KU Leuven
Biomedical Sciences Group
Faculty of Medicine
Department of Oral Health Sciences
Prosthetics, BIOMAT

Effect of high-frequency loading on peri-implant bone remodelling

Xiaolei Zhang

Jury:

Promoter:	Prof. Dr. Joke Duyck, KU Leuven
Co-promoter:	Prof. Dr. Ignace Naert, KU Leuven
Co-promoter:	Prof. Dr. Ir. Harry van Lenthe
Chair:	Prof. Dr. Dominique Declerck, KU Leuven, Belgium
Secretary:	Prof. Dr. Wim Teughels, KU Leuven, Belgium
Jury members:	Prof. Dr. Reinhilde Jacobs, KU Leuven, Belgium
	Prof. Dr. Lies Geris, U. Liège , Belgium
	Prof. Dr. Astrid D. Bakker, ACTA, Netherlands

Dissertation presented in partial fulfilment of the requirements for the degree of Doctor in Biomedical Science

November 2015

Acknowledgements

Wow, this is it! When the moment really comes, I feel too much to say. This PhD has been a long journey way beyond my expectation and has rendered me so many thanks to express. During the time I am in Leuven and outside of the campus, I have met many great people that, in one way or another, have helped me in reaching this point. My sincere gratitude is addressed to all of them. Some of their names are especially deserved to acknowledge here.

With great respect, I'd love to express the utmost appreciation to my promoter Prof. J. Duyck. She is such an excellent scholar and mentor who guide me on the road of science. When I get stuck in pits of my study and life, she is always there as a source of creative ideas and a solid support.

I am grateful to my co-promoter Prof. I. Naert. He offered me the opportunity of starting a PhD at KU Leuvn. As a poor young man who went to a foreign country for the first time in his life, I always remember my first a few hard weeks in Leuven. Prof. Naert and his son Philip kindly brought a bed, a mattress and a cabinet to my newly-rented empty studio and help me settle down. I'm sorry Prof. Naert. I cannot return the furniture to you because I don't know where they are after all these years. But your kindness and generosity is always in my heart.

I would like to thank my co-promoter Prof. H. van Lenthe. He is one of the most gentle and intelligent scientists I've ever met. His wisdom and profound knowledge broaden my understanding of the project. It's a great honor and pleasure to work with him.

For being part of the jury of this PhD, and for their critical remarks on the thesis, I owe my gratitude to Prof. Dominique Declerck, Prof. Wim Teughels, Prof. Reinhilde Jacobs, Prof. Dr. Lies Geris, and Prof. Astrid D. Bakker

This work would not have been accomplished without the help of many colleagues. Dr. Amol Chaudhari, my dear friend and office roommate, it's an unforgettable time to spend with you on brain-storming and Grote Markt hanging out. Dr. Toru Ogawa, my very important partner of the animal surgeries and whole-body-vibration studies, is a

true Japanese researcher who dedicates all his time to the project. Dr. Marcio Vivan Cardoso always impressed me with his novel ideas and gentle personality. Dr. Antonia Torcasio, the work with her on the quantification of peri-implant bone strain really is a linchpin of this thesis.

Many thanks to the BIOMATers. All of you mean a lot to me. Jan De Munck, Annelies Van Ende, Pong Pongprueksa, Xin Li, Athina Mavridou, Selvi Palaniappan, Marissa Chatterjee, Atsushi Mine, Yuji Suyama, Kohki Hatori, Shuhei Hoshika, Anne-Katrin Lührs, and Simone Gonçalves Moretto. We are a family of BIOMAT! Lovely department secretaries, Ms. Sonja Meulemans and Ms. Sandra Winnen, you are very appreciated for you professional and careful arrangements for this defense.

I also want to address the special gratitude to my fellow compatriots in Leuven. Dr. Yan Huang is an extreme warm-hearted man and a good friend. We definitely will have a life-long contact and collaboration back in China. Dr. Guozhi Zhang is one of the first groups of friend I made in Leuven. He is cocky and cold for the first sight. But it wouldn't take long to realize that he actually is just a simple, frank and reliable youngster. My life in Leuven is colorful because of the named and the unnamed above.

I'd like to appreciate Prof. Junqi Ling, the dean of School and Hospital of Stomatology Sun Yat-sen University, for her offer of an academic position to me. Prof. Zhengmei Lin and Prof. Xi Wei, the directors of the department of conservative dentistry and endodontics, are also grateful for their supporting me to finalize this PhD thesis.

And at last (but not the least), I would like to thank my family. 感谢父母多年来的培养和支持，希望妻女能平安、健康，你们永远是我前进的动力！

Xiaolei Zhang

张晓磊

This thesis is based on the following publications:

Paper One Zhang X., Duyck J., Vandamme K., Naert I., Carmeliet G. Ultrastructural characterization of the implant interface response to loading. ***Journal of Dental Research*** 2014 Mar;93(3):313-8.

Paper Two Ogawa T., Zhang X., Naert I., Vermaelen P., Deroose C., Sasaki K., Duyck J. The effect of whole body vibration on peri-implant bone healing in rats. ***Clinical Oral Implants Research*** 2011 Mar;22(3):302-7.

Paper Three Ogawa T., Possemiers T., Zhang X., Naert I., Chaudhari A., Sasaki K., Duyck J. Influence of loading time on the impact of whole body vibration on peri-implant bone healing: a histomorphometrical study on rat. ***Journal of Clinical Periodontology*** 2011 Feb;38(2):180-5.

Paper Four Ogawa T., Vandamme K., Zhang X., Naert I., Possemiers T., Chaudhari A., Sasaki K., Duyck J. Stimulation of titanium implant osseointegration through high frequency vibration loading is enhanced when applied at high acceleration. ***Calcified Tissue International*** 2014 Nov;95(5):467-75.

Paper Five Zhang X., Vandamme K., Ogawa T., Torcasio A., Van Lenthe H., Naert I., Duyck J. *In vivo* assessment of the effect of controlled high- and low-frequency mechanical loading on peri-implant bone healing. ***Journal of the Royal Society Interface*** 2012 Jul 7;9(72):1697-704.

Paper Six Zhang X., Naert I., Van Schoonhoven D., Duyck J. Direct high-frequency stimulation of peri-implant rabbit bone: a pilot study. ***Clinical Implant Dentistry and Related Research*** 2012 August; 14(4):558-64.

Paper Seven Zhang X., Torcasio A., Vandamme K., Ogawa T., Van Lenthe H., Naert I., Duyck J. Enhancement of implant osseointegration by high-frequency low-magnitude loading. ***PLoS ONE*** 2012;7(7): e40488.

These studies were granted by
the Research Fund of Research Council KU Leuven (No. OT 07/059).

Table of contents

List of symbols

ε	Strain
µ	Micron
ø	Diameter
ABC	Avdin-biotin-peroxides complex
ALP	Alkaline phosphatase
BA	Bone area
BF	Bone fraction
BFR	Bone-formation rate
BIC	Bone-to-implant contact
BMU	Basic multicellular unit
BS	Bone surface
C.Ar	Callus area
Col1al	Collagen type 1 alpha 1
CTR	Control
Ctsk	Cathepsin K
H&E	Hematoxyline and erythrosine
HF-LM	High-frequency low-magnitude
HF-HM	High-frequency high-magnitude
Hprt1	Hypoxanthine phosphoribosyl transferase 1
Hz	Hertz
L	Length
LF-LM	Low-frequency low-magnitude
LF-HM	Low-frequency high-magnitude
MAR	Mineral apposition rate
MSCs	Mesenchymal stem cells
N	Newton
OC	Osteocalcin
Opg	Osteoprotegerin

Opn	Osteopontin
PBS	Phosphate buffered saline
PEMS	Pulsed electromagnetic stimulation
PMMA	Poly(methyl methacrylate)
qRT-PCR	quantitative Real-time polymerase chain reaction
RANK	Receptor activator of NF kappa B
RANKL	Receptor activator of NF kappa B ligand
ROI	Region of interest
Runx2	Runt-related transcription factor 2
SD	Standard deviation
SEM	Standard error of the mean
SG	Strain gauge
SUV	Standardized uptake value
T.Ar	Tissue area
Ti	Titanium
TRAP	Tartrate-resistant acid phosphatase
VA	Vessel area
WBV	Whole body vibration

Chapter 1
General introduction

1.1 Bone remodelling and tissue mechanics

Bone is a metabolically active tissue capable of adapting its shape and structure to mechanical stimuli and repairing structural damage through the process of remodelling. Bone remodelling, the resorption of bone followed by focal bone formation by the basic multicellular unit (BMU), is carried out by active bone resorbing osteoclasts and is followed by bone formation by osteoblasts. The regulation of these two arms of remodelling is not necessarily sequential, but are probably multidirectional and highly regulated so that the volumes of bone resorbed and formed are titrated in a manner appropriate to the local mechanical requirements (Parfitt, 2001).

Described as the biological process of activation→resorption→formation (A→R→F), the adaptive and reparative bone remodelling can be affected by a number of stimuli (*i.e*. hormones, cytokines, and mechanical signals) (Turner *et al*., 2009). For the mechanical signals, specifically, osteocytes within the bone are believed to sense the signals, and further convert them into biochemical signals to trigger cellular responses (a process called mechanotransduction) (Huang *et al*., 2004). Further, osteocyte apoptosis is believed to involve in the mechanism to attract osteoclasts to sites that develop a bone-remodelling unit. The loading-induced micro-cracks impair osteocyte processes in their canaliculi, causing osteocyte apoptosis (Hazenberg *et al*., 2006). These apoptotic osteocytes will provide topographical information needed to identify the location and size of the damage. In this way, osteocytes might also contribute to direct bone remodelling (Seeman, 2006; Verborgt *et al*., 2000).

Piles of studies have enriched our understanding on how the mechanical signals are converted into an anabolic or catabolic bone response. In brief, when mechanical loading is applied at low- (associated with relatively high-magnitude) or high- (associated with relatively low-magnitude) frequency, the bone will experience the deformation, which is defined as strain. The strain can induce a fluid flow in the bone lacuna-canalicular bone matrix, which will be sensed by the bone cells (mainly osteocytes), which in turn will trigger the down-stream signal cascades. The activity of bone functional cells, osteoblasts and osteoclasts, will then be mobilized and remodel the bone (Figure 1.1) (Bonewald and Johnson, 2008; Ehrlich and Lanyon, 2002; Judex

et al., 2009; Turner, 2006).

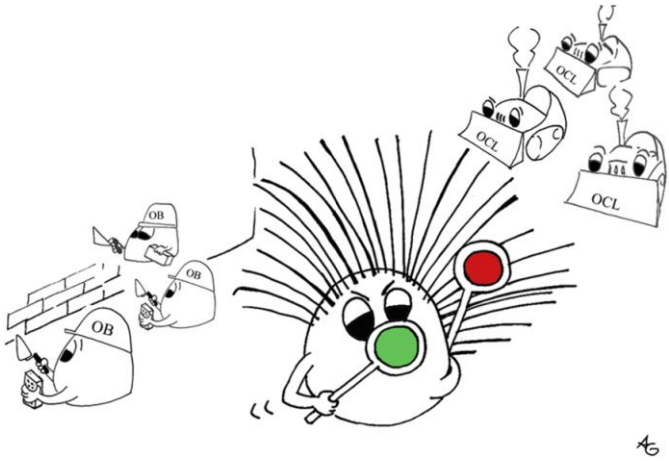

Figure 1.1 *Schematic representation of the central role of osteocytes in bone remodelling. Osteocytes sense the mechanical load and subsequently produce signaling molecules that can regulate the activity of the effector cells, the osteoclasts and the osteoblasts, which subsequently leads to adequate bone mass and architecture. OB, osteoblast; OCL, osteoclast. (Klein-Nulend J, et al., Bone 2013) (Reprinted from Bone, 54(2), Klein-Nulend J, Bakker AD, Bacabac RG, Vatsa A, Weinbaum S, Mechanosensation and transduction in osteocytes, 182-90, Copyright (2013), with permission from Elsevier).*

Extensive research indicates that not only the basic loading components (*e.g*. magnitude and frequency), but also other load parameters play a role in the resulting bone response to mechanical loading. According to contemporary literature, the following notions were made (Burr *et al*., 2002; Judex *et al*., 2009; Ozcivici *et al*., 2010a; Robling and Turner, 2009): (1) dynamic rather than static loading leads to bone remodelling; (2) the anabolic response can be initiated by very little mechanical stimuli (*e.g*. a few strain cycles and/or a short loading time in minutes or seconds); (3) bone cell accommodation: an initial change in bone (re)modelling by mechanical stimuli will eventually die out as the bone cells accommodate to the new environment; (4) recovery of the mechanical sensitivity of the bone cells: a load-free resting time between loading cycles or sessions can help regain the sensitivity.

1.2 Osseointegration and peri-implant bone healing: effect of loading

Osseointegration refers to a direct structural and functional connection between ordered, living bone and the surface of a load-carrying device/implant (Branemark, 1959; 1983). Besides the above concept by Branemark, more definitions of osseointegration have been adopted at multiple levels, including clinically (Adell *et al*., 1981), anatomically (Branemark *et al*., 1983), histologically, and ultrastructurally (Linder *et al*., 1983), broadening the meaning of osseointegration from different aspects.

In skeleton biology, the mechanical and histological response of bone to trauma has been intensively studied. Similar to the process of bone trauma healing, main host responses and histological events (including hematoma formation, mesenchymal tissue development, woven bone formation through the intramembranous ossification, and lamellar bone formation *via* remodelling of woven bone) are observed during the peri-implant bone healing and hence lead in most cases to the successful connection of bone to the implant, coined osseointegration (Davies, 2003). Accordingly, these histological changes will be addressed by three events, *e.g*. the host tissue response to implantation, peri-implant bone formation and peri-implant bone remodelling. As widely recognized, the healing can be influenced by the surgical technique as well as by host-related (immune response, vascularization, bone type, systemic diseases, *etc*.), implant-related (surface properties, design, *etc*.), environmental (*e.g.* oral microflora, smoking), and biomechanical factors (Fini *et al*., 2004; Liddelow and Klineberg, 2011; Novaes *et al*., 2010; Soballe *et al*., 1992).

1.2.1 Initial tissue response to implantation

Although not fully understood yet, a cascade of cellular and extracellular biological events occurs at the bone-implant interface, which determines the early tissue response as well as the bone formation at the interface thereafter. The first biological component in contact with an endosseous implant is blood. After being entrapped at the implant surface, the blood cells are activated and hence release cytokines and growth factors (Davies, 1998). Around the implant, the newly formed blood clots result in a fibrin network serving as an osteoconductive scaffold for the migration of osteogenic cells

and induce the eventual differentiation of these cells in the healing compartment (Berglundh *et al*., 2003; Davies, 1998; Meyer *et al*., 2004).

With the conduction of the fibrin clot, the osteogenic cells (*i.e*. pre-osteoblasts and/or mesenchymal cells) can migrate and attach to the implant surface as early as the first day of implantation. Successively, they deposit bone-related proteins and create a noncollagenous matrix layer on the implant surface that regulates cell adhesion and binding of biomolecules. Similar to the bone cement lines and laminae limitans that forms a continuous and thick layer rich in calcium, phosphorus, osteopontin and bone sialoprotein (Meyer *et al*., 2004; Murai *et al*., 1996), this matrix is an early-formed calcified afibrillar layer on the implant surface, allowing further bone formation.

During the bone healing, the newly formed bone is laid down on the resorbed surface of the pre-existing bone after osteoclastic activity. Meanwhile, cement lines of poorly mineralized osteoid define the area where bone resorption was completed and bone formation initiated. A few days after implantation, osteoblasts were found to deposit collagen matrix directly on the early formed cement line/lamina limitans layer along the implant surface (Meyer *et al*., 2004). In the process of matrix secretion and mineralization, some osteoblasts become entrapped and buried in the calcifying matrix, which later on are clustered as osteocytes in bone lacunae (Murai *et al*., 1996).

1.2.2 Peri-implant bone formation

The bone formation in the peri-implant region, *via* intramembranous ossification, can occur in two directions (Davies, 1998; 2003): (1) the healing of the pre-existing bone approaching to the biomaterial (distance osteogenesis); (2) the new bone extending from the implant toward the pre-existing bone (contact osteogenesis / *de novo* bone formation).

The early deposition of new calcified matrix on the implant surface results in an early implant anchorage. Containing a sufficient vasculature, marrow tissue supports active recruitment of mononuclear precursors for osteoclasts so that bone trabeculae remodel faster than cortical bone (Franchi *et al*., 2005).

With the establishment of early implant osseointegration, a certain degree of resistance to early implant loading is achieved. This bony network also offers a biological scaffold for further cell attachment and bone deposition resulting in biological fixation (Franchi *et al*., 2005; Probst and Spiegel, 1997). Successively, peri-implant woven bone is remodelled into lamellar bone that may reach a high degree of mineralization. (Probst and Spiegel, 1997).

1.2.3 Peri-implant bone remodelling

Peri-implant bone undergoes remodelling as adaptation to mechanical loading. The turnover of peri-implant mature bone in osseointegrated implants is confirmed by the presence of basic multicellular units (containing osteoclasts, osteoblasts, mesenchymal cells and lymphatic/blood vessels) in the neighborhood of the implant surface (Franchi *et al*., 2005; Matsuo *et al*., 1999; Slaets *et al*., 2006; 2007; Slaets *et al*., 2009).

Peri-implant bone remodelling actually starts early after implantation. Recent studies on early osseointegration (from hours to days) have demonstrated that the upregulation of genes responsible for bone formation *ALP* (alkaline phosphatase, *ALP*) and *OC* (osteocalcin, *OC*) was coupled with upregulation of genes expressed by osteoclasts indicating that the bone remodelling phase is triggered much earlier than what has previously been assumed (Omar *et al*., 2010; Omar *et al*., 2011). Similar results were observed with other surfaces where the over expression of collagen 1 and OC was coupled with higher expression of TRAP (tartrate-resistant acid phosphatase, TRAP) in cells adherent to coin titanium implants retrieved from rabbit tibia after 8 weeks of implantation (Monjo *et al*., 2008). An intimate cross-talk is established between osteogenic cells and osteoclasts, *e.g*. the surface receptor RANK (receptor activator of NF kappa B, RANK) on osteoclasts recognizes and binds to osteoblast membrane-associated factor RANKL (receptor activator of NF kappa B ligand, RANKL) during the osteoclastic differentiation from the monocytic lineage (Katagiri and Takahashi, 2002). The presence of basic remodelling units in the peri-implant bone can already be observed 7 days after implantation (Slaets *et al*., 2006; Slaets *et al*., 2007).

Taken together, active bone resorption and bone formation processes are taking place over a wide time range and starting already during the first days after implantation.

1.2.4 Effect of mechanical loading on peri-implant bone healing

Peri-implant bone healing involves bone apposition and remodelling. At the cellular level, the invasion of capillaries into the mesenchymal zone, as well as the differentiation of mesenchymal cells into osteoblasts are crucial for the healing process. Abundant evidence has shown that the differentiation of mesenchymal cells into osteoblasts is tightly regulated by mechanical loading (Kelly and Jacobs, 2010). According to *in vitro* studies, once loaded *via* oscillatory fluid flow, a series of biological responses of mesenchymal cells to the loading occurs and hence leads to the osteoblast differentiation including increased intracellular Ca^{2+}, higher proliferation rate, upregulation of osteoblastic genes (*e.g*. *Runx2*, *Sox9*), and decreased ALP activity (Arnsdorf *et al*., 2009; Li *et al*., 2004). A relevant finding, which confirmed the effect of mechanical loading on peri-implant osteogenesis and angiogenesis, was reported by Geris *et al*. (Geris *et al*., 2010). They revealed the consistence between the results of mathematical modelling and *in vivo* experiments, and hence indicated that the stimulation of mechanical loading indeed affects the angiogenic and osteogenic processes (*i.e*., osteoblast and endothelial cell proliferation and osteogenic MSCs differentiation) during implant healing.

In brief, mechanical loading does affect peri-implant bone healing by (1) directing neighboring mesenchymal cells into osteoblasts for intramembranous ossification and by (2) influencing peri-implant bone remodelling favoring bone gain. The latter, *i.e*. the effect of mechanical loading on bone remodelling, has widely been acknowledged

1.3 Effect of *in vivo* mechanical loading on peri-implant healing and clues from skeleton research

For a long time, it was assumed that premature loading limited the peri-implant osteogenesis, favoring a peri-implant fibrous tissue formation, thereby preventing osseointegration. A direct bone-to-implant contact (osseointegration) was not established as required for predictably withstand functional loads (Branemark *et al*., 1977; Branemark *et al*., 1983). On the contrary, controlled mechanical loading does even promote peri-implant osteogenesis (Meyer *et al*., 2004; Romanos *et al*., 2003; Romanos, 2004; Simmons *et al*., 2001a). Peri-implant tissue formation is strongly

related to the local mechanical environment at the bone-implant interface during healing (Szmukler-Moncler *et al*., 1998; Vandamme *et al*., 2007c).

As mentioned previously, loading magnitude and frequency are the basic components of dynamic mechanical loading, which will lead to a range of strains and strain rates in the bone. To address the findings of *in vivo* studies about mechanical loading and adaptive/reparative (peri-implant) bone remodelling, we reviewed and sorted these studies by two loading categories the so-called: "low-" (< 10Hz) and "high-frequency" (> 10Hz) loading.

1.3.1 Mechanical loading at so-called "low-frequency" (< 10"Hz)

1.3.1.1 Clues from skeleton research

During the eighties of the last century, *in vivo* experiments have been performed to investigate the effect anabolic mechanical signals at low-frequency (< 10Hz) on the skeleton. Most studies have focused on loading magnitudes that are relatively large (*i.e*. the load-induced deformation is higher than the suggested remodelling threshold of $\sim$ 1000 με) (Frost, 2004). Other variations, including loading waveform, duration, rest interval between loading events and strain rate, were addressed as well.

In table 1.1, we summarized *in vivo* studies indicating the anabolic effect of low-frequency mechanical loading, *e.g.* leading to the periosteal bone formation (Lee *et al*., 2002), inhibiting disuse-induced bone loss (Inman *et al*., 1999) and facilitating the early callus formation during fracture healing (Takeda *et al*., 2004). Within a range of parameters (*e.g*. magnitude, frequency and loading duration), several clues are noted.

(1) *Effect of loading magnitude*: up to a certain limit, a higher loading magnitude, inducing a higher strain, is associated with increased osteogenic response (Cullen *et al*., 2001; Forwood *et al*., 1998; Gross *et al*., 2002; Mosley *et al*., 1997; Silva and Brodt, 2008).

(2) *Effect of loading frequency*: according to Warden and Turner (Warden and Turner, 2004), an increased loading frequency can lead to an improved response with a plateau of 5-10Hz. At the same time, they also reported that the change of loading frequency did not significantly influence the mechanical strain per unit load (Warden and Turner,

2004). Hence, under the same loading magnitude, this improved response by increased loading frequency can be explained by the growth in number of loading events per unit time. Not surprisingly, when loading cycles were solely prolonged, more bone response can be found (Cullen *et al*., 2001).

(3) *Combined effect of loading magnitude and frequency (i.e. strain rate)*: in a compressive loading model of the rat ulna, an interesting fact was revealed that less loading magnitude was required to evoke the bone (re)modelling when loading frequency was increased (Hsieh and Turner, 2001). The importance of the combined effect (*i.e.* strain rate) was then subject to investigation and was proven (LaMothe *et al*., 2005; Mosley and Lanyon, 1998).

(4) *Cell accommodation and recovery*: the mechanical loading causes an initial change in bone (re)modelling, but the reaction will eventually die out as the bone cells accommodate to the new environment (Cullen *et al*., 2000). As stated by Turner (Turner, 1999), bone cells continuously adjust their mechanosensitivity in response to their mechanical loading history. To either recover the mechanosensitivity or retard the cell accommodation, the loading strategy of applying a load-free interval between loading sessions (Robling *et al*., 2001a) or loading cycles (Srinivasan *et al*., 2003; Srinivasan *et al*., 2007) has been tested and been proven to result in more bone response than the continuous loading.

(5) *Resonance effect*: the stochastic resonance can be evoked by a low-frequency loading when composed with a vibration. Under the condition of stochastic resonance, a significant increase of new bone formation on the periosteal surface was reported, when compared to the unloaded control and the low-frequency loading alone (Tanaka *et al*., 2003).

The site-specific response of host bone to loading seems to be related to the loading magnitude. With the local strain less than 1000 με, more active bone (re)modelling was found at the trabecular site than the cortical site (Fritton *et al*., 2005). Under the loading regimes resulting in around 2000 με at the midshaft of both tibia and ulna, the cortical bone adaptive response to loading was more pronounced in the tibia compared to the ulna (Kuruvilla *et al*., 2008). The authors proposed that the difference might be

due to the variation of the osteoblast density and cell sensitivity to loading between tibia and ulna. When the local strain of around 3000 με was achieved, the osteogenic response was found at both cortical and trabecular sites (De Souza *et al*., 2005; Lee *et al*., 2002).

1.3.1.2 Implant studies

1.3.1.2.1 Direct implant loading via force-controlled loading through the implant axis

A series of studies was carried out to explore the effect of mechanical loading through bending force on implant osseointegration (De Smet *et al*., 2005; De Smet *et al*., 2006; De Smet *et al*., 2007; 2008). Screw-shaped implants were installed in the distal part of guinea pig tibiae, mainly consisting of cortical bone, and a sinusoidal loading was applied 1 week after implant installation. The implant stability (measured by resonance frequency) was increased due to the mechanical loading regime (De Smet *et al*., 2005). When loading regimes with different strain rates (from 1620 to 12000 με/s) were applied, the lowest strain rate loading regime (1620 με/s, corresponding to 3 Hz and 540 με) induced a significant increase in bone mass in the medullar cavity around the implant surface. This implies an inverse correlation between strain rate amplitude and peri-implant bone response (De Smet *et al*., 2006). When the strain rate was kept constant at 1600 με/s, the low-frequency high-magnitude loading protocol (3 Hz 533με) induced the most bone formation in the medullar cavity (De Smet *et al*., 2007). 267με at 3 Hz with 800 με/s appeared to be the optimum loading regime, compared to both lower and higher strain rates (133με-3 Hz-400με/s, 533με-3Hz-1600με/s respectively) (De Smet *et al*., 2008).

This loading regime did not have the same effect in a rabbit tibia model though. However, an increased new bone formation was observed in the endosteal and periosteal area (Slaets *et al*., 2009). To determine the effect of axial loading on the peri-implant bone formation, Clark *et al*. (Clark *et al*., 2005) applied a conventional cyclic loading protocol on implants, which were installed in the proximal femur region of the rabbit and were left to heal for 6 weeks before the mechanical stimulation. After a 12-day mechanical stimulation (200mN-1Hz-10min/day), a significantly greater bone

volume, endocortical osteoblast-like cell number per bone surface (BS), mineral apposition rate (MAR), and bone-formation rate (BFR/BS) than the contralateral control were found. The above mentioned data support the idea that mechanical forces delivered by axial loading of the implant can stimulate the peri-implant bone formation and increase the osseointegration.

1.3.1.2.2 Direct axial implant loading via displacement-controlled micromotion through the implant axis

Several experiments indicated that the micromotion at the tissue-implant interface, caused by "excessive" mechanical forces applied too early in the osseointegration process, can lead to fibrous encapsulation and subsequent implant loosening (Brunski *et al*., 2000; Cameron *et al*., 1973; Pilliar *et al*., 1986; Soballe *et al*., 1992). It has been suggested that the early micromotion leads to the differentiation of cells at the bone-implant interface into fibroblasts that produce a fibrous capsule around the implant instead of the desired bone (Szmukler-Moncler *et al*., 1998). Although some degree of micromotion is tolerated, a certain threshold should not be surpassed. This threshold is set at various levels by different researchers. The studies, however, are difficult to compare due to the differences in study set-ups, *e.g*. different surgical techniques, implant loading conditions, implant geometry, implant surface, and implantation site (related to bone quality). An implant displacement of 100 μm, for instance, does not necessarily lead to an interfacial micromotion of 100 μm. The factors, including implant design and surface roughness, affect the actual resultant micromotion at the interface. A study on the effect of a pure micromotion on implant osseointegration revealed that a micromotion as small as 30 μm might already impair osseointegration (Duyck *et al*., 2006).

The implant loading, however, does not lead solely to micromotion at the bone-implant interface, but also to the transfer of forces to the surrounding tissues. Whereas interfacial micromotion tends to have a compromising effect on implant integration, a favorable force transfer might have a positive effect on the latter. The proportion of micromotion and force transfer depends on the degree of osseointegration and other factors such as implant geometry, surface characteristics, *etc*. For example, a centrally

applied load does not necessarily coincide with the micromotion at the bone-implant interface when the direction of the implant movement differs from that of the bone-implant interface. In addition, the tissues between screw threads or porosities are protected from the full impact of the centrally applied load, leading to a less micro-motion at the bone-implant interface.

By use of a bone chamber model in rabbit tibia, Duyck and co-workers proved that well-controlled immediate implant loading can enhance the peri-implant bone quantity and quality, and accelerate the implant osseointegration in case of a restriction of interfacial micromotion and a good force transfer from the implant towards the surrounding tissues (Duyck *et al*., 2006; Duyck *et al*., 2007; Vandamme *et al*., 2007a; Vandamme *et al*., 2007b; c). Both implant design (screw-shape instead of cylinder) and surface roughness favored the mechanical stimulation of the peri-implant tissues and therefore enhanced peri-implant bone healing and osseointegration. The screw-shaped implant design not only improved the primary stability by increasing the implant bone contact surface, but also promoted osseointegration by providing a favorable local mechanical environment for bone formation, compared with the cylindrical implant.

Leucht *et al*. (Leucht *et al*., 2007) applied a 150 μm micromotion (1Hz, 1min/day, 7days) to implants inserted in tibiae of mice, immediately after implant insertion. They found that in areas of excessively large strains (*i.e*. at the base of the implant), osteochondroprogenitor cells occupied the site but failed to differentiate into osteoblasts. However, osteoblast differentiation and bone matrix deposition took place in close proximity to the implant surface where moderate strains predominated. A histological assessment of the gap regions indicated that the amount of new bone that formed by post-surgical day 7 in the motion cases was equivalent to the amount of new bone that was formed by day 14 in the stable implants. Collectively, the moderate strain induced by axial micromotion could increase osteogenesis around the implant.

1.3.1.2.3 Direct implant loading perpendicular to the implant axis

Besides loading through the implant axis, the lateral loading was applied in several studies to assess its effect on the peri-implant bone response. By use of bone

scintigraphy, the effect of loads applied by lateral coil springs on the peri-implant bone metabolism was evaluated 8 weeks after implant installation in the rabbit tibia (Sasaki *et al*., 2008). The highest metabolic activity was observed in the animals that received more loading (2N *vs.* 4N) and was increased in a time-dependent way. A stepwise loading protocol was applied on the same animal model after an implant healing time of 3 months (Wiskott *et al*., 2008). No significant difference in the bone-to-implant contact was found between the loading and control animals. An increased bone volume and density were observed, however, in the peri-implant area in the loading group by microcomputer tomography analysis. The controlled lateral force seemed to improve the peri-implant bone and at least maintain the implant osseointegration. For implants exhibiting mucositis or ligature induced peri-implantitis, the static lateral loading (1) failed to induce peri-implant bone loss, or (2) failed to enhance the bone loss (Gotfredsen *et al*., 2002).

Table 1.1 *In vivo studies of mechanical loading at "low" frequency*

Range of local peak strain(με)	Research target	Loading system	Local peak strain (με)	Frequency (Hz)	Wave form	Timing (cycles, durations)	Results	Reference
≤1000	mouse, tibia	horizontal oscillatory loading on tibia	wild-type mice, 720 ±90 με; IGF-1-overexpressing mice, 600 ±75 με	1	haversine	100 cycles/session, 4w	↑periosteal bone formation in wild-type mice; ↑↑periosteal bone formation in IGF-mice	Gross *et al*., 2002
	mouse, ulna	compressive	735	2(with/without vibration for SR)	haversine	30 s/day, 2days	↑↑new bone formation on the periosteal surface by loading + vibration; ↑new bone formation on the periosteal surface by loading alone	Tanaka *et al*., 2003
	mouse, tibia	compressive	800	4	a load ramp of 0.075s duration followed by a unload ramp of 0.075s	1200 cycles/day, 5 days/week, 2/6weeks	↑mineral content in the cortico-cancellous proximal metaphysic (14%) and in the cortical mid-shaft (2%); ↑bone volume fraction (15%); ↑average trabecular thickness (12%)	Fritton *et al*., 2005
	mouse, tibia	3-point like bending system	900/1400	1	n/a	100 cycles/day, 5days	for loading of 900 με, no difference of BFR/BS between loaded wild-type mice and loaded thrombospondin 2 knock-out mice; for loading of 1400 με, a significant two-fold increase in BFR/BS was in loaded thrombospondin 2 knock-out mouse	Hankenson *et al*., 2006
	mouse, tibia	3-point like bending system	1000	1	trapezoidal	60 s, 5 days/week, 4 weeks	higher strain rates evoked greater adaptive responses on the periosteal surfaces in mature bone	LaMothe *et al*., 2005
	mouse, tibia	3-point like bending	1000/1250/1600	1	trapezoidal (10-s rest at zero load inserted between each load cycle)	10/50/250 cycles/day, 3 days/week, 3 weeks	effect on the bone formation: 1600 ＞1250 ＞ 1000με; ↑periosteal bone formation rate by rest-period insertion	Srinivasan *et al*., 2007
	mouse, tibia	3-point bending	1000/2000	1	triangle	60 cycles/day, 5 days/week, 2weeks	effect on bone formation: 2000με＞ 1000με	Silva and Brodt., 2008
	rat, tibia	4-point bending	800/1000	2	sinusoidal	40/120/400 cycles, 3 days/week, 3 weeks	at constant frequency, as number of cycle↑, the bone response↑	Cullen *et al*., 2001
1000～2000	mouse, tibia	horizontal oscillatory loading on tibia	1200/2400 in tibia mid-shaft	1	trapezoidal	50 cycles/d, with or without 10/20 s rest time between each cycle, 2 w	For the loading of 1200με, loading with 10-s rest time insertion ↑periosteal bone formation rates 2-fold higher than that of the pure loading group in aged mice; no extra benefit of bone formation was found by increasing loading magnitude or increasing time of rest	Srinivasan *et al*., 2003
	mouse, tibia/ulna	compressive	1200/1350	10	trapezoidal	40 cycles,10-s' rest between each cycle, 3 d/w, 2 w	↑osteogenic response in trabecular and cortical bone by combination of loading with PTH treatment	Sugiyama *et al*., 2008

	mouse, ulna	compressive	1750±204	1/5/10/20/30	haversine	5 min/day, 3 days/week, 4 weeks	Loading frequency had no effect on mechanical strain per unit load	Warden and turner. 2004
	rat, tibia	4-point bending	1200	2	n/a	36 cycles/day, 6/12/18 weeks	↑periosteal lamellar bone formation; periosteal formation is elevated transiently for 6–12 wk and returns to age-matched control levels by week 18 of loading. After 12 wk of loading, bone adaptation reached a steady state.	Cullen *et al*., 2000
	rat, tibia	4-point bending	1400	2	n/a	36 cycles/day, 3 weeks	↑periosteal mineralization and maintained bone mineral density; attenuating the loss in bone strength incurred with disuse and concurrent calcium deficiency	Inman *et al*., 1999.
	rat, tibia	4-point bending	1756/2001/2467	2	haversine	36 cycles/day, 3 days/w, 3 weeks	collagen-induced arthritis↓bone formation induced by mechanical loading.	Kameyama *et al*., 2004
2000～000	mouse, ulna/tibia	compressive/4-point bending	2000	2	haversine	99 cycles/day, 3 days/week, 3weeks	↑bone formation greater in the tibiae than the ulnae	Kuruvilla,*et al*., 2008
	mouse, ulna	compressive	2000	4	trapezoidal	10 min, at a strain rate of 0.1 sec (-1) for 5 days/week for 2 weeks.	↑lamellar periosteal bone formation; no endosteal response	Lee *et al*., 2002
	mouse/rat, ulna	compressive	2200	2	n/a	360 cycles/day, 1/2 days	↓↓Sost transcripts and sclerostin protein levels	Robling *et al*., 2008
	mouse, ulna	compressive	2566±315	1/5/10/20/30	haversine	120 cycles/day, 3 days	↑cortical bone adaptation with increasing loading frequency up to 5–10 Hz; to plateau with frequencies beyond 10 Hz.	Warden and Turner. 2004
	rat, ulna	compressive	2000	2	ramped square wave	10 min, killed after 6 hours	↑eNOS protein expression in osteoblast/osteocyte lineage; no effect on the eNOS mRNA.	Zaman *et al*., 1999
	rat, tibia	4-point bending	2400	2	haversine	36 cycles(pulse every 0.5, 3.5, 7 or 14 s rest), 15 days	8 h of recovery was sufficient to restore full mechanosensitivity to the cells	Robling *et al*., 2001(b)
	rat, tibia	4-point bending	2500	2	haversine	36 cycles/day, 3days/w, 2 weeks	BPM7↑loading-induced endosteal lamellar bone formation rate	Cheline *et al*., 2002
	rat, tibia	4-point bending	420 - 2664	2	haversine	18 sec, every second day for 10 days	↑new bone formation at periosteal and endocortical surfaces with a dose response to the loaded strain	Forwood *et al*., 1998
≥3000	mouse, tibia	compressive	500-3000	2Hz(with 10s rest-period between cycles)	n/a	40 cycles/days, 3 days/week, 2 weeks	↑both trabecular and cortical bone in the tibia	De Souza RL *et al*., 2005

	mouse, ulna	compressive	3000	4	trapezoidal	10 min, at a strain rate of 0.1 sec (-1) for 5 days/week for 2 weeks.	↑a mixed woven/lamellar periosteal response and lamellar endosteal bone formation.	Lee *et al*., 2002
	rat tibia/ulna	4-point bending/compressive	3000/3600	2	haversine	360 cycles/day, 9 days	loading-induced bone formation ↓by PTH inhibitor	Li *et al*., 2003
	rat tibia/ulna	4-point bending/compressive	3000/3400	2	haversine	360 cycles/days,	loading-induced BFR and MS/BS ↓by Cox-2 inhibitor on effect on loading-induced MAR	Li *et al*., 2002
	rat ulna	compressive	3400	2	ramped square wave	10 min/d	loading-induced bone response was involved by the activity of estrogen receptor alpha	Zaman *et al*., 2006
	rat, ulna	compressive	4000	2	ramped square wave	1200 cycles/day, 5 days	neither a single nor five consecutive daily periods of *in vivo* mechanical loading produced any significant effect on different NOS isoform mRNA expression	Zaman *et al*., 1999
	rat, ulna	compressive	4000	2	trapezoidal	1200 cycles were applied on days 4–8 and 11–15, inclusive. A standard high dwell time of 50 μsec was used, when the load was held constant.	a high rate of strain change provides a greater osteogenic stimulus than the same peak strain achieved more slowly	Mosley and Lanyon. 1998
	rat, ulna	compressive	1610,2640,3660,4680/850,1400,1950,2500/360,580,800,1020	1/5/10	haversine	360 cycles/day, 5 days/week, 2 weeks	↑periosteal rBFR/BS and rMS/BS in a dose-response manner with peak compressive strain and frequency; Loading frequency would affect the positive dose-response relationship between mechanical strain and osteogenesis	Hsieh & Turner.2001
Not mentioned	rat, tibia	compressive and distractive	n/a	1	sine	30 min/day, 3 days/week, 3 days/1w/2w	↑callus formation in the early stage of bone fracture healing	Takeda *et al*., 2004
	rat, ulna/tibia	compressive	n/a	1	sinusoidal	300 cycles/day, 4 days	protein expression of GluR ↑in bone lining cells	Szczesniak *et al*., 2005
	rat, tibia	4-point bending	n/a	2	haversine	300 cycles,7days,2/3/4/5 weeks	COX-2 inhibitor postponed the increased woven bone formation induced by loading	Gregory, *et al*., 2007
	rat, tibia	4-point bending	n/a	2	haversine	300 cycles	↑IGF gene expression in osteocytes	Reijnders *et al*., 2007

In summary, the mechanical loading at low-frequency has shown its potential to improve osseointegration and peri-implant bone healing. However, the so-called "optimal" loading protocol (*i.e.* loading magnitude, frequency spectrum and loading mode) still has to be defined.

1.3.2 Mechanical loading at so-called "high-" frequency (> 10 Hz)

1.3.2.1 Clues from skeleton research

Bone can respond to very small mechanical loading when applied at high-frequency. Table 1.2 shows the findings of *in vivo* studies on this theme. The loading frequency seems to be a more determinant factor compared to loading magnitude in case of high-frequency loading (Judex *et al.*, 2007). The inspiring point is that the therapeutic potential of the loading has been proven in clinic cases (Table 1.3). Its application in implant dentistry is therefore worth considering.

The exact mechanism of how mechanical loading affects bone is yet unclear. However, the available evidence suggests that the anabolic mechanical loading at high- or low-frequency may be sensed by the host tissue in a different strain-dependent manner.

(1) Under the low-frequency regime (< 10 Hz), relatively large loading magnitudes were needed to induce an anabolic response. When keeping the loading frequency and the number of loading events constant, variations in strain magnitude can explain differences in the osteogenic response: the larger the deformations generated in host bone, the greater the increases in bone mass (Cullen *et al.*, 2001; Gross *et al.*, 2002; Mosley *et al.*, 1997; Torrance *et al.*, 1994). This can be interpret with relatively simple models such as the mechanostat (Frost, 2004) and the fluid flow theory (Klein-Nulend *et al.*, 2005). According to the fluid flow theory, the load-induced fluid shear stress performed as the activating signal by acting on osteocytes and cell processes in the lacunar-canalicular system. ***Therefore, the anabolic effect of low-frequency loading on bone was associated with the activating signal depending on the load-induced strain magnitude.***

(2) Under the high-frequency regime, relatively small loading magnitudes were needed to induce an anabolic response. Local strains on the tibia surface have been recorded

less than 10 με in the whole body vibration (Judex *et al*., 2007; Xie *et al*., 2006). Apparently, the induced strain is extremely small, far less than the (re)modelling threshold of 1000 με under the low-frequency regime (Frost, 2004). The anabolic response of the host tissue was mainly dependent on the loading frequency, rather than the loading magnitude (Christiansen and Silva, 2006; Judex *et al*., 2007; Judex and Rubin, 2010). Some explanations of this dependence were suggested by the theoretical models of You *et al*. (You *et al*., 2001) and Han *et al*. (Han *et al*., 2004). Their models were based on the facts that (1) osteocyte processes were attached along their length by tethering filaments, and (2) the actin filament bundle in dendritic processes led to a highly polarized cell whose processes were several hundred times stiffer than the osteocyte cell body (Han *et al*., 2004). Hence, the flow-induced drag on these filaments would produce a tension that could greatly amplify the very small whole tissue strains at the cellular level. By predicting the strain amplification ratio from the tissue to the cell level, they found that this amplification ratio not only increased with loading frequency, but also decreased with loading magnitude (You *et al*., 2001). ***Therefore, in case of high-frequency loading, low bone strains were amplified most, suggesting a more efficient mechanotransduction process by cellular perception of high-frequency signals, compared to high-magnitude strains.*** Another possible explanation for the anabolic effect of high-frequency/vibration loading was proposed by Rubin *et al* (Rubin *et al*., 2002). *I.e*., during daily movements, a living subject normally experiences high-frequency plus low magnitude events of around 10 Hz and 0.05-0.5 με. Once the subject was confronted with the loading with relatively higher frequency and magnitude (17-90 Hz and 1-10 με), there was a shift in the mechanical environment. ***This shift of mechanical environment could be responsible for the bone's adaptive response.***

1.3.2.2 Implant studies

Because of its anabolic effect observed in *in vivo* and clinical studies in the skeleton field, the high-frequency mechanical loading is a tempting strategy to boost implant healing. A variety of high-frequency loading regimes applied onto the implant was explored in different studies to observe the peri-implant bone response.

An early study on the effect of mechanical loading on bone growth into a porous implant was performed by Rubin and McLeod (Rubin and McLeod, 1994). The strains of 150 με were generated in the cortex immediately adjacent to the implant by means of host bone bending in the turkey ulna disuse model (Rubin and McLeod, 1994). The 20 Hz loading regime induced the most favorable bone response, while the 1 Hz loading only prevented the bone resorption caused by the disuse.

A favorable peri-implant bone response was also found in case of high-frequency loading *via* whole body vibration (WBV). After an early (the implants were left to heal for one week after implantation) WBV for 2 weeks, the peri-implant bone response in the ovariectomized rat tibia model was quantified by micro-CT evaluation (Akca *et al*., 2007). Compared to the pulsed electromagnetic stimulation (PEMS) group and the control (no loading and no PEMS) group, the low-magnitude high-frequency loading (5 N and 50 Hz) induced the highest amount of relative bone volume around the peri-implant bone area. This non-invasive mechanical intervention was proven to be more effective to bone healing around the implant than the PEMS in the ovariectomized rat and the control.

1.4 Clinical views on the effect of mechanical loading on implants

Being aware of the fact that an excessive interfacial micromotion early after implantation interferes with local bone healing and predisposes to a fibrous tissue interface instead of osseointegration, the conventional implant loading protocol was generally accepted since 1977 (Branemark *et al*., 1977). The latter implies a load-free healing time for 3 months in the mandible and 6 months in the maxilla to allow uncompromised osseointegration and hence minimize the risk of soft tissue encapsulation (Brunski *et al*., 1979). However, it is not the absence of loading *per se* that is critical for osseointegration but rather the absence of excessive micromotion at the bone-implant interface (Szmukler-Moncler *et al*., 1998). Due to optimized surgical techniques, implants, *etc*., there is a definite trend towards early or even immediate loading after implant installation, in which the forces are applied on the implant *via* the prosthesis. Based on data of clinical studies, the immediate loading protocol achieved similar high success rates as that noted for the conventional protocols (Avila *et al*.,

2007; Esposito *et al*., 2009a; Esposito *et al*., 2009b). Within the theme of this thesis introduction, *i.e*. the mechanical loading on implant healing, the clinical view on both so-called “overloading” and immediate loading will be addressed in this section.

Table 1.2 *In vivo studies of mechanical loading at "high" frequency*

Loading Set-up	Species	Animal Model	Frequency (Hz)	Magnit (g)	Loading Protocol	Duration	Microstrain (με)	Analysis	Outcome	Reference
Local Vibration										
Ground-based hindlimb vertical vibration	Sheep(Warhill, intact ewes, 6-8y, female)	Normal	30	0.3	20min/d, 5d/w	1y	5 με at the left tibial midshaft	BMD of tibia, femur and radius were quantified by DXA pQCT	↑trabecular bone density of proximal femur by 34.2% (trabecular space ↓36.1%, trabecular number ↑45.6%); no change found on cortical bone	Rubin, *et al*., 2002
	Sheep(female)	Normal	30	0.3	20min/d, 5d/w	1y	5 με at the left tibial midshaft	BMD of tibia, femur and radius were quantified by DXA pQCT	trabecular bone density of proximal femur ↑34.2%, BV/TV↑32%	Rubin, *et al*., 2001
	Sheep(Warhill, intact ewes, 6-8y, female)	Normal	30	0.3	20min/d, 5d/w	1y	5 με at the left tibial midshaft	BMD of medial condyle of femur was quantified by microCT, mechanical test on the bone shaft	↑bone quantify (BMC↑10.6%, trabecular number↑8.3%, space ↓11.3&); stiffness ↑12.1%; failure strength ↑26.7%	Rubin, *et al*., 2002
	Sheep(Warhill, intact ewes, 6-8y, female)	Normal	30	0.3	20min/d, 5d/w	1y	5 με at the left tibial midshaft	BMD of medial condyle of femur was quantified by microCT, finite element model analysis	trabecular stiffness ↑17% in the longitudinal, 29% anterior–posterior, 37% medial-lateral	Judex *et al*., 2003
	Sheep(female,2-3y)	a transverse osteotomy in the right metatarsus and externally stabilized	20	0.02mm displacement	loading 2 w after surgery, 5 min/d	8w	n/a	QCT and mechanical test	callus formation ↑11%; no other significant difference was found	Wolf, *et al*., 2001
Constrained tibia vibration	male C57Bl/6 mouse, 5–6 month	normal	20-150	0.5	n/a			strain measurement, finite element model	for *in vivo* leg, best transmissibility occur on 60Hz at 0.5g.	Christiansen *et al*., 2008
	male C57Bl/6 mouse, 5–6 month	normal	70/140	0.5	15min/day	5 w	at 70 Hz, the local strain (330 με with heavy mass125 g, 59 με with low mass 40 g, 17 με with fixed mass)	microCT and histomorphological analysis	No difference was found between the control and tested legs.	Christiansen, *et al*., 2009

							on tibia midshaft			
horizontal oscillatory loading on tibia	(19 w) female C57BL/6J (B6) mice	without weight-bearing	45	0.3/0.5	15 min/d, 5 d/w	3w	in the proximal tibia, 1.1 με at 0.3 g, 2.2 με at 0.5g	microCT and dynamic histomorphological analysis	at 0.3g, BFR↑88%,MS/BS↑64% in tibia metaphysis; at 0.5g, BFR↑66%,MAR↑22% in tibia metaphysis;	Garman *et al*., 2007
	female adult (4-month old) BALB/cByJ mice	without weight-bearing	45	0.6	25 min/d, 5 d/w	3w	n/a	microCT, finite element model	trabecular stiffness↑38% than the internal control, but still 44.7% lower than the weight-bearing bone	Ozcivici *et al*., 2007
	(16 w) female C57BL/6 mice	normal	30		100s with or without 10-s rest time inserted between each 1-s loading pulse, 5 d/w	3w	800 με (lateral tibial middiaphysis).		without rest, periosteal surface BFR/BS↑88%, MAR↑ 48%; with rest, BFR/BS↑91%,MAR↑126%	LaMothe and Zernicke. 2004
Whole Body Vibration										
	Female Sprague Dawley rats (3 mon)	ovx	30	0.6/3	20 min/d, 5 d/wk	4/8w	14.07±5.09 με 23.40±7.53 με	qCT, histomorphology	Longitudinal analysis: no differences in cortical or trabecular BMD by pQCT; cross-sectional analysis: no differences in histomorphometric analysis; *in vitro* analysis: vibration at 3 g ↑ total cortical and medullary areas and periosteal and endosteal perimeter in OVX rats	Rubinacci *et al*., 2008
	Female Sprague Dawley rats (6–8 mon)	ovx	45/90	0.15	10 min/d, 5d/w	4w	2.12 με/0.74 με.	microCT, histomorphology	90 Hz: ↑ BFR, BV/TV and Tb.Th	Judex *et al*., 2007
	Female Wistar rats (1 y)	ovx	17/30/45	0.5/1.5/3	30 min/d, 5d/w	17w	n/a	mechanical test_3point-bending, histomorphology	45 Hz: ↑ periosteal BFR and ↓ OVX-induced endocortical resorption, ↓ declines in biomechanical properties	Oxlund *et al*., 2003
	Female Wistar rats (12 w)	ovx	50	2	30 min/d, 5d/w	12w	n/a	mechanical test, DEXA scan,	↓ OVX-induced bone loss; ↑ BMD	Flieger *et al*., 1998
	Female adult rats	ovx	90	0.3	2 x 20 min/d, 5d/w	6w	n/a	micro-CT at 0, 2, 4, 6 w after wbv, 3-point-bending of mechanical test	no effect	Brouwers *et al*., 2009

Female Sprague Dawley rats (3 mon)	ovx	90	0.5 mm displacement	2 x 15min/d	35d	n/a	flat-panel volumetric CT, mechanical testing, histomorphometrics	↑biomechanical properties ↑bone density (trabecular > cortical bone),	Sehmisch *et al*., 2009
Female SD rats (12w)	ovx+implant on tibia	50	5newton	14min/d, 5d/w, applied one week after implantation.	2w	n/a	microCT	↑relative bone volume around implant	Akca *et al*., 2007
Female Sprague Dawley rats (6–8 mon)	disused	90	0.25	10 min/d	4w	n/a	bone histomorphology	↑ BFR and MS/BS with normalized BFR in vibration + HU group similar to CON	Rubin *et al*., 2001
adult rat	closed femoral shaft fracture	35	0.3	?	2/4w	n/a	plain radiography, micro-CT, histomorphometry	↑callus formation, mineralization and fracture healing	Leung *et al*., 2009
Male SD rats(4mon)	5-mm bilateral defect on cranium	45	0.4	20 min/d, 5 d/w, applied 1 w after surgery for 3w, no treatment for another 4 ws	3w	n/a	microCT	↑osseous regenerative processes, particularly in the presence of a supporting scaffold.	Hwang *et al*., 2009
BALB/cByJ mice (8 w)	normal	45	0.3	15 min/d, 5d/w	6w	n/a	microCT, histomorphology, TRAP-staining	proximal tibial metaphysis: ↑ MS/BS; cortical bone: ↑ BV, periosteal bone area, bone marrow area, cortical area and moment of inertia; ↑ soleus cross-sectional area	Xie *et al*., 2008
C57BL/6 mice (12 w)	normal	0-50	2N	30 s'/d, 3 d/w	4w	500-4000 με		No effect of vibration on periosteal bone formation	Castillo *et al*., 2006
Female mice (2 mon)	normal	45	0.3	15 min/d	3w	10 microstrain on the periosteal surface of the proximal tibia	bone histomorphology	↓ osteoclastic activity; ↑ BFR	Xie *et al*., 2006
Male mice (7 mon)	normal	45	0.1/0.3/1	15 min/d	5w	n/a	microCT, cell culture for OB activity	↑ trabecular bone BV/TV in 0.1 and 1.0 g groups	Christiansen *et al*., 2006
C57BL, BALB/c, and C3H mice	normal	45	0.25	10 min/d		n/a	histomorphology	↑ BV/TV in C57BL only (85%); ↑ BFR/BS in BALBc (32%).; ↔ in C3H	Judex *et al*., 2002
C3H mice (12 w)	defect in cranial bone	30	0.3 g	20 min/d, 5d/w	28d	5 με	microCT	↑healing capacity of the bone	Omar *et al*., 2008

Table 1.3 *Clinical studies of mechanical loading at "high" frequency*

Subject Population	Subject Condition	Loading Protocol	Analysis	Outcome	Reference
Healthy Volunteers (33+/-7 y)	bed rest (BR) for 90 d	0.3/0.5g, 30 Hz, 10 min/d	MRI and CT (0, 60, 90, 90+7D after bed resting)	attenuate swelling of the intervertebral disc; ↓the incidence of low back pain	Holguin *et al*., 2009
Healthy Volunteers (22-29 +/- 7 y)	high protein intake for 5 d	3.5g, 30Hz, 10 min/d	daily urine test for calcium, phosphate, titratable acid, urea and c-telopeptide	↓the high expression of calcium, phosphate excretion and c-telopeptide	Cardinale *et al*., 2007
PMP at least for 1 y	postmenopausal	28 Hz, 3×2 min/session, 2 session/w, 6 months	Blood and urine test for PTH, CV. Muscle power was assess by jumping test. pQCT on tibia for bone density, mass and geometry.	↑muscle power by 5%; No change was found on cortical bone density and biomarkers of bone turnover.	Russo *et al*., 2003
PMP (58-74 y)	postmenopausal	2.28-5.09 g, 35-40 Hz, 30 min, 3 time/w, 24 w	DXA measure the hip bone density. Serum tests the biomarkers of bone turnover. Muscle strength test	↑hip BMD and leg muscle strength. No change of the biomarkers of the turnover	Verschueren *et al*., 2004
PMP (57 y)	postmenopausal	0.2 g, 30 Hz, 2×10 min/d, 12 mon	BMD measured by DXA on femur, spine.	↑BMD was found on femoral neck and spine; Lighter subject benefit more; Bone density was not influenced.	Rubin *et al*., 2004
PMP (55-88 y)	postmenopausal	0.7-4.2 mm(displacement), 20Hz, 4 min/session, 1 session/w, 12 mon	Lumber BMD measured by DEXA, urine NTX and serum ALP level tested by ELISA.	no difference was found on BMD and NTX, ALP. ↓the chronic back pain	Iwamoto *et al*., 2005
PMP (66 y)	postmenopausal	3 mm (displacement), 12.5 Hz, 6×1 min, 3 times/w, WBV *vs*. walking, 8mon	Hip and lumbar BMD (g.cm-2) were measured using dual-energy X-ray absorptiometry and balance was assessed by the blind flamingo test	↑the BMD femoral neck; ↑the balance. No change of BMD on lumbar spine	Gusi *et al*., 2006
pre- or postpubertal disabled children (4-19 y)		0.3 g, 90 Hz, 10 min/d, 5 times/w, 6 mon	vTBMD was measured by QCT on tibia and spine.	↑vTBMD of proximal tibia; No change was found on cortical bone and muscle parameters	Ward *et al*., 2004
Low-BMD female (15-20 y) with fracture history		0.3 g, 30 Hz, 10 min/d, 12 mon	QCT to measure the bone and muscle mass	the cancellous bone in thelumbar vertebrae and cortical bone in the femoral midshaft of the loaded group↑by 2.1% and 3.4%; paraspinous musculature↑by 4.9% greater	Gilsanz *et al*., 2006

1.4.1 Implant "overloading"

The inherent difference between the tooth and implant is that an endosseous implant is in direct contact with the bone while a natural tooth is suspended in the bone by a periodontal ligament. Therefore, implants lack the adaptive facility of teeth to develop reversible increased mobility when loaded. Implants are more rigidly attached to the bone and may be displaced 3-5 μm vertically and 10-50 μm laterally with forces applied of 2000 g (Kim *et al*., 2005). Some have suggested the occlusal "overloading" as one of the main causes for peri-implant bone loss and/or loss of osseointegration of successfully integrated implants (Adell *et al*., 1981; Isidor, 1996; 1997; Miyata *et al*., 2000; Quirynen *et al*., 1992; Rangert *et al*., 1989; Rosenberg *et al*., 1991). In comprehensive reviews by Esposito *et al*. (Esposito *et al*., 1998a; b), the prevalence of late implant failures from 19 different publications with Branemark implants with a machined surface was assessed. Of the failures observed after more than 1 year of loading, the occlusal overload was estimated to account for approximately 90% and peri-implantitis for 10% of the few late failures (4.6% of the inserted implants). The observations, including screw loosening or fracture, abutment or prosthesis fracture, bone loss, implant fracture, have been considered as the signs of implant overloading (Zarb and Schmitt, 1990).

However, the so-called "overloading" in some implant literature seems to be an inappropriately used term when its definition is taken into account. According to Frost's mechanostat (Frost, 2004), the mechanical strain magnitude over 3000 με should lead to a catabolic reaction of bone (*i.e.* net bone loss). Hence, the "overloading", by its definition, should theoretically induce a mechanical strain of > 3000 με at the implant-bone interface and a net loss of peri-implant bone. Unfortunately, neither clinical nor animal implant study have ever convincingly proven their "overloading" cause a mechanical strain of > 3000 με at the implant-bone interface. As commented by Mellal *et al*., the stress and strain evoked at the implant-bone interface remain impossible to be quantified today in the animal/clinical settings (Mellal *et al*., 2004). Confronted with the above challenge, an alternative way to explore the cause-and-effect relation between "overloading" and implant failure is to

assess the peri-implant bone response after "overloading". In a recent systematic review, Naert *et al*. (2012) concluded that there is insufficient evidence that the so-called overload can lead to peri-implant bone loss or implant failure. Some studies even reported an anabolic effect from loading (Naert *et al*., 2012). One study, however, indicates a possible detrimental effect of loading when combined with peri-implant infection (Kozlovsky *et al*., 2007).

1.4.2 Predictability of immediate implant loading

Based on the consensus obtained from ITI Consensus Conference at Stuttgart (Germany) in August 2008, Weber *et al*. reported that the immediate implant loading can be defined as being loaded earlier than 1 week subsequent to implant installation (whereas up to 2 months for early loading and >2 months for conventional loading) (Weber *et al*., 2009). The immediate implant restoration with functional loading can provide faster patient comfort by allowing quick masticatory function and esthetics. In addition, it also eliminates the inconvenience of a second surgery approach for placement of transepithelial abutments. This often leads to an early soft tissue healing and results in an early stabilization of the peri-implant mucosa. Undisturbed implant healing by conventional loading was considered for long to be the main factor necessary to achieve predictable high success (Albrektsson *et al*., 1981). The immediate implant loading was believed to possess potential risks that the clinician and patient must be aware of. These include: a possible implant failure due to increased implant micromovement and unable to predict final soft and hard tissue outcomes (Avila *et al*., 2007). So, the question whether or not the immediate implant loading works as good as the conventional loading has been a concern.

According to Gapski *et al*. (Gapski *et al*., 2003) and Avila *et al*. (Avila *et al*., 2007), factors that influence the outcomes of immediate implant loading can be divided into 4 categories: (1) Surgery-related factors, pertaining to primary implant stability and a non-traumatic surgical technique; (2) Host-related factors, pertaining to bone quantity and quality (density), proper bone healing environment, oral hygiene/patient compliance; (3) Implant-related factors, pertaining to the influence of macro- (thread) and micro- (surface coating) structure of the implant; and (4) Load-related factors,

pertaining to the importance of occlusal forces and prosthetic design. When the outcomes of immediate implant loading were compared with that of the conventional loading, no significant difference was reported both for the partial implant-retained restoration and the complete implant-retained overdenture, based on the systematic review of clinical trials/cases (Carrillo Garcia *et al*., 2008; Kawai and Taylor, 2007). In a recent review of randomized controlled clinical trials of immediately *versus* early *versus* conventionally loaded implants, in which 1852 implants in 1024 patients after 1 year of function were included, no difference in prosthesis failure, implant failure and marginal bone level changes was found between immediately and conventionally loaded implants (Esposito *et al*., 2009a). Although it is still unclear whether it is beneficial to avoid occlusal contacts during the implant osseointegration process, the present studies and clinical experiences have shown that the immediate implant loading achieved similar success rates as those reported for conventional implant protocol. At the same time, in order to achieve this predicatively high success rates, it is crucial for dentists to keep the following in mind: (1) a high degree of primary stability at implant insertion, which is associated with an adequate insertion torque, is a key prerequisite; (2) a careful selection of cases with an adequate treatment plan; (3) a proper control of the influencing factors (*e.g*., surgery-related, host-related, implant-related and load-related). Accordingly, in the case of poor primary implant stability or other suspected negative prognostic variables, it might be preferable to wait for early or even conventional healing period to offer bone enough time to properly heal around the implant.

1.5 Conclusions and prospectives: from lab to chair-side

From the literature, it's not difficult to note that the dynamic mechanical loading can lead to bone remodelling. The anabolic bone response to mechanical loading can be initiated by very little mechanical stimuli (*e.g*. a few strain cycles and/or a short loading time in minutes or seconds). Further, the mechanical loading can influence peri-implant bone remodelling favoring bone gain and hence improve peri-implant bone healing.

As mechanical loading – at either low or high frequency - appears to be a potent signal for adaptive and reparative bone remodelling, the application strategy of mechanical loading is yet to define. The questions including when (immediate *vs.* conventional loading), how long (loading duration), what (low- *vs.* high-frequency loading) and how (indirect *vs.* direct implant loading) are open to explore.

When compared to the reports on general skeleton, the effect of high-frequency loading on peri-implant bone is much less reported in literature. Considering the promising effect of high-frequency loading on bone, this PhD research focuses on the peri-implant bone response to high-frequency loading. We intend to explore the potential of high-frequency loading to obtain better and faster peri-implant bone healing.

The overall objective of this PhD research is to investigate the effect of mechanical loading, in particular high-frequency loading, on peri-implant bone healing and remodelling. The following hypotheses were addressed:

- Healing and healed peri-implant bone tissues respond differently to mechanical loading (*i.e.* immediate *versus* conventional loading).
- High-frequency mechanical loading can stimulate osseointegration and peri-implant bone remodelling.
- The effect of high-frequency loading on peri-implant bone depends on time-related parameters.
- The effect of high-frequency loading on peri-implant bone depends on the applied loading parameters, in particular load magnitude and frequency.
- The effect of high-frequency mechanical loading on peri-implant bone depends on the mode of load application (whole body vibration *vs.* direct implant loading *vs.* indirect implant loading).

To fulfill the research objective and to test the related hypotheses, a series of experiments was performed and reported in 5 chapters of this thesis (Chapters 3 to 7).

In Chapter 3, the peri-implant tissue response to immediate and conventional loading was evaluated.

Because of the abundant evidence of whole body vibration on the bone stimulating potential, the effect of such high-frequency loading on peri-implant bone remodelling was investigated in 3 continuous studies (Chapter 4).

As the exact local mechanical stimuli cannot be clearly defined in case of whole body vibration, the assessment of the controlled high-frequency loading was the logical next step. This was performed through a well-controlled compression of the tibia containing the implant (the indirect loading in Chapter 5) and through the direct implants loading (Chapters 6 and 7).

Studies in Chapter 5 and 7 were performed in close collaboration with the department of Biomechanics and Engineering Design of KU Leuven. Peri-implant cortical strains resulting from tibia compression (in Chapter 5) or from direct implant loading (in Chapter 7) were measured *ex vivo* using strain gauges. These strain gauge measurements, combined with micro-finite element analyses, based on micro-CT scan data, allow translating the applied load into the resulting tissue strains in the peri-implant regions (Torcasio *et al.*, 2011, 2012).

Chapter 2
Materials and methods

2.1 Animal models

2.1.1 Rat tibia

3-month old male Wistar rats were used. Rats were housed 3 to 4 animals per standard cage under 12-h dark–light photoperiods.

Surgeries were performed under general gas anesthesia with 2.5% isoflurane (Isoflurane USP®, Halocarbon, New Jersey, USA). Implants were placed in the mesio-proximal part of both tibiae. The primary implant stability was obtained through bicortical implant fixation. The implant cavity was drilled at low rotational speed under constant saline cooling and was 0.3 mm undersized compared to the implant diameter. The implants were manually installed by means of a custom-fit torque wrench, with a complete submersion of the screw part (5 mm) of the implant into the bone. Resorbable sutures (Vicryl 3-0, Ethicon GmbH, Norderstadt, Germany) were used to close the wound.

The animals of all groups were sacrificed by cervical displacement under isoflurane-induced anesthesia at the end of the experimental term.

2.1.2 Rabbit tibia

6-months old female New Zealand white rabbits (body weight, 3.7 ± 0.5 kg) were selected for this experiment. The rabbits were all pathogen free and kept in quarantine for 1½ months before the study was started.

Under general anesthesia (intravenous, Diprivan 1%, 0.4 ml/kg; Astra Zeneca, Brussels, Belgium), a total of four implants was inserted in the two tibia epiphyses of each rabbit by two implant surgeries at 1 week and 4 weeks before the sacrifice. Postoperatively, the animals were given a dose of an intramuscular injection of 0.05 mg/kg buprenorphine as analgesics and 300.000E/d antibiotics (penicillin, Kela, Hoogstraten, Belgium) for 3 days.

At the end of the experiment, the animals were sacrificed with a 0.1ml/kg intravenous injection of an embutramide, mebenzoniumiodide, and tetracaine hydrochloride solution (T61; Intervet, Mechelen, Belgium).

2.2 Histological preparation

2.2.1 Tissue preparation

2.2.1.1 Paraffin sections

Specimens were fixed in 2% paraformaldehyde immediately after sacrifice. The bone segments were decalcified in 0.5M EDTA (pH 7.4)/PBS at 4 ℃ and paraffin-embedded, whereupon the implants were gently unscrewed. Next, the samples were re-embedded into paraffin. Then, longitudinal or transversal sections of 5-µm thickness were cut with a rotary microtome (HM360; Microm, Walldorf, Germany).

2.2.1.2 PMMA sections

At sacrifice, the implants and surrounding tissues were isolated and immediately fixated in a $CaCO_3$–buffered formalin solution, dehydrated in an ascending series of ethanol concentration and embedded in polymerized methylmethacrylate (PMMA) resin. The tissue-implant blocks were sectioned along the longitudinal direction of the tibia and the implant's axis by means of a diamond saw (Leica SP1600, Wetzer, Germany). After polishing to a final thickness of 20 to 30 µm (Exakt400 CS, Exakt Technologies Inc., Germany), the sections were ready for further staining.

2.2.2 Histochemical staining

Before histological staining, paraffin sections were de-waxed by immersion in xylene and rehydrated in descending concentration of ethanol. After staining, sections were dehydrated and covered by cover-glass (Menzel-Glaser®, Gerhard Menzel GmbH, Braunschweig, Germany) with histological mounting medium (Histomount ™, National Diagnostics, Atlanta, USA).

2.2.2.1 H&E (paraffin sections)

The sections were stained with Harris hematoxyline and erythrosine (H&E) for approximately 2 and 5 minutes, respectively.

2.2.2.2 Stevenel's blue and Von Gieson's picrofuchsin red (PMMA sections)

The sections were stained with Stevenel's blue and Von Gieson's picrofuchsin red for 20 and 7 minutes, respectively, visualizing mineralized (red) and non-mineralized tissues (blue).

2.2.3 Immunohistochemical staining of CD31

The paraffin sections were firstly de-waxed by immersion in xylene and rehydrated in descending concentration of ethanol. Secondly, they were incubated in the Antigen Retrieval solution (DAKO, Denmark) for 20 minutes at 95 ℃ and washed in PBS. Then, sections were incubated in 0.3% H_2O_2 in methanol for 20 minutes, followed by 3 rinses with PBS. Unspecific binding was blocked by incubating the sections for 30 minutes in PBS with 2% BSA. Subsequently, sections were incubated overnight with primary antibody of CD 31 (DAKO, Denmark). After 3 washes with PBS, the incubation with secondary antibody was performed for 1 hour, followed by 3 additional washes with PBS. Sections were then exposed to a biotin-mediated reaction (the avdin-biotin-peroxides complex, ABC) for 30 minutes. Next, the antibody bindings were visualized on the color substrate diaminobenzidine. Finally, the slides were counterstained with hematoxylin.

2.3 Histomorphometric analysis

Quantitative assessments were performed by light microscopy (Leica Laborlux, Wetzlar, Germany) and a high sensitivity video camera (AxioCam MRc5, Zeiss, Göttingen, Germany). As the sections were made along the long axis of the tibia and the implant, histomorphometric analyses were carried out on both proximal and distal sides of the implant.

2.3.1 With paraffin sections

2.3.1.1 Bone density in-between implant threads

The bone area (BA, %), representing the percentage of bone occupying the V-thread regions located in the bone marrow, was scored as 1, 2, 3 or 4, corresponding to 0-25%, 25-50%, 50-75% or 75-100% of the thread region consisting of bone tissue. The mean BA was calculated for on average 12 regions per sample (Figure 2.1A).

2.3.1.2 Vascularization

The blood vessel area (VA, %) represents the area of blood vessels visualized by CD31 immunostaining. VA was evaluated in 3 regions: (1) the V-thread tissues in the upper cortex (region of cortical bone), (2) the 1st V-thread area beneath the upper cortex (a region where fast bone regeneration occurs due to endosteal callus formation) and (3) the 1st V-thread tissues in the bone marrow (region of bone marrow) (Figure 2.1B).

2.3.1.3 Endosteal callus formation

In the peri-implant endosteal and central bone marrow region, the size and the mineralization of the formed callus were quantified. To do so, a rectangular tissue area (T.Ar) was defined spanning the region between the endosteal side of upper and lower cortex and up to 1.5 mm distance from the implant surface. The callus area (C.Ar/T.Ar, %) was quantified as the percent tissue area filled with callus tissue. The callus bone area (B.Ar/C.Ar, %) was defined as the percent bone filling of the callus tissue (Figure 2.1C).

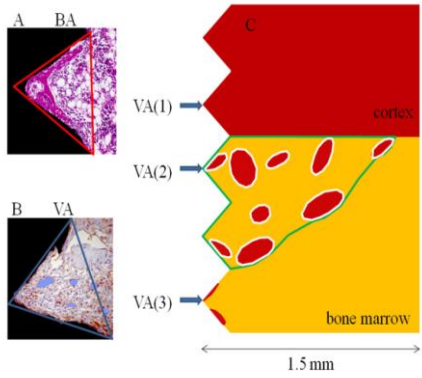

Figure 2.1 *Illustrations and schematic representation of the measurements performed on paraffin-embedded implant-tissue samples. (A) In the region of peri-implant medulla, the percentage bone filling of the implant V-threads (red-outlined triangular area) was calculated and allocated to a quartile category (Bone area – BA, %); (B) The blood vessel area (VA, %) was quantified in 3 regions by the ratio of the vessel surface area (highlighted in blue) to the tissue surface area (blue-outlined area); (C) Axisymmetric schematic representation of the 3 different regions where VA was recorded, and of the quantification of the endosteal callus size and mineralization.*

2.3.2. With PMMA sections

2.3.2.1 Bone-to-implant contact

Bone-to-implant contact (BIC, %) = 100 × (summation of the lengths of bone-to-implant contact / the implant length from first till last bone-to-implant contact).

2.3.2.2 Bone fraction

Bone fraction (BF, %) = 100 × (area of bone / area of the region of interest). Three different regions of interest (ROI) were defined: 0-100 μm (ROI 1), 100-500 μm (ROI 2) and 500-1000 μm (ROI 3) away from the implant surface. The height of all ROI's was set from first till last bone-to-implant contact (Figure 2.2).

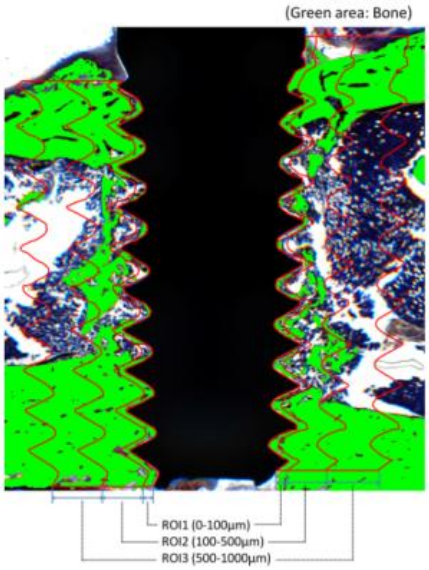

Figure 2.2 *Illustration of the reference sites for the peri-implant bone fraction (BF) evaluation. ROI 1 ranged from 0 (implant surface) to 100 μm, ROI 2 from 100 to 500 μm and ROI 3 from 500 to 1000 μm.*

2.4 Gene expression analysis

By use of quantitative real-time PCR (qRT-PCR), the osteoblast- and osteoclast-related gene expressions were assessed in peri-implant cortical bone.

2.4.1 Sample collection

The cortical bone chips remaining on the implant neck were harvested immediately after removal of the implant, and snap-frozen in liquid nitrogen. According to

standard protocols of quantitative real-time PCR (qRT-PCR), total RNA was retrieved by extraction with TRIzol® reagent (Invitrogen, Merelbeke, Belgium). The RNA integrity and amount were checked using a spectrophotometer (Pharmacia, model 80-2103-98, LKB Biochrom, England).

2.4.2 Sample analysis

Random-primed cDNA was synthesized from 1µg of total RNA using the SuperScript™ II RT Kit (Invitrogen, Merelbeke, Belgium). Equal volumes of cDNA were used to program amplifications through real-time PCR reactions (ABI Prism 7500 Fast Real-Time PCR System, Applied Biosystems, Halle, Belgium) using primers of genes encoding for bone formation and bone resorption. Quantification of gene expressions of the different markers was performed using the comparative threshold cycle method (ΔΔCt) (Livak and Schmittgen, 2001) with hypoxanthine phosphoribosyl transferase 1 (*Hprt1*; Applied Biosystems TaqMan® Assay ID Rn01527840_m1) as the endogenous reference.

Bone formation-related gene expression

Specific primers of genes encoding for runt-related transcription factor 2 (*Runx2*), collagen type 1 alpha 1 (*Col1a1*), osteopontin (*Opn*) and osteocalcin (*Oc*) were used, in the presence of TaqMan Universal PCR Master Mix (Applied Biosystems). The primers were home-designed (for primer sequences, see Table 2.1), except for *Runx2* (Applied Biosystems TaqMan® Assay ID Rn01512296_m1).

Bone resorption-related gene expression

The mRNA expression of the osteoclast-related genes, including receptor activator of NF kappa B ligand (*RANKL*), osteoprotegerin (*Opg*) and cathepsin K (*Ctsk*), were analyzed by the TaqMan® Gene Expression Assays (Applied Biosystems; ID Rn00563499_m1; ID Rn00589289_m1 and ID Rn00580723_m1 respectively).

Table 2.1 *Primer and probe sequences for qRT-PCR.*

Gene	**Primer and probe sequence (5'→3')**	
Oc	Forward primer	GCTGGCCCTGACTGACTGCATT
	Reverse primer	TGGACATGAAGGCTTTGTCAGA
	Probe	CAGGTGCAAAGCCCAGCGACTCTG
Col1a1	Forward primer	CGATGGCGTGCTATGCAA
	Reverse primer	ACTTCTGCGTCTGGTGATACATATTC
	Probe	CCCAACCCCCAAAAACGGGAGG
Opn	Forward primer	TGACTTTAAGCAAGAAACTCTTCCAA
	Reverse primer	TGCATGGTCTCCATCGTCAT
	Probe	CAACTCCAATGAAAGCCATGACCACATG

The primer source is the rat for all genes.

2.5 Statistical analysis

Comparison between quantitative data of two groups was done by two-sided Student's t-test. Paired sample t-test was applied in case of two pair-wised groups. Multiple groups were analyzed by ANOVA adjusted by Tukey's multiple correction. Statistical software was used to do the above analysis (SPSS for Windows 10.0, Chicago, IL, USA). *P*-values inferior to 0.05 were considered significant. The data were reported as the mean ± standard error of the mean (SEM).

Chapter 3
In Vivo study of the peri-implant tissue response to controlled immediate and conventional loading

This chapter is based on the publication "**Zhang, X.**, Duyck, J., Vandamme, K., Naert, I., Carmeliet, G. (2014). Ultrastructural characterization of the implant interface response to loading. ***Journal of Dental Research*** 2014 Mar; 93(3):313-8."

Abstract

***Objective*:** Well-controlled mechanical loading can improve peri-implant bone formation. The study aimed to further explore the peri-implant tissue response to immediate and conventional loading.

***Materials and methods*:** Screw-shaped, titanium implants were installed in rat tibiae, in which one implant was loaded (test) while the other served as unloaded control. The test implant was loaded either immediately after implantation or after a healing period of 28 days (conventional loading). Rats were sacrificed after 4, 7, 14, 21, or 28 days of loading. The samples were routinely processed into paraffin sections for histological analyses. Additional samples loaded for 28 days were resin-embedded to evaluate the bone-implant interface, while others loaded for 7 days were used for gene quantification by quantitative real-time PCR. Statistical analyses were performed with the significance set at $p < 0.05$.

***Results*:** Compared to the unloaded control, bone-to-implant contact increased significantly by immediate loading for 28 days ($p<0.05$), but not in case of conventional loading. No effect was observed of the immediate or conventional loading on the bone area in-between the implant threads, the blood vessel area and the endosteal callus formation. After loading for 7 days, relative to the unloaded control, a 2.3-fold increase of *Runx2* in peri-implant bone was induced in case of immediate loading ($p<0.01$) without a change of the *RANKL/Opg* ratio. Conventional loading for 7 days upregulated *Runx2* (4.3-fold, $p<0.01$) as well as *Opg* (22.3-fold, $p<0.05$) compared to the unloaded control, resulting in a decreased *RANKL/Opg* ratio.

***Conclusions*:** These results suggest that only immediate implant loading can enhance bone-to-implant contact. On the other hand, immediate and conventional loading seem not to manifestly influence the cellular response of peri-implants tissues, although molecular adaptations are clearly present and different between immediate and conventional loading.

Key words: bone; mechanical loading; rat; titanium implant; vascularization.

3.1 Introduction

Bone is a metabolically active tissue capable of adapting its mass, shape and structure to the mechanical environment. Consequently, bone can repair the (micro)damage caused by loading through the process of remodelling (Ozcivici *et al*., 2010a). Inversely, an anabolic mechanical environment can result in bone gain. The anabolic effect of mechanical loading also applies to bone around titanium implants (Duyck *et al*., 2006; Duyck *et al*., 2007; Isidor, 2006). Evidence has been provided that well-controlled mechanical loading can improve implant integration into the bone and can stimulate peri-implant bone formation (De Smet *et al*., 2005; Duyck *et al*., 2006; Duyck *et al*., 2007; Vandamme *et al*., 2007c; Vandamme *et al*., 2008).

Implant success requires direct apposition of bone to the implant surface, referred to as osseointegration. Long-term success rates of more than 90% have been reported for the conventional loading osseointegration protocol (Jemt *et al*., 2011). This prosthetic protocol adopts an implant healing time of 3 up to 6 months prior to functional loading by means of prosthesis. Today, a tendency towards early (within 6 weeks after implant placement) and immediate (within 7 days after implant surgery) implant loading is prevailing in the clinics offering a faster masticatory function and a better patient comfort. High success rates for the immediate loading protocol have been reported in animal experimental (Lee *et al*., 2009; Romanos *et al*., 2010) and in clinical studies (Esposito *et al*., 2009a; Mertens and Steveling, 2011). However, this has been evidenced exclusively for studies with well-defined situations, in selected patients and relatively short-term follow-up periods.

The rationale of the conventional loading protocol is based on earlier reports indicating that premature loading increases the risk of fibrous tissue encapsulation of the implants rather than forming direct bone apposition (Akagawa *et al*., 1986; Brunski *et al*., 1979). However, studies have pointed out that well-controlled immediate loading *per se* does not necessarily lead to fibrous tissue formation at the implant interface (Klinger *et al*., 2006; Szmukler-Moncler *et al*., 1998). More likely, surpassing a certain threshold of micromotion at the tissue-implant interface during the healing phase jeopardizes the bone repair around the implant (Duyck *et al*., 2006; Szmukler-Moncler *et al*., 1998).

Thorough insight in the tissue response to implant loading during and after osseointegration is still limited although required to scientifically support the clinical shift from conventional to early or immediate loading protocols. Acquiring knowledge on the implant's optimal biomechanical environment promoting osseointegration is useful, as this would contribute to optimize implant prognosis in case of immediate and early loading protocols.

The aim of the present rat study was to define the peri-implant tissue response to immediate and conventional implant loading at tissue, cellular and molecular level. The study hypothesis was twofold: (i) controlled implant loading accelerates osseointegration, and (ii) the peri-implant tissue response to loading depends on the timing of load application (immediate or conventional). Unraveling the specific peri-implant tissue response relative to the load-timing regime could be of considerable importance for clinical implant rehabilitation protocols.

3.2 Experimental design

3.2.1 Animals, implants and surgical procedure

130 male Wistar rats were used in the present study. The animals were randomly distributed over 10 experimental groups, depending on the loading protocol (immediate loading; conventional loading) and on the duration of the experiment (4, 7, 14, 21 and 28 days) (Table 3.1). Cylindrical screw-shaped implants (Ø: 2 mm × L: 10 mm) were custom-made from titanium rods (99.6%, Goodfellow Cambridge Ltd., Huntingdon, England). The implants were etched with HF (4%) and HNO_3 (20%), ultrasonically cleaned with distilled water, and sterilized prior to surgery. The surface treatment resulted in an average Ra-value of 0.45 µm and an Sdr value of 1%, as determined by scanning white-light interferometry (Wyko NT 3300; Veeco Metrology Inc., Tucson, AZ, USA). Implants were placed in the mesio-proximal part of both tibiae. Surgery was described in 2.1.1.

Table 3.1 *Overview of the different loading experiments and type(s) of analyses performed*

		Duration of loading (days)				
		4	7	14	21	28
Loading	Immediate (n)	10	10+5	10	10	10+10
	Conventional (n)	10	10+5	10	10	10+10
Analysis	BIC					x
	BA - VA	x	x	x	x	x
	C.Ar/T.Ar – B. Ar/T.Ar	x	x	x	x	x
	Gene expressions		x			

n, number of animals; BIC, bone-to-implant contact; BA, bone area; VA, blood vessel area; C.Ar/T.Ar, callus area/tissue area; B.Ar/C.Ar, bone area/callus area.

3.2.2 Mechanical loading

The loading procedure was similar to previously described protocols (De Smet *et al*., 2005; De Smet *et al*., 2006; Slaets *et al*., 2009). In brief, a sinusoidally varying bending moment was applied with a force-controlled electro-mechanical shaker (Model 4810, Bruel and Kjaer, Naerum, Denmark) through a lever connected onto the upper part of implant. The horizontal lever was screw-retained onto the implant and positioned in alignment with the long axis of the tibia. During loading, the tibia was firmly fixed by an alginate casting to the base plate of the stimulator to ensure reproducible mechanical loading. For each animal, one hind limb was randomly selected to harbor the implant that was loaded (= test). The implant at the contralateral tibia served as internal unloaded implant (= control).

Two loading regimes were defined. For the immediate loading protocol, the loading started the day following surgery. For the conventional loading regime, a healing time of 28 days prior to loading was respected. The same loading protocol was used for both regimes, *i.e*. 1800 load cycles of 1 Newton, inducing a deformation of about 1500 με at the cortical surface adjacent to the implant, at a frequency of 3 Hz for 5 days per week. The loading was applied for 4, 7, 14, 21 or 28 days, corresponding to 5

experimental groups for each loading regime. The loading parameters applied were chosen based on previous *ex vivo* strain gauge measurements and experimental findings of our group, indicating the osteogenic potential of these parameters (De Smet *et al*., 2005; De Smet *et al*., 2006; Slaets *et al*., 2009).

3.2.3 Processing and analysis of implant-bone samples

Different sample processing methods were applied, depending on the type of the analysis that was aimed for (Table 3.1).

3.2.3.1 Tissue and cellular analysis

3.2.3.1.1 Sample processing

Tissue and cellular analyses were performed on either resin-embedded (refer to 2.2.1.1) or paraffin-embedded sections (see 2.2.1.2).

Undecalcified resin-embedded sections containing implant and peri-implant tissue were stained (see 2.2.2.2) and used for assessment of implant osseointegration (see 2.3.2.1).

Paraffin-embedded sections were used to investigate the bone formation, remodelling and vascularization of the peri-implant tissues, as well as the callus formation in the endosteal and bone marrow region. Tibia specimens were fixed in 2% paraformaldehyde immediately after sacrifice. The bone segments were decalcified in 0.5M EDTA (pH 7.4)/PBS at 4°C and paraffin-embedded, whereupon the implants were gently unscrewed. Next, the samples were re-embedded by paraffin and 5-µm sections were made (HM360; Microm, Walldorf, Germany) parallel to the long axis of the long bone and of the implant. The central sections were selected for staining with hematoxyline eosine to investigate the general morphology (refer to 2.2.2.1). The vessel endothelial cells were visualized by CD31 immunohistochemical staining (refer to 2.2.3).

3.2.3.1.2 Quantitative assessment

Quantitative assessments were performed under light microscopy (Leica Laborlux, Wetzlar, Germany) and a high sensitivity video camera (AxioCam MRc5, Zeiss,

Göttingen, Germany). As the sections were made along the long axis of the tibia and the implant, histomorphometric analyses were carried out on both proximal and distal sides of the implant. To assess osseointegration, peri-implant bone formation, vascularization and callus formation, the following parameters were measured using image-analysis software (Axiovision 4.0, Zeiss, Göttingen, Germany):

At the implant interface

Bone-to-implant contact (BIC, %) was performed exclusively on the samples of the 28-days loading experiment (refer to 2.3.2.1) (See Table 3.1).

In the V-thread areas of the implant

Two measurements were performed on the tissue spikes residing in the V-thread areas of the implant: bone area and vessel area.

The bone area (BA, %), representing the percentage of bone occupying the V-thread regions located in the bone marrow, was scored (refer to 2.3.1.1 and Figure 2.1A). The mean BA was calculated for on average 12 regions per sample.

The blood vessel area (VA, %) represents the area of blood vessels visualized by CD31 immunostaining. VA was evaluated in 3 regions on both sides of the sample (refer to 2.3.1.2, Figure 2.1B and Figure 2.1C).

In the peri-implant endosteal and marrow region

In the peri-implant endosteal and marrow region, the size and the bone content of the formed callus were quantified (refer to 2.3.1.3 and Figure 2.1C).

3.2.3.2 Molecular analysis

Sample collection and analysis were carried out by use of real-time PCR protocol to spot both bone formation- and resorption-related gene expression (refer to 2.4).

3.3 Results

Histological observations

Qualitative histological analysis at consecutive time points revealed that in general a similar pattern of bone repair was observed in the test (loaded) and control (unloaded) implants, but those differences in responses were noticed between the immediate and conventional loading regimes. For the immediate loading regime, both new bone formation as well as bone remodelling was perceived. At the peri-implant cortex, bone

apposition from the host bone towards the implant as well as bone remodelling was observed at all experimental time points. In the peri-implant medullar region, woven bone was observed, originating from the endosteum and extending along the implant surface. Over time, this newly-formed bone was remodelled into denser, lamellar bone. For the conventional loading regime, mainly bone remodelling, rather than new bone formation, was observed. In the peri-implant cortex, signs of remodelling were noticed but without obvious changes of the cortical bone adjacent to the implant. In the peri-implant medullar region, dense bone was noticed in close contact with the implant and was found to remain stable over time.

Histomorphometry

Implant osseointegration

Bone-to-implant contact, indicating the degree of implant osseointegration, was measured in the 28-days loading experimental groups (see Table 3.1). Compared to the unloaded control, an increased BIC was induced by immediate loading (77.67% ± 2.17% *vs.* 65.71% ±3.49%, test *vs.* control, $p < 0.05$), while no significant effect on BIC was observed in the conventional loading implants (75.91% ± 6.71% *vs.* 76.1% ± 5.67%, test *vs.* control, $p > 0.05$).

Bone formation and vascularization of the implant V-thread areas

Loading had no manifest effect on the bone formation (BA) in either the immediate or conventional loading regime. However, BA significantly evolved over time ($p<0.01$) in the unloaded as well as loaded conditions. In the immediate loading regime, the BA score consecutively increased from day 4 to day 28 ($p<0.01$). In the conventional loading regime, on the other hand, higher BA scores were observed on day 21 and 28, compared to day 4 and 7 ($p<0.01$).

The vascularization of the tissues (VA) was found to be unaffected by immediate or conventional loading in the 3 defined V-thread areas. A significant change in the vascularization over time was detected in both loading regimens, but only at the 1st V-thread tissue beneath the cortex (VA2) ($p<0.01$): in the immediate loading regime, VA increased from day 4 and reached its peak on day 7, and then gradually decreased till day 28 (Figure 3.1 A); in the conventional loading regime, VA remained stable over all

observation time points except on day 28 when a slight increase was noticed, compared to day 7, 14 and 21 (p<0.01) (Figure 3.1 B).

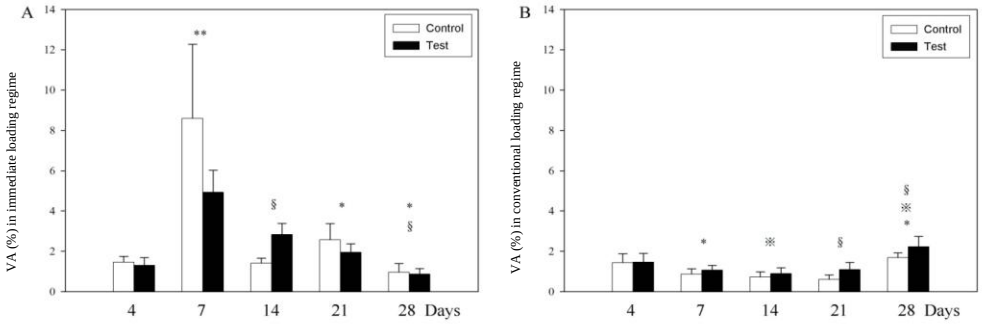

Figure 3.1 *Blood vessel area (VA, %) in the 1st V-thread area beneath the cortex. Identical symbols refer to a significant difference between these time points regardless of loaded or unloaded (p<0.05, ANOVA). The double sign (**) indicates the significant peak of VA on day 7 compared to all other time points (p<0.01, ANOVA and post-hoc Tukey's test).*

Callus and bone formation in the peri-implant endosteal and bone marrow region

No loading effect on the size of the callus (C.Ar/T.Ar) and its bone content (B.Ar/C.Ar) was found in either the immediate or conventional loading regime. An increase of C.Ar/T.Ar over time was only observed after 28 days in the immediate loading regime, which was significantly different from 21 days (Figure 3.2 A). However, a constant increase in the amount of bone matrix in the callus (B.Ar/C.Ar) was clearly noticed in case of immediate regime (Figure 3.2 B) from 4 to 28 days. These temporal changes in C.Ar/T.Ar and B.Ar/C.Ar were not detected in the conventional loading regime.

Gene expressions in the peri-implant cortical bone tissue

Molecular assessment of the peri-implant bone response to loading was performed for the 7-days experiments (see Table 3.1). The average RNA yield was 53.95 (±4.94) µg per explants. Immediate loading significantly upregulated *Runx2* expression, with a 2.3-fold change (p<0.01) (Figure 3.3 A). No differences in the expression of the other bone formation markers, neither of the bone resorption markers was observed.

Similarly, conventional loading resulted in an increase of *Runx2* (4.3-fold; $p<0.01$). Additionally, a 22.3-fold upregulation of *Opg* ($p < 0.05$) (Figure 3.3 B) and an accompanying striking decrease of the *RANKL/Opg* ratio in response to conventional loading was found ($p<0.01$) (Figure 3.4).

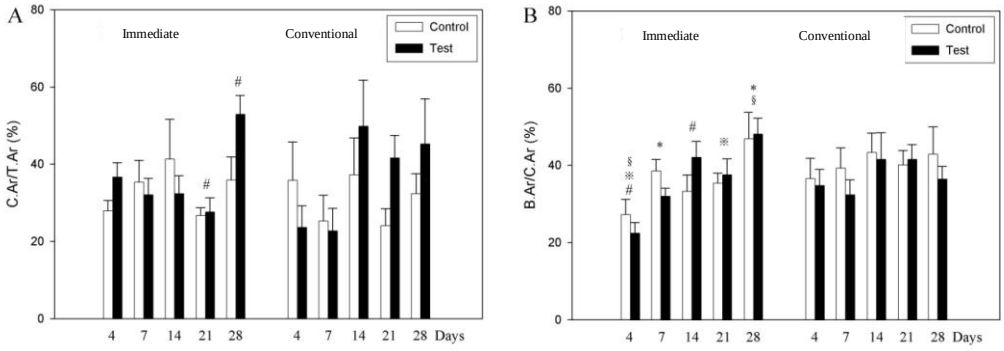

Figure 3.2 *Callus formation (C.Ar/T.Ar; %) and bone content (B.Ar/C.Ar; %) in the peri-implant endosteal and bone marrow region. Identical symbols refer to a significant difference over time (p<0.01, ANOVA and post-hoc Tukey's test).*

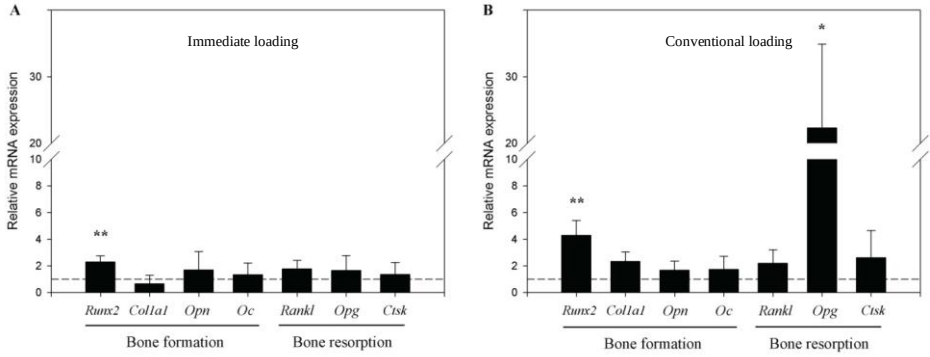

Figure 3.3 *Gene expression in the peri-implant cortical bone in response to immediate (A) and conventional (B) loading for 7 days (dotted line: normalized control; *p<0.05, **p<0.01, compared to the normalized control, ANOVA).*

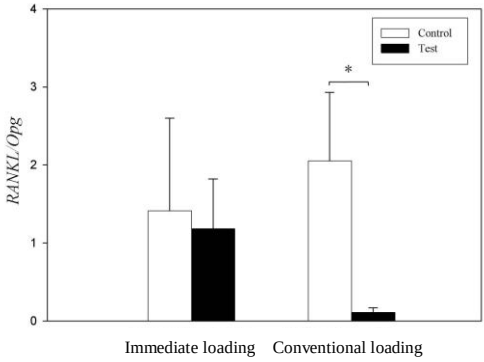

Figure 3.4 *The ratio of RANKL/Opg expression in the peri-implant cortical bone in response to 7 days immediate and conventional loading (*p<0.05, ANOVA).*

3.4 Discussion

The peri-implant tissue response to well-controlled immediate and conventional loading was investigated. It was hypothesized that (i) controlled implant loading accelerates osseointegration, and that (ii) the type and extent of the peri-implant tissue response to loading depends on the timing of load application (immediate or conventional). The formulated hypotheses are only partly confirmed: controlled implant loading does stimulate osseointegration but exclusively when applied immediately after implantation. However, neither immediate nor conventional loading was found to induce significant tissue and cellular changes in the peri-implant region during the experimental period. In contrast, the molecular analysis of the peri-implant cortical bone revealed a different upregulation of osteoblast/osteoclast-related genes for the two loading protocols after loading for 7 days.

Histological observations and histomorphometrical analyses revealed the temporal peri-implant tissue characteristics at early (< 28 days, *i.e*. immediate loading regime) and late (>28 days, *i.e*. conventional loading regime) post-implantation stage. At the early stage, bone (re)modelling occurred in the peri-implant cortical region. Concurrently, woven bone was formed in the peri-implant bone marrow *via* intramembranous healing (Leonard *et al*., 2009; Vignoletti *et al*., 2009). Originating from the endosteum of the peri-implant cortex, this newly formed bone is considered to be an inherent response of early healing in the long bone (Eriksson *et al*., 2007). At the late stage, the cortical bone in the peri-implant region, as well as the dense lamellar bone in close contact with the implant in the bone marrow region, was hardly modified

over time. This finding reflects a rather stable peri-implant bone tissue at this stage of healing.

Controlled immediate loading - opposite to conventional loading - was found to enhance implant osseointegration. Immediate loading for 28 days resulted in a significant increase in BIC compared to the unloaded control, which is in line with previous findings from our group (De Smet *et al*., 2005; Duyck *et al*., 2006; Duyck *et al*., 2007; Vandamme *et al*., 2007c; Vandamme *et al*., 2008). Also, the absence of an effect of conventional loading on implant osseointegration corroborates available data (Sasaki *et al*., 2008; Wiskott *et al*., 2008). In contrast, Kim *et al*. (Kim *et al*., 2008) reported an enhanced BIC by conventional loading (with a load-free healing time for 3 months) compared to immediate loading. As no unloaded group was included as internal control in their study, the BIC difference between the two groups may be explained by the difference of healing time. In the present study, the implants that were immediately loaded for 28 days obtained a similar degree of osseointegration (BIC: 77.67% ± 2.17%) as the implants that received conventional loading for 28 days (75.91% ± 6.71%) or that were left to heal for 56 days (76.1% ± 5.67%). In this respect, the immediate loading accelerates implant osseointegration, although BIC data of immediate and conventional loading at earlier time points (*e.g*. 7, 14 or 21 days) are lacking. This study limitation excludes to assess the impact of immediate loading on the onset and extent of osseointegration (BIC).

Regarding the bone density of the tissue spikes residing in the V-thread areas of the implant, no significant loading effect was observed for the two loading regimes. Only the bone area change over time was confirmed. An increase in bone area over time after implant surgery was also observed in previous rabbit studies, representing the healing dynamics of the host tissue in response to implantation (Slaets *et al*., 2006; 2007). On the other hand, some evidence of increased peri-implant bone density induced by conventional loading is available (Wiskott *et al*., 2008), indicating that the formed peri-implant bone can be triggered to adapt to an altered biomechanical challenge. The discrepancy between this report and our results is likely due to the

applied loading protocol and the experimental period (*e.g.* loading magnitude stepwise up to 100 N and loading duration up to 14 weeks in the referred study).

Peri-implant tissue vascularization is crucial to both peri-implant bone modelling and remodelling (Marco *et al.*, 2005). Increased peri-implant vessel density can be found in the inflammatory stage of both physiological (*e.g.* implant healing) (Marco *et al.*, 2005) and pathological (*e.g.* peri-implantitis) conditions (Cornelini *et al.*, 2001). According to the results of the present study, the peri-implant vascularization increases and reaches its maximum 7 days after implantation (*i.e.* in the immediate regime). At the later stage after implantation (*i.e.* in the conventional regime), the peri-implant vascular density remains constant for most of the time. With reference to mathematical models and *in vivo* experiments, Geris *et al.* (Geris *et al.*, 2010) suggested a consistent effect of immediate loading on improving angiogenesis in the peri-implant tissues. However, according to our data, both immediate and conventional loading failed to induce significant changes in blood vessel area. A likely explanation is that the effect of loading on tissue vascularization is overruled by the healing response. Another explanation may be linked to the complexity of the vessel growth around implants and the variables that influence the vessel growth. A mesh-like appearance of a very intricate vessel network around implants was observed after loading for 1 year (Traini *et al.*, 2006). The growth and distribution of peri-implant blood vessels was proposed to form and comply themselves into their environments. The environments include multiple variables (*e.g.* implant placement, loading, and host bone characteristics) that can either alone or in association influence the vascularization and its distribution (Traini *et al.*, 2006). Nevertheless, more research on understanding angiogenesis and the vascular structure in peri-implant tissues is needed.

Around all implants, endosteal callus formation was observed. However, neither immediate nor conventional loading was found to influence the size and bone content of the callus, when compared to the unloaded implants. An increase of the callus bone content was observed from 4 to 28 days, but this was no longer seen at later time points. Other than our findings, an enlarged endosteal callus induced by immediate loading was found in a rabbit study; whereas the bone composition of the callus was

not affected (Slaets *et al*., 2009). These contradictory results are probably due to differences in animal model and reference area selection. Compared to rodents, the rabbit displays faster skeletal adaptation and bone turnover (Pearce *et al*., 2007) and these characteristics may contribute to a different bone response to loading. In addition, a rather large reference area (2500 µm distance from the implant surface) was used in the rabbit model, whereas a smaller region was chosen in the current study (1500 µm). The latter resulted in higher endosteal callus values for both loaded and unloaded implants. The callus tissue farther away from the implant was excluded from the present selection area, but these tissues may be particular prone to loading as it is a less mature tissue with larger surfaces exposed to mechanical influences (Carter *et al*., 1998). Hence the loading-mediated increase in endosteal callus, as reported by Slaets *et al*. (Slaets *et al*., 2009), could not be confirmed here.

In vitro and *in vivo* studies support the notion that the mechanical environment affects gene expression of the cells adjacent to implants (Kokkinos *et al*., 2009; Vandamme *et al*., 2011). The results of the current study demonstrated that immediate implant loading upregulated *Runx2*, a key regulator of osteoblastogenesis (Datta *et al*., 2008). Likewise, conventional implant loading promoted *Runx2* expression, with an additional upregulation of *Opg* (anti-osteoclastic marker) and a depressed *RANKL/Opg*. Bone remodelling is tightly controlled by *RANKL* and *Opg* and the ratio of *RANKL/Opg* is considered as the best marker to reflect the effect on bone resorption. (Boyce and Xing, 2008). It has been demonstrated that excessive micromotion at the bone-implant-interface – a key determinant in biological implant failure – can promote *RANKL* and inhibit *Opg*, thereby inducing an accelerated peri-implant bone resorption, even as early as 1 hour after the applied micromotion (Stadelmann *et al*., 2008). Other than excessive micromotion, the mechanical loading exerted onto the implant in the present study displayed a beneficial effect at the molecular level. Moreover, this anabolic potential was found to depend on the timing of application (*i.e*. immediate or conventional loading).

In conclusion, controlled, moderate loading does not restrain the establishment nor the maintenance of implant osseointegration, and the peri-implant tissue remodelling. An

enhanced osseointegration can be expected when loading is initiated immediately after insertion. The finding that bone (re)modelling and vascularization in the peri-implant tissues was unaffected by both loading regimes suggests a strict localized effect of the controlled moderate implant loading. However, the observed gene expression changes in the tissues in the implant's vicinity in response to loading support the need for further exploration of the mechanisms underlying implant mechanobiology.

Acknowledgements: The authors acknowledge N. Smets and K. Moermans (Laboratory of Experimental Medicine and Endocrinology, KU Leuven) for their guidance on molecular biology and histology. Sincere gratitude is expressed to D. Lin (Leuven Biostatistics and Statistical Bioinformatics Centre, KU Leuven). This work was supported by the Research Council KU Leuven (OT/07/059) and by the Research Foundation - Flanders (G.0500.08 and G.0982.11 to FWO). The authors declare no potential conflicts of interest with respect to the authorship and/or publication of this article.

Chapter 4
The effect of whole body vibration on peri-implant bone healing

This chapter is based on the publications:

"Ogawa T., **Zhang X.**, Naert I., Vermaelen P., Deroose C.M., Sasaki K., Duyck J. The effect of whole body vibration on peri-implant bone healing in rats. ***Clinical Oral Implants Research*** 2011 Mar;22(3):302-7."

"Ogawa T., Possemiers T., **Zhang X.**, Naert I., Chaudhari A., Sasaki K., Duyck J. Influence of loading time on the impact of whole body vibration on peri-implant bone healing: a histomorphometrical study on rat. ***Journal of Clinical Periodontology*** 2011 Feb;38(2):180-5."

"Ogawa T., Vandamme K., **Zhang X.**, Naert I., Possemiers T., Chaudhari A., Sasaki K., Duyck J. Stimulation of titanium implant osseointegration through high frequency vibration loading is enhanced when applied at high acceleration. ***Calcified Tissue International*** 2014 Nov;95(5):467-75."

The principal investigator of the above publications is Dr. Toru Ogawa. The contribution of the PhD candidate to this chapter is to design and perform the experiments, and to prepare the manuscripts.

4.1 Introduction

In this chapter, the beneficial effect of immediate controlled high-frequency mechanical loading, *via* whole body vibration (WBV), on peri-implant bone and bone-to-implant contact was tested in 3 series of rat experiments. The null hypotheses to be tested are, (1) the immediate high-frequency loading has a positive effect on the peri-implant bone and bone-to-implant contact and (2) that loading frequency, duration and acceleration (magnitude) are determining factors.

Study 4.1 serves as an exploratory study to investigate whether or not WBV has a stimulatory effect by use of a step-wise frequency band from 12 to 150 Hz with a constant acceleration of 0.3 g.

Study 4.2 describes a successive experiment to assess the effect of loading duration and sequence of WBV on peri-implant bone healing and osseointegration. It was hypothesized that the osteogenic response increases with increasing load duration and with the inclusion of a rest period.

Study 4.3 deals with a study to explore the optimal combination of frequency and acceleration parameters of WBV in stimulating titanium implant osseointegration. It was hypothesized that (i) WBV loading is anabolic for titanium implant osseointegration, and that (ii) the most pronounced response of the peri-implant bone to WBV would be obtained for the loading regime with highest frequency and acceleration.

4.2 Experimental design

Animals and implants

Adult male Wistar rats received an implant in the proximal metaphysis of one of both tibia (Figure4.1 a and b). The protocol of implant surgery was described in 2.1.1. The custom-made cylindrical screw-type implants (Ø: 2 mm × L: 10 mm) were obtained from a titanium rod (99.6%, Goodfellow Cambridge Ltd., Huntingdon, England) (Figure4.1 a). The implants were ultrasonically cleaned, etched with HF (4%) and HNO3 (20%), yielding a Ra value of 0.45 mm, and sterilized before surgery.

Vibration device

A custom-made vibration device was used (Department of Mechanical Engineering, Division of Biomechanics. KU Leuven) (Figure4.1 c). As shown, the device can induce various loading conditions (Table 4.1).

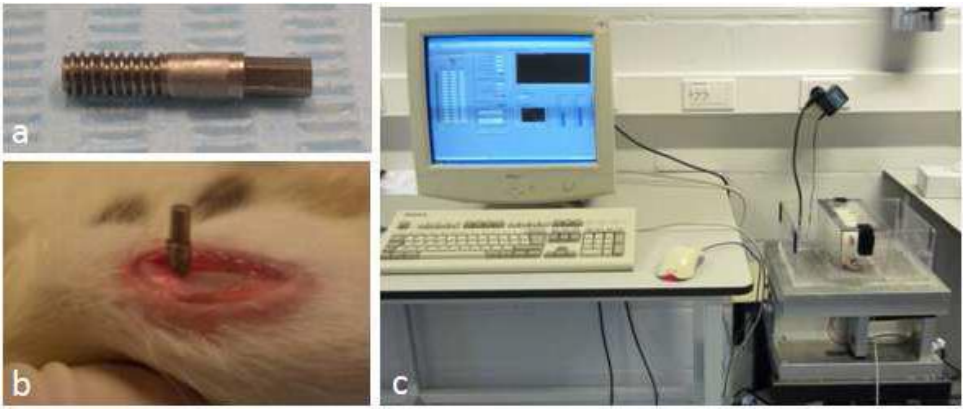

Figure 4.1 *(a) Custom-made cylindrical screw-shaped implants (Ø: 2 mm×L:10 mm) obtained from a titanium rod (99.6%, Goodfellow Cambridge Ltd., Huntingdon, England). (b) Implant was placed in the proximal metaphysis of tibia. (c) Custom-made vibration device (Department of Mechanical Engineering, Division of Biomechanics. KU Leuven)*

Specimen preparation and analysis

After sacrifice of the animals, the implants and their surrounding tissues were retrieved, processed into PMMA sections (refer to 2.2.1.2), stained (2.2.2.2) and analyzed histomorpgologically. The measurements of BF and BIC, as well as selection of the region of interest (ROI), have been described in Section 2.3.2.

Table 4.1 *Characteristics of the vibration device*

Specification	Value
Range of frequency	1-150 Hz
Range of accelerations	0.015-5 g
Tolerances	10%
Weight of the animal	Maximum 1 kg
Surface of the plate available for the animal	300×300 mm

PET imaging （For Study 4.1）

Small-animal PET imaging was performed using micro PET (Focus 220, Siemens Medical Solutions, Knoxville, TN, USA), which has a transaxial resolution of 1.35mm in full-width at halfmaximum (Figure 4.2). The images were taken 1 day before implant installation, as well as 3, 5, 7, 10, 14 and 21 days after implantation (Figure 4.2 b and c).

Rats were injected with approximately 18.5MBq of [^{18}F]sodium fluoride into a tail vein under 2.5% isoflurane gas anesthesia. To allow a reproducible positioning of the rats during scanning, the rats were secured on a fixation plate with four markers. Lower extremity images with a 15min acquisition time were obtained 80min after radioactive tracer injection. Data were acquired in a 128×128×95 matrix with a pixel size of 0.475 mm and a slice thickness of 0.796mm. PET scan images were reconstructed using both filtered back projection and a statistical maximum posteriori probability algorithm (MAP). The contralateral proximal tibial metaphysis was used as a reference site. Plain radiographs of the lower limb with the fixation plate including the markers were taken to identify the implant and the reference site (Figure 4.2 d).

PET data were analyzed and quantified using AMIDE (version 0.9.1, http://amide. sourceforge. net/index.html) (Loening and Gambhir, 2003). Regions of interest (ROIs) with an ellipsoid configuration (size: 5×3×3 mm) were defined around the implant and contralateral tibia within the same animal. The mean signal intensity (MBq/cc) was calculated using the AMIDE data analysis tool and converted to a standardized uptake value (SUV). Data were evaluated by two blinded observers. The uptake ratio (SUV implant ROI/SUV contralateral ROI) was compiled and analyzed at each time point.

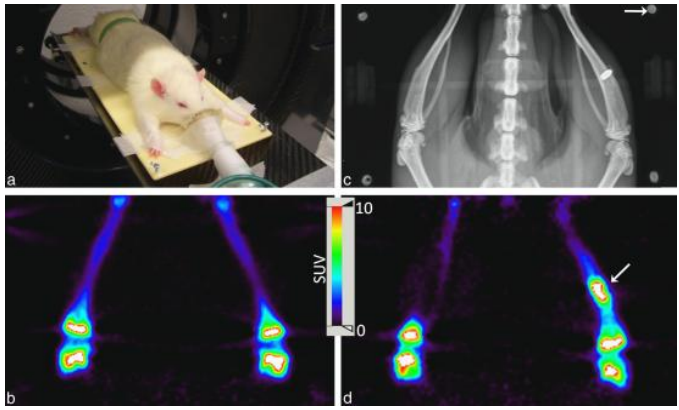

Figure 4.2 *(a) MicroPETscan session (Focus 220, Siemens Medical Solutions). Examples of positron emission tomography (PET) images taking (b) before the implant installation and (c) 7 days after implantation. The arrow indicates [^{18}F]fluoride accumulation around the implant. (d) Plain radiographs of the lower limb including four markers (arrow).*

Loading protocol

WBV started the next day post implant surgery.

(1) For Study 4.1, a daily WBV was applied on the test group from the day of surgery onwards. The WBV consisted of 15 consecutive frequency steps (12, 20, 30, 40, . . ., to 150 Hz). Each of these 15 frequencies was applied for 2000 cycles, at an acceleration of 0.3 g, for 5 days a week. The total WBV lasted 11min per day. The animal allocation according to loading protocol and experimental duration was showed in Table 4.2.

Table 4.2 *Animal allocation according to loading protocol and experimental duration (for Study 4.1)*

Experimental duration (days)	3	7	14	25
WBV (n)	5	5	5	7
Control (n)	5	5	5	5

(2) For Study 4.2, animals were randomly divided into two groups of different healing times. In one group (n=45 animals), the implants healed for 1 week, whereas the implants in the other group (n=50) healed for 4 weeks. Each group was subdivided into five groups with different loading times: a control group (no loading) and four test groups with 1.25, 2.5, 5 and twice 1.25 min (interval of 4 h) of loading. The vibration started the next day after surgery. The daily vibration consisted of 15 consecutive frequency steps (12, 20, 30, 40 . . . 150 Hz), applied in a randomized way, and all with a 0.3 g acceleration. Table 4.3 shows the loading scheme and animal allocation.

(3) For Study 4.3, animals were randomly divided into 2 groups with different experimental periods. In one group (n=60) the experiment lasted 1 week, while in the other group (n = 60), the experiment endured for 4 weeks. Each group was subdivided into 6 groups: one unloaded control group (C) and 5 WBV loaded groups. Attempting to cover a wide range of peri-implant bone reactions, specific combinations of frequency ranges (classified as 'low (F_L)', 'medium (F_M)' or 'high (F_H)') and accelerations (classified as 'low (A_L)', 'medium (A_M)' or 'high (A_H)') were applied. The following WBV loading regimes were defined: 12-30 Hz at 0.3g (F_LA_H); 70-90 Hz at 0.075g (F_MA_M); 70-90 Hz at 0.3g (F_MA_H); 130-150 Hz at 0.043g (F_HA_L); and130-150 Hz at 0.3g (F_HA_H) (Table 4.4). Each test group received 5 steps of loading. For example, for the animals of the group F_MA_H, WBV was applied at 70, 75, 80, 85 and 90 Hz loading in a randomized way for 1 minute per frequency (total loading duration of 5 minutes). Groups F_LA_H, F_MA_H and F_HA_H were loaded with the same loading acceleration but with varying loading frequencies. Groups F_MA_M and F_MA_H, as well as group F_HA_L and F_HA_H shared common loading frequency ranges but with varying loading accelerations. Vibration loading started the day following surgery ('immediate implant loading' as defined in the consensus report on the classification of loading protocols (Esposito *et al*. 2009) and was applied 5 days per week for either 1 week or 4 weeks.

Table 4.3 *Loading scheme and animal allocation (for Study 4.2)*

Group	Experimental Duration (week)	Loading time (min)	Frequency (Hz)	Acceleration (g)
Control	1 (n=9) 4 (n=10)	0	0	0
Test 1	1 (n=9) 4 (n=10)	5 20s per each frequency	12-150	0.3
Test 2	1 (n=9) 4 (n=10)	2.5 10s per each frequency	12-150	0.3
Test 3	1 (n=9) 4 (n=10)	1.25 5s per each frequency	12-150	0.3
Test 4	1 (n=9) 4 (n=10)	1.25×2 5s per each frequency	12-150	0.3

Table 4.4 *Frequency and acceleration parameters of the different loading regimes (for Study 4.3)*

	Frequency (Hz)		Acceleration (*g*)	
Group	Range	Classification	Value	Classification
C	-	-	-	-
F_L A_H	12-30	low	0.3	high
F_M A_M	70-90	med	0.075	med
F_M A_H	70-90	med	0.3	high
F_H A_L	130-150	high	0.043	low
F_H A_H	130-150	high	0.3	high

C, control; F, frequency; A, acceleration; L, low; M, medium; H, high

4.3 Results

4.3.1 Results of Study 4.1

One rat in the test group died 7 days after implantation. In the control group, one rat was excluded after 14 days because of skin infection at the implant site. All other 40 rats presented an uneventful implant healing.

Histological data from 7-day healed implants clearly showed an osteogenic reaction around the implants, particularly in the test group (Figure 4.3). After 25 days of healing, the peri-implant bone appeared to be denser (Figure 4.3).

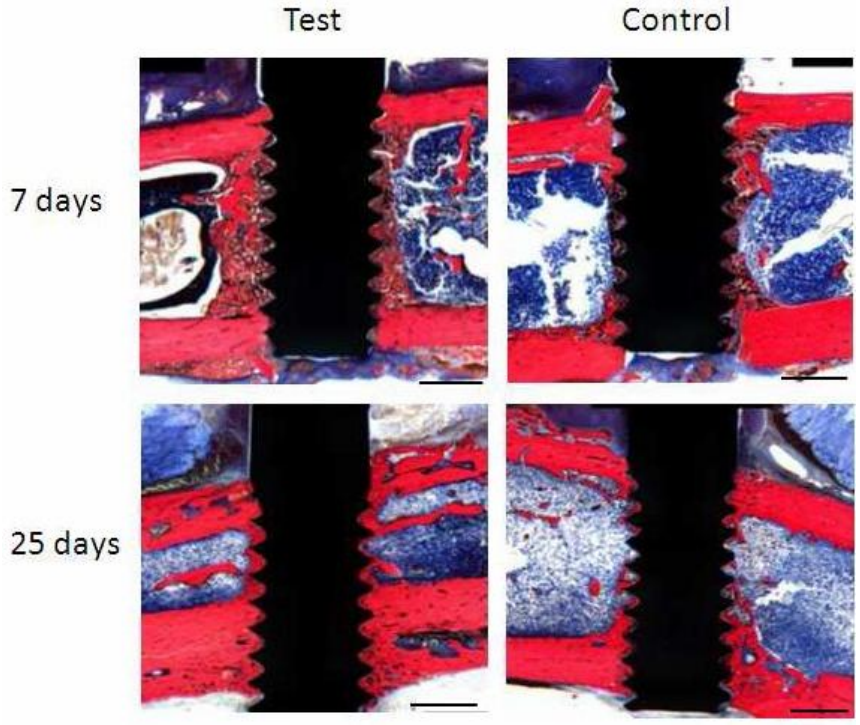

Figure 4.3 *Histological sections of the test and control group after 7 and 25 days of healing. Scale bars: 1mm.*

Histomorphometrically, BIC and BF (ROI 1 and ROI 2) were significantly influenced by the loading and the healing time ($p<0.01$, ANOVA), whereas BF (ROI 3) was only significantly influenced by the loading ($p<0.05$, ANOVA) (Figure 4.4).

The uptake ratio of [^{18}F]fluoride increased during the first week after implant insertion and then decreased gradually (Figure 4.5). This tendency was observed in both the test and the control groups. Although no significant difference was found between the test and the control groups, the healing time did have a significant effect ($p<0.001$, Friedman test).

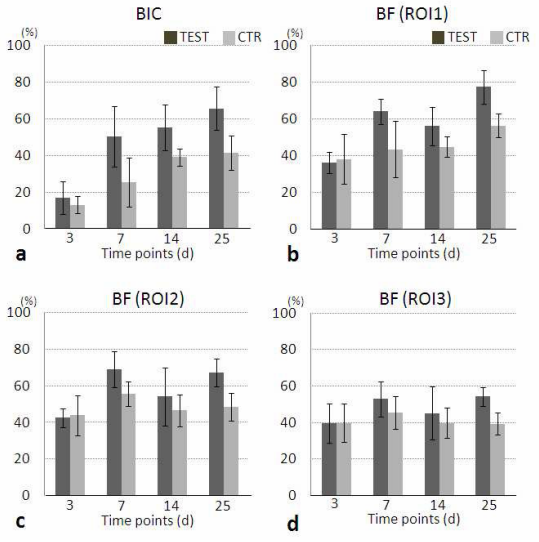

Figure 4.4 *Histomorphometrical results of the bone-to-implant contact (BIC) and peri-implant bone fraction (BF). The graphs show means and standard deviations of the BIC (a) and BF (b–d) for the different healing periods. BIC and BF (ROI 1 and ROI 2) were significantly influenced by the loading and the healing time ($p<0.01$, ANOVA). BF (ROI 3) was only significantly influenced by the loading ($p<0.05$, ANOVA).*

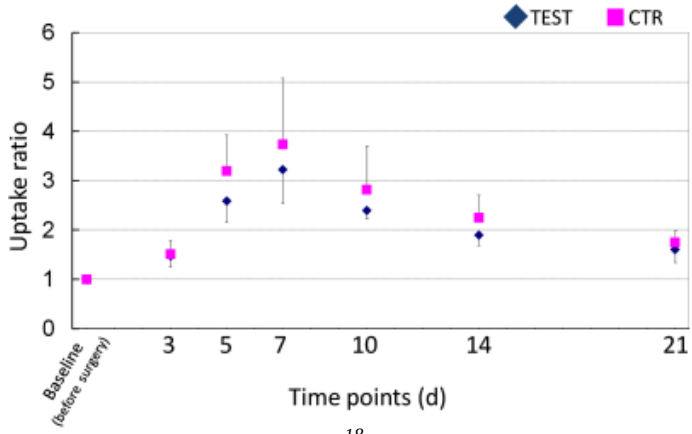

Figure 4.5 *Change in uptake ratio of [^{18}F]fluoride before and after the implant installation.*

4.3.2 Results of Study 4.2

In the 4-week healing period, three samples were excluded from histomorphometrical analyses because of skin infection or technical failure during sample processing.

Histological observations

Figure 4.6 shows a representative example of a loaded implant that was allowed to heal for 1 or 4 weeks. After 1 week of healing, a clear osteogenic response was observed. After 4 weeks of healing, the immature bone around the implant reorganized and became much denser.

BIC analysis

In Figure 4.7 a, BICs of the two healing periods are shown. BIC was significantly influenced by the loading time as well as by the healing period (ANOVA; $p<0.01$). A subsequent post hoc analysis indicated that the BIC of each test group was significantly higher than that of the control group in both the 1- and the 4-week healing periods (Tukey's HSD test; $p<0.05$ or $p<0.01$). Moreover, in the 4-week healing period, BIC was significantly higher in the twice 1.25 min loading group compared with the 1.25min loading group (Tukey's HSD test; $p<0.05$).

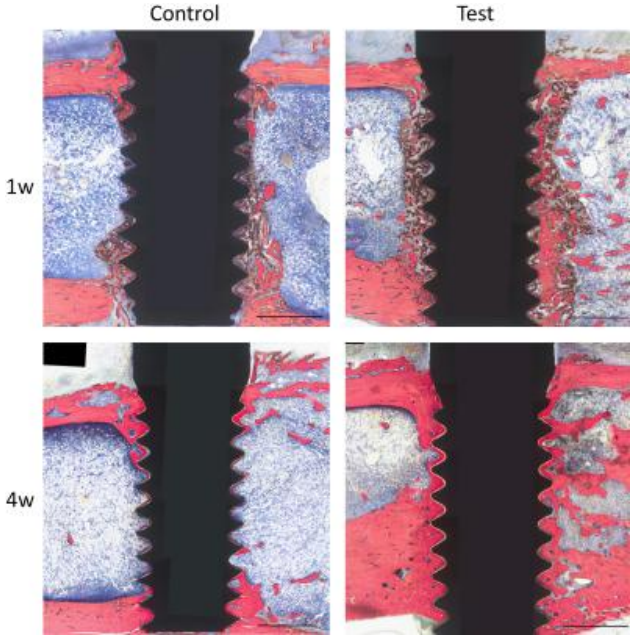

Figure 4.6 *Representative images of the test and control group from the 1-week healing period (a) and the 4-week healing period (b). Scale bars: 1 mm.*
BF analysis

BF at 0–100 μm (ROI 1)

Although no significant difference in BF was observed between the two healing periods (ANOVA; $p>0.05$), BF was significantly influenced by the loading time (ANOVA; $p<0.01$) (Figure 4.7 b). In the 1-week healing period, it was found that the test groups, except for the 2.5 min loading group, showed a significantly higher BF than the control group (Tukey's HSD test; $p<0.05$ or $p<0.01$). In the 4-week healing group, a significant difference was found between the control and the 5 min loading group (Tukey's HSD test; $p<0.05$) and also between the control and the twice 1.25 min loading group (Tukey's HSD test; $p<0.01$). Moreover, BF of the twice 1.25 min loading group was significantly higher than both of the 1.25 min and the 2.5 min loading groups (Tukey's HSD test; $p<0.05$).

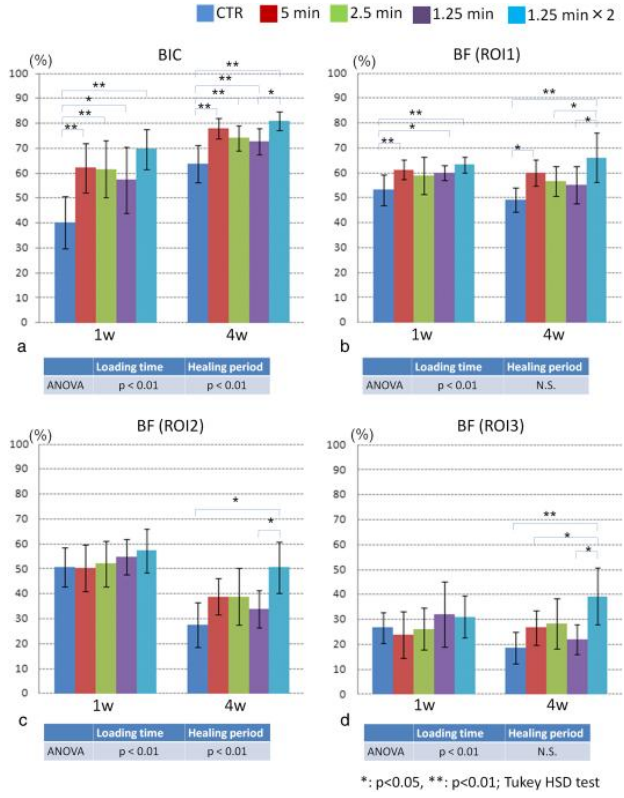

Figure 4.7 *Histomorphometrical results of the bone-to-implant contact (BIC) and bone fraction (BF). The graphs show the means and standard deviations of the BIC (a) and BF (b–d) for the different healing periods (Tukey's HSD test; *:p<0.05,**:p<0.01).*

BF at 100–500 μm (ROI 2)

BF (ROI 2) was significantly influenced by the loading time as well as by the healing period (ANOVA; $p<0.01$). In the 4-week healing period, a statistical difference between the twice 1.25 min loading group and the control group, as well as between the twice 1.25 min and the 1.25 min loading group, was found (Tukey's HSD test; $p<0.05$) (Figure 4.7 c).

BF at 500–1000 μm (ROI 3)

Although no statistical difference in BF was observed between the two healing periods, BF was significantly influenced by the loading time (ANOVA; $p<0.01$) (Figure 4.7 d).

For the 4-week healing period, the BF of the twice 1.25 min loading group is statistically higher than the control group and the other loading groups, except for the 2.5 min loading group (Tukey's HSD test; $p<0.05$ or $p<0.01$).

4.3.3 Results of Study 4.3

All but 1 implant healed uneventfully. The latter implant (unloaded, 1 week CTR-group) was excluded from the study.

Histological observations

A representative example of an unloaded *vs*. WBV loaded implant for 1 week and 4 weeks of loading is shown in Figure 4.8. An osteogenic response at the implant surface and in the implant vicinity could be observed histologically already 1 week after implant installation. At the cortical level, bone remodelling with necrotic bone remnants as well as newly formed bone trabeculae was seen. In the medullar region – a region devoid of bone tissue prior to implant installation – newly formed tissue was observed around the implant, consisting of fibrovascular stroma with bone trabeculae. The bone formation occurred exclusively *via* a primary repair sequence, without a cartilaginous intermediary. In unloaded conditions, the amount of newly formed bone along the implant surface decreased with increasing distance from the cortex. This reflects the process of appositional bone growth, originating from the endosteal cortical trabeculae. This was observed in particular at the distal side, the side without native metaphyseal bone trabeculae. Owing to the osteoconductivity of a titanium

implant, the peri-implant bone growth extended further towards the middle of the implant. In case of WBV loading however, it was observed that the width of the peri-implant bone collar along the entire implant length was more uniform, suggesting that other (*i.e*. progenitor cells) than resident bone cells, in response to mechanical stimulation, contributed to the bone formation. Indirect implant loading through whole body vibration for 1 week resulted in a non-site-dependent anabolic bone response at the medullar level.

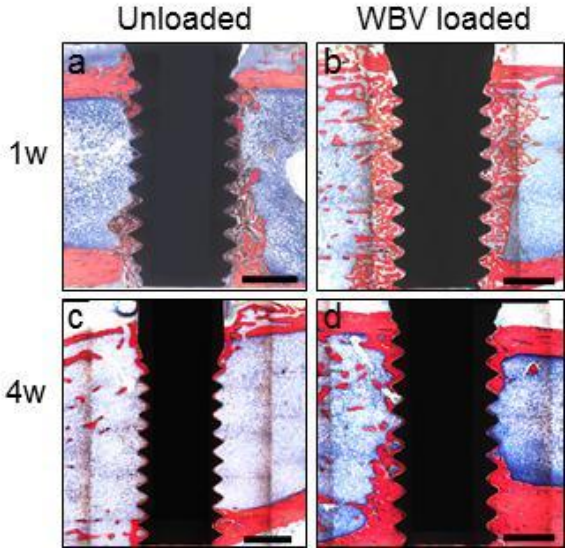

Figure 4.8 *Representative image of unloaded and WBV loaded implants from the 1-week and the 4-week experimental period. Scale bar: 1 mm. Bone formation took place adjacent to the implant in the medulla after 1 week of healing for both unloaded (a) and loaded (b) implants. Reorganization of the newly formed peri-implant bone, indicative for bone remodelling, led to dense bone adjacent to both unloaded (c) and WBV loaded (d) implants.*

After 4 weeks of unloaded or loaded healing, irrespective of the applied WBV loading regime, the newly formed bone had matured and was reorganized into lamellar, *i.e*. an orderly deposition of the collagen fibers as observed by microscopy, bone tissue. At the same time, less cuboidal-shaped osteoblasts were noticed in both the cortical and medullar region, indicative for a restricted bone formation activity. Furthermore, the amount of the lamellar bone deposited onto the implant surface was found to be

dependent on the loading protocol. In the absence of loading, a thin bone 'shell' of uniform thickness along the entire implant was observed. In contrast, in response to WBV loading, a striking increase in the width of the peri-implant bone could be discerned: a thick bone 'collar' around the implant was formed, starting from both the medial and lateral cortex and almost connecting.

Histomorphometrical analysis

Bone-to-implant contact (BIC)

BIC was significantly influenced by HF-LM loading as well as by the duration of the loading period, without interaction between the factors (ANOVA; $p < 0.0001$) (Table 4.5). BIC increased over time (Figure 4.9). Post-hoc analysis exploring differences in BIC between the different loading regimes revealed that BIC in each WBV loaded group was significantly higher compared to the unloaded group (Tukey HSD test; $p < 0.0001$). Furthermore, the loading regimes at medium and high frequency combined with a high acceleration protocol (F_MA_H and F_HA_H) resulted in the highest BIC values, which were significantly different from BIC values obtained after WBV stimulation at low frequency high acceleration (F_LA_H) and at medium frequency with medium acceleration (F_MA_M) (Tukey HSD test; $p < 0.02$ and $p < 0.005$ respectively) (Figure 4.9).

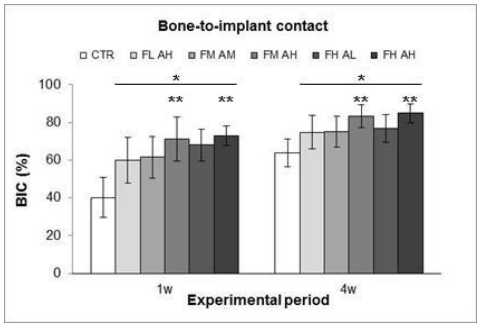

Figure 4.9 *Histomorphometrical results of BIC. Means and standard deviations for the 2 experimental terms and for the different loading conditions are shown. * Significant different versus control group (CTR); ** Significant different versus F_LA_H and F_MA_M (Post-hoc Tukey HSD test).*

Peri-implant bone formation (BF)

The peri-implant bone formation reaction to WBV HF-LM loading was significantly influenced by the duration of the loading term, with a decrease over time (ANOVA; $p < 0.0001$). Furthermore, BF was significantly influenced by WBV loading, but solely in the region closest to the implant surface (BF_ROI_1) (ANOVA; $p < 0.001$) (Table 4.5). No interaction was found between the duration and the loading mode factors. In contrast to BIC where an overall significant increase was found between WBV loaded and unloaded implants, post-hoc analyses revealed selected increases for the peri-implant BF in response to WBV loading (Tukey HSD test; $p < 0.02$ for F_LA_H and F_HA_M, and $p < 0.001$ for F_MA_H and F_HA_H) (Figure 4.10). No significant differences for BF_ROI_1 were found between F_MA_M loaded and unloaded control implants. Moreover, likewise the BIC results, the highest BF responses were found for the loading regimes at medium and high frequency combined with a high acceleration protocol (F_MA_H and F_HA_H). These differed significantly from the results of the F_MA_M loading protocol (Tukey HSD test; $p < 0.005$ and $p < 0.001$ respectively) (Figure 4.10).

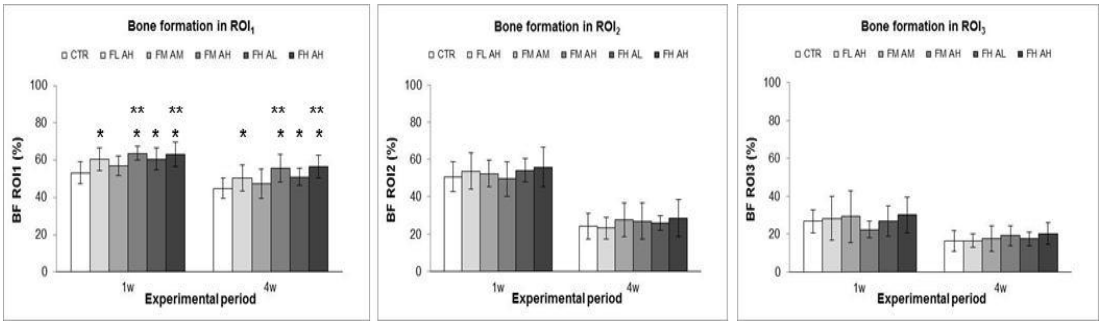

Figure 4.10 *Histomorphometrical results of BF for the 3 regions of interest (a to c). Means and standard deviations for the 2 experimental terms and for the different loading conditions are shown. An asterisk denotes a statistically significant difference relative to the unloaded group (CTR).A double asterisk denotes a statistically significant difference relative to the F_MA_M (Post-hoc Tukey HSD test).*

Table 4.5 *ANOVA results of the effect of the independent variables (i.e. the duration of the experimental period, of the loading mode and their interaction) on the dependent variables (i.e. BIC and BF)*

	Duration	Loading_Mode	Duration*Loading_Mode
BIC	$p < 0.0001$	$p < 0.0001$	$p = 0.190$
BF_ROI_1	$p < 0.0001$	$p < 0.001$	$p = 0.962$
BF_ROI_2	$p < 0.0001$	$p = 0.519$	$p = 0.753$
BF_ROI_3	$p < 0.0001$	$p = 0.555$	$p = 0.524$

4.4 Discussion

4.4.1 Discussion on Study 4.1

An explorative investigation was firstly performed to assess the potential effect of HF-LM loading, *via* WBV, on peri-implant bone healing and implant osseointegration. The main hypothesis, stating that HF-LM loading has a positive effect on peri-implant bone healing and implant osseointegration, is confirmed by the histomorphometrical results.

A comparable study evaluated the vibration effect on peri-implant bone in ovariectomized rats after a 14-day healing period by means of microCT (Akca *et al*., 2007). The results inferred that HF-LM loading remarkably enhanced bone volume density and trabecular number around titanium implants compared with the controls. Also in bone defect healing, a positive effect of HF-LM loading was reported (Omar *et al*., 2008). This suggests that HF-LM loading has the potential to positively affect peri-implant bone healing and osseointegration, which was in line with the findings of the current research.

To evaluate the effect of the HF-LM loading in relation to the presence of the implant, three different peri-implant sites were defined in this study. Whereas both vibration loading and healing time appeared to have a significant effect on the BF in ROI 1 and ROI 2, only the vibration effect was significant in ROI 3. This might reflect the effect of the loading stimulation to bone, independent of the peri-implant bone healing. Although significant loading effects were found in all reference sites, the loading effect seems to fade along with the distance from the implant, as indicated by the F-value of

the loading effect (ROI 1: 16.5, ROI 2: 10.2, ROI 3: 5.2, ANOVA). The higher this F-value, the more distinct the loading effect. These findings suggest that HF-LM loading had an accelerating effect on the peri-implant bone healing exceeding the pure osteogenic stimulus to the mature bone.

This study also validated the potential of PET imaging with [^{18}F]fluoride to evaluate bone metabolism changes due to implant installation and WBV. The uptake of [^{18}F]fluoride is proportional to the degree of active bone remineralization during homeostatic bone turnover. Implant installation caused a significant increase in bone metabolic activity around the implant. This uptake around the implants increased until 7 days after implantation and gradually decreased thereafter, which is in line with previous studies (McCracken *et al*., 2001; Sasaki *et al*., 2008).

The uptake ratio around the implant relative to a control region in the contralateral region was calculated for the test (loaded) animals as well as for the control (unloaded) animals. As the whole body of the test animals was subjected to the HF-LM loading, the contralateral control region was also subjected to this stimulation. In the control animals, neither the peri-implant nor the contralateral bone was loaded. The uptake ratio therefore reflects the impact of implant installation on the bone metabolic activity rather than the effect of the loading. This is the major reason for the lack of difference in the uptake ratio between the test and the control animals.

There was, however, a tendency towards higher uptake ratios in the control animals compared with the test animals. This implies that the relative importance of implant installation on the bone metabolic activity was the highest in the absence of loading. For the test animals, the WBV loading seemed to minimize the dominant impact of implant installation on the bone metabolic activity.

4.4.2 Discussion on Study 4.2

Based on the first study, which found a positive effect of the HF-LM loading on peri-implant bone (Ogawa *et al*. 2010), here we further investigated the influence of time factors on the impact of the HF-LM loading on peri-implant bone. It was hypothesized that these time factors do play a role on peri-implant bone healing and osseointegration.

To test our hypothesis, the loading group was subdivided into four groups with different loading durations and with or without a recovery period. The overall results of the post hoc analysis (Tukey's HSD test) clearly showed that the twice 1.25 min loading group exhibited the most pronounced stimulating effect on BIC and BF in all three ROIs after 4 weeks of healing. The positive influence of the twice 1.25 min loading can be explained by the inclusion of a rest period between two loading sessions per day. Robling *et al*. (Robling *et al*., 2000; Robling *et al*., 2002) already indicated the beneficial effect of such rest periods on loading induced bone formation. They found that division of a given bout of loading cycles into several loading sessions could lead to an increase of the bone response to the mechanical intervention. This rest period seems to allow an optimal recovery of the cell's mechanosensitivity, which was believed to decrease along with loading due to bone cells possessing the ability to accommodate their physical and biological environment (Turner, 1999). As proposed by Robling *et al*. (Robling *et al*., 2000), the loss of mechanical sensitivity, and subsequent resensitization following a load free recovery period, is mediated in part by the actin cytoskeleton in bone cells.

Not just the insertion of a rest period but also the duration of this rest period is important for the positive effect on BIC and BF. This rest period was 4 h in the current study. Some researchers investigated the optimal recovery period of mechanosensitivity in more detail (Robling *et al*., 2001a; Umemura *et al*., 2002). Robling *et al*. (Robling *et al*., 2001a) reported that a rest period as short as 10 s after each loading cycle within a bout can transform an otherwise ineffective loading regime into a highly osteogenic stimulus. Furthermore, it was shown that a rest period of 4 h presented a significantly improved osteogenic effect than the no-rest group (Robling *et al*., 2001a). This positive effect of the 4 h rest-time between loading sessions on the loading-induced bone response might offer a reasonable explanation for the findings in our study.

Regarding the loading duration, no significant differences were observed among the 5, 2.5 and 1.25 min loading groups. Nevertheless, several studies (Rubin and Lanyon, 1984; Turner *et al*., 1994; Umemura *et al*., 1997) indicated that the prolonged duration

of loading could significantly increase the bone formation rate and the bone mineral content. However, it was also reported that after a certain threshold, saturation occurs and results in a plateau (Burr *et al*., 2002; Turner *et al*., 1994; Umemura *et al*., 1997). This might be an explanation for the lack of a significant difference among the 5, 2.5 and 1.25 min loading groups.

Interestingly, the results of the current as well as our previous study (Ogawa *et al*., 2011b) reveal that the loading effect seems to be more distinct in the area closest to the implant (BIC and BF of ROI 1). There are three possible reasons to explain for this. The first is that differentiating tissues react better to loading than non-differentiating tissues in a condition such as bone healing (Goodship *et al*., 2009; Omar *et al*., 2008; Shi *et al*., 2010). As the differentiating tissues are mainly located at the interface, the loading effect is supposed to be more distinct in the neighboring region. Secondly, there could be an additional loading-related influence on peri-implant bone healing and osseointegration because of the interface between the titanium implant and its surrounding bone. Because of the different material properties of titanium and bone, these materials will behave differently to the loading, thereby creating a certain mechanical environment at the interface, which is likely to differ from the rest of the bone (Duyck *et al*., 2007; Vandamme *et al*., 2007b). This particular mechanical situation might be responsible for a different kind of cell triggering and deposition of, *e.g*. ions such as calcium and phosphate ions (Ho & Melbin, 2005), which may also contribute to faster osseointegration. Finally, there is the combination of the two previously mentioned reasons. However, these mentioned possibilities need further investigation.

Clear differences were observed between the results after 1 *versus* 4 weeks. BIC was significantly higher after 4 weeks of healing. This observation can probably be explained by the process of osseointegration. After 1 week, BIC can be established by bone apposition from the surrounding bone in those implant regions that were initially not in direct contact with the bone. In the areas where the bone was in direct contact with the implant, a process of bone resorption needs to precede the bone apposition (Botticelli *et al*., 2003; Botticelli *et al*., 2005). This implies that there is a phase of

decreasing BIC before the implant becomes biologically integrated. After 1 week of healing, considerable woven bone formation is observed in the medullar area. After 4 weeks, this newly formed bone decreased in volume and has rearranged into denser and better organized bone, often in contact with the implant.

As mentioned before, besides time factors, there are many more loading parameters such as magnitude or frequency that affect the loading effect. These factors, as well as their interaction, should be investigated in order to establish an optimal bone-stimulating loading regime to enhance peri-implant bone healing and osseointegration.

4.4.3 Discussion on Study 4.3

An attempt to further analyze the role of particular vibration parameters on the bone response around integrating titanium implants, the third study was performed. The provided evidence that the extent of the bone reaction to WBV depends on the characteristics of the composing parameters (Rubin & McLeod 1994; Oxlund *et al*. 2003; Judex *et al*. 2007; Hwang *et al*. 2009) was anticipated for the implant osseointegration setting in the present study. More in particular, the constituting parameters (*i.e*. 'frequency' and 'acceleration') on the bone tissue kinetic response around titanium implants were under investigation. Frequencies of 12-30 Hz, 70-90 Hz and 130-150 Hz, and accelerations of 0.043*g*, 0.075*g* and 0.3*g* were applied. It was hypothesized that (i) WBV has an anabolic effect on implant osseointegration and that (ii) the loading regime with the highest frequency and acceleration results in the most pronounced constructive peri-implant bone reaction.

Mechanical loading plays a pivotal role in bone homeostasis. Bone's sensitivity to mechanical demands in the negative and positive direction is illustrated by disuse and exercise studies respectively (Vico *et al*. 2000, Kontulainen *et al*. 2003). At the same time, it is well known that bone has a constant level of activity, aiming to keep bone tissue strains at an optimal level by altering bone structure designated as remodelling (Frost 2004). In response to injury or biomaterial installation, bone healing (modeling) precedes the bone remodelling. The response to the trauma of inserting a screw in the tibial bone was on the one hand cortical bone remodelling, and on the other hand medullar trauma-induced membranous bone formation with subsequent remodelling.

The new bone formation is important for the strength of screw fixation, and increased bone formation at early stages in the incorporation process may provide a better long-term prognosis (Ryd *et al*. 1995). The findings revealed that the least marked bone apposition onto the implant (quantified by 'bone-to-implant contact') was recorded when the rats were normal weight bearing (unloaded group), resulting in a retarded and a depreciated implant osseointegration compared to all tested loading regimes. Furthermore, an impressive anabolic medullar bone response to whole body vibration loading in the implants' vicinity (measured as 'peri-implant bone formation') was observed, reflecting that this peri-implant modeling- and remodelling-based bone formation is noticeable influenced by vibration loading. These findings confirm the amply provided evidence for an enhanced implant osseointegration through mechanical loading (Duyck *et al*. 2006; De Smet *et al*. 2006; Leucht *et al*. 2007), and the corroborating evidence for the positive effect of HF-LM loading on titanium implant osseointegration (Akca *et al*. 2007, Chen *et al*. 2011, Ogawa *et al*. 2011a, Ogawa *et al*. 2011b). The 1st hypothesis – *i.e.* WBV loading is anabolic for titanium implant osseointegration – was herewith sustained.

Analogous to the findings of the pilot experiments of the authors' group (Ogawa *et al*. 2011b, Ogawa *et al*. 2011a), a significant decrease in peri-implant bone formation with increased time lapse was noted. Furthermore, the amount of medullar callus tissue declined with extending distance from the implant surface. These findings illustrate the progressive stages of ossification of the repair tissue which was formed by the osteoprogenitor cells in the marrow, the endosteal surface and the adjacent trabeculae (Xu *et al*. 2009), in interplay with the osteoconductive property of titanium (Le Guehennec *et al*. 2007). Finally, differences between loaded and unloaded samples in this medullar bone formation were observed. Absence of stimulation resulted in the removal of the newly formed bone in this area and maximal reestablishment of the medullary canal, whereas loading preserved the bone. As these loading-related differences were significant for the reference area closest to the implant surface (ROI_1), and not for the distant areas ROI_2 and ROI_3, it is suggested that the loading, although applied indirectly through whole body vibration – and not directly through direct implant loading – exerted its effect *via* the titanium implant and created site-specific

mechanical conditions. The local mechanical environment resulted in loading stimulus perception by differentiating interfacial tissues rather than by the established distant tissue.

In order to gain a better understanding into the contribution of the component(s) that control the bone response to HF-LM loading, efforts were made on deconstructing the dynamic loading cycle into its frequency and acceleration constituent elements. Frequencies and accelerations classified as low, medium or high were assigned and combined. It was observed that the loading mode with the highest acceleration (0.3*g*), combined with medium (70-90 Hz) or high (130-150 Hz) frequency (groups F_MA_H and F_HA_H respectively) resulted in significantly more bone apposition onto the implant (bone-to-implant contact) compared to the corresponding loading mode at low frequency (F_LA_H; 12-30 Hz at 0.3*g*) and to the medium frequency and acceleration protocol (F_MA_M; 70-90 Hz; 0.075*g*). These data establish bone's ability to discriminate between vibration frequencies when loading at high acceleration, and indicate that focusing on the loading bouts frequency and on the duration for a specific frequency is an attractive strategy for the optimization of WBV intervention in biomaterial integration. The F_MA_H and F_HA_H loading regimes were also the best performing in terms of formation of bone adjacent to the implant surface (bone formation in ROI_1), but solely significantly differing from F_MA_M. Our 2nd hypothesis – *i.e.* the loading regime with the highest frequency and acceleration will result in the most pronounced constructive peri-implant bone reaction – could only partly be confirmed: the loading regime at medium frequency - high acceleration is as potent as the F_HA_H protocol for enhancing titanium implant osseointegration.

The degree by which variations in the parameters defining a WBV intervention alter the efficacy of the low-level mechanical signals for the implant setting are now starting to become unraveled. However, the importance of the host bone characteristics, *i.e.* the quality and the related vascularization, has not been profoundly recognized in this context. It has been repeatedly shown that WBV can serve as an anabolic signal to a skeleton even upon the withdrawal of estrogen (Verschueren *et al*. 2004, Rubin *et al*. 2006, Akca *et al*. 2007, Judex *et al*. 2007, Sehmisch *et al*. 2009,Tezval *et al*. 2011). But

while interference of osteoporosis with the implant-tissue integration process has been evidenced (Ozawa *et al*. 2002, Vandamme *et al*. 2011), only 2 studies were published on the effect of HF-LM mechanical vibration on peri-implant bone volume in osteoporotic rats (Akca *et al*. 2007, Chen *et al*. 2011). Future studies probing the interdependence of WBV mechanical parameters and covering the host bone properties will provide important clues towards identification of the physical mechanisms by which WBV perturbs bone's cellular activity.

Several limitations of this study need to be addressed. We did not do any measurements to shed light on the mechanical fixation of screws, nor of the induced strain environment. This information, particularly at the initial phases of implant osseointegration, would be valuable for the interpretation and further optimization of HF-LM loading protocols. Furthermore, not all possible combinations of 'frequency' and 'acceleration' (L-M-H) for the 2 experimental periods (1w-4w) were investigated, thereby rendering the full exploration of their interaction effects in a 3-way ANOVA and consequently of their selective individual effects on the peri-implant bone incomplete. Finally, the evidence provided in the present and in previous studies on the positive effect of high-frequency loading on implant osseointegration is mainly derived from tissue level findings. Bone generation in peri-implant bone regeneration in response to mechanical loading needs to be further explored in terms of the implicated molecular regulatory mechanisms. Advanced gene and protein expression approaches may contribute towards an understanding of the mechanisms involved in bone mechanotransduction at the *in vivo* titanium bone-implant interface.

Acknowledgements: The authors highly acknowledge Dr. Siegfried Jaecques (KU Leuven) for his assistance in the development and production of the vibration device. This study was funded by the Research Council of the KU Leuven (Belgium) (OT07/059) and the Fund for Scientific Research Flanders (G.0726.09). We would like to thank Dr. H. van Lenthe for his scientific advice.

Chapter 5

In vivo assessment of the effect of controlled high- and low-frequency mechanical loading on peri-implant bone healing

This chapter is based on the publication "**Zhang X.**, Vandamme K., Torcasio A., Ogawa T., van Lenthe G.H., Naert I., Duyck J. *In vivo* assessment of the effect of controlled high- and low-frequency mechanical loading on peri-implant bone healing. ***Journal of the Royal Society Interface*** 2012 Jul 7;9(72):1697-704."

Abstract

***Objective*:** The aim of this study was to investigate the effect of controlled high- and low-frequency mechanical loading on peri-implant bone healing.

***Materials and methods*:** Custom-made titanium implants were inserted in both tibiae of 69 adult Wistar rats. For every animal, one implant was loaded by compression through the axis of tibia (test) while the other one was unloaded (control). The test implants were randomly distributed among 4 groups receiving different loading regimes which were determined by *ex vivo* calibration. Within the high- (HF, 40Hz) or low-frequency (LF, 2Hz) loading category, the magnitudes were chosen as low- and high-magnitude respectively (LM, HM), leading to constant strain rate amplitudes for the two frequency groups. This resulted in the 4 loading regimes: (i) high-frequency low-magnitude (HF-LM, 40Hz-0.5N); (ii) high-frequency high-magnitude (HF-HM, 40Hz-1N); (iii) low-frequency low-magnitude (LF-LM, 2Hz-10N); and (iv) low-frequency high-magnitude (LF-HM, 2Hz-20N) loading. Loading was performed 5 times per week and lasted for 1 or 4 weeks. Tissue samples were processed for histology and histomorphometry (bone-to-implant contact (BIC) and peri-implant bone fraction (BF)) at the cortical and medullar level. Data were analyzed statistically with ANOVA and paired *t*-tests with the significance level set at 0.05.

***Results*:** For the one-week experiments, an increased BF adjacent to the implant surface at the cortical level was exclusively induced by the LF-HM loading regime (2Hz-20N). Four weeks of loading resulted in a significant effect on BIC (and not on BF) in case of HF-LM loading (40Hz-0.5N) and LF-HM loading (2Hz-20N): BIC at the cortical level significantly increased under both loading regimes, whereas BIC at the medullar level was positively influenced only in case of HF-LM loading.

***Conclusions*:** Mechanical loading at both high- and low-frequency affects osseointegration and peri-implant bone fraction. Higher loading magnitudes (and accompanying elevated tissue strains) are required under low-frequency loading to provoke a positive peri-implant bone response, compared to high-frequency loading. A sustained period of loading at high-frequency is needed to result in an overall enhanced osseointegration.

Keywords: animal; implant; loading frequency; mechanobiology; osseointegration.

5.1 Introduction

In orthopedics and implant dentistry, a variety of strategies have been explored to achieve a solid and rapid osseointegration, which is required for early implant loading. Accordingly, the biological basis of such an objective is a controlled and fast peri-implant bone healing, which implies bone regeneration and remodelling. The mechanical environment plays an important role in bone (re)modelling by which the existing bone's mass, shape and structure is adapted to its mechanical challenge (Judex *et al.*, 2009; Ozcivici *et al.*, 2010a). In line with this general concept, the effect of mechanical loading on bone regeneration and remodelling also applies to bone around titanium implants (Duyck *et al.*, 2006; Duyck *et al.*, 2007; Isidor, 2006). Findings from *in vivo* studies have shown that well-controlled mechanical loading at low-frequency can improve bone formation at the implant surface and in the peri-implant region (Duyck *et al.*, 2006; Duyck *et al.*, 2007; Isidor, 2006; Vandamme *et al.*, 2007c; Vandamme *et al.*, 2008).

The interest in high-frequency mechanical loading – *i.e.* a frequency beyond the physiological frequency (~3 Hz of human mastication) – grows because an increasing number of studies indicate its stimulating effect on bone formation and fracture healing (Goodship *et al.*, 2009; Hwang *et al.*, 2009; Judex *et al.*, 2007; Omar *et al.*, 2008). Together with the findings of clinical studies (Gilsanz *et al.*, 2006; Judex *et al.*, 2009; Rubin *et al.*, 2004), the advantages of mechanical loading at high-frequency are believed to be safe and efficient. The latter refers to the evidence that high-frequency mechanical loading improves the bone's mechanical properties, thereby promoting its properties to withstand the physiological demands (Ozcivici *et al.*, 2010a). This makes high-frequency mechanical loading a potent non-pharmacological intervention for osteoporosis, fracture healing and beyond (Gilsanz *et al.*, 2006; Ozcivici *et al.*, 2010a; Rittweger *et al.*, 2010; Rubin *et al.*, 2004).

Several *in vivo* systems for applying high-frequency loading have been successfully used, such as whole body vibration (Hwang *et al.*, 2009; Judex *et al.*, 2007) and individual limb compressive loading (Christiansen *et al.*, 2009; De Souza *et al.*, 2005). Whole body vibration experiments have evidenced the beneficial effect of high-

frequency loading on bone (Goodship *et al.*, 2009; Hwang *et al.*, 2009; Judex *et al.*, 2007) and on titanium implant osseointegration (Akca *et al.*, 2007; Ogawa *et al.*, 2011b). On the other hand, the accessibility of local strain quantification and the feasibility of controlling the individual loading parameters render the compressive loading mode appropriate for performing a parametric study. However, the compressive loading model has not been tested for the peri-implant setting thus far. Moreover, the specific contribution of the individual loading parameters (magnitude, frequency, rate, duration of loading) on the resulting peri-implant bone tissue response to high-frequency loading remains partly unknown.

In an effort to further optimize mechanical loading protocols that enhance implant osseointegration, we tested the hypothesis that a high-frequency signal may be more effective in stimulating implant osseointegration than a low-frequency signal, and that the differential sensitivity is dependent on the induced loading magnitude. To do so, the peri-implant tissue response to mechanical loading at high- and low-frequency was assessed by means of the rat tibia compression model.

5.2 Experimental design

Animals and surgical procedure

Seventy-seven male Wistar rats were used in the present study. Eight of these rats were used for the determination of the loading protocol by means of *ex vivo* strain gauge measurements. The remaining 69 rats were used for the *in vivo* evaluation of peri-implant tissue response to loading.

Custom-made cylindrical screw type implants (ø: 2 mm × L: 8 mm) were obtained from titanium rods (99.6% Ti, Goodfellow Cambridge Ltd., Huntingdon, England) (Figure 5.1 a). The implants were ultrasonically cleaned with distilled H_2O and etched with a solution of HF (4%) and HNO_3 (20%), resulting in a roughness value Ra of 0.45 µm. Implants were sterilized prior to surgery. Implants were installed bi-laterally in the medioproximal site of tibia (refer to 2.1.1).

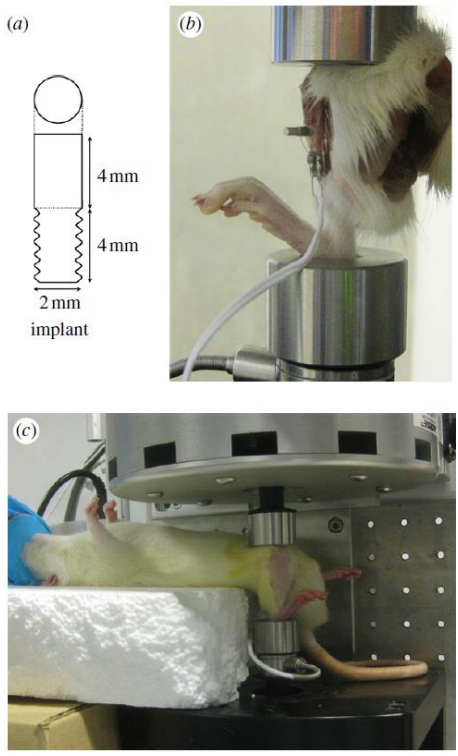

Figure 5.1 *Implant design, ex vivo calibration and in vivo loading are illustrated. (a) Commercially pure titanium custom-made screw-shaped implant (ISO M2 screw-thread protocol). (b) Ex vivo strain gauge measurements were performed on excised hind limbs in order to determine the relation between the applied loading force and the resulting strain in proximity of the implant. (c) An in vivo axial compressive loading was applied by two custom-made loading cups of a testing system (Bose TestBench LM1, EnduraTEC Systems Group, Bose Corp., Minnetonka, MN, USA).*

Quantification of peri-implant bone strains

Bone strains measured on 8 excised rat hind limbs before and after implant placement (Torcasio *et al*., 2011; Torcasio *et al*., 2012) were used to establish the relationship between the applied load and the resulting bone strain. In short, a single element strain gauge (type FLG-02-11, TML, Tokyo Sokki Kenkyujo Co., Ltd.) was glued onto the exposed lateral bone surfaces of the intact tibiae at 25 % of the tibia length. The limbs were placed in between 2 loading cups of a testing device (BOSE TestBench LM1,

EnduraTEC Systems Group, Bose Corp., Minnetonka, MN, USA) and strain was measured at compressive forces of 2.5, 5.0, 7.5 and 10 N, respectively, at a rate of 0.5 mm/sec. Measurements were performed five times after complete removal and repositioning of the limbs into the loading cups. The experiments were repeated on each specimen after the insertion of a titanium screw-shaped implant of 2 mm diameter 1.5 mm distal to the strain gauge site. Mean strain and standard deviation over the 5 repetitions were calculated for each limb before and after implant insertion.

In vivo mechanical loading

Rats were randomly allocated to 8 groups, corresponding to 4 different loading regimes and 2 experimental periods (Table 5.1). The 1-week and the 4-week loading groups were loaded consecutively. The loading regimes consisted of high-frequency (40 Hz; HF) and low-frequency (2 Hz; LF) protocols. Within each frequency category, the strain amplitude varied 2-fold (*i.e.* low- (LM) and high- (HM) magnitude, respectively). The combined loading frequency and magnitude resulted in identical strain rate amplitudes between the frequency categories (identical strain rate amplitudes for HF-LM and LF-LM, and for HF-HM and LF-HM). The test tibiae (= loaded) were held in loading cups and subjected to dynamic axial loads (Figure 5.1 c). Loading was initiated one day post implant installation. The load application took 10 minutes per session and was performed 5 times a week. The implant in the contralateral tibia served as unloaded control (= unloaded). Anesthesia induced by Isoflurane inhalation (Isoflurane USPR, Halocarbon, NJ, USA) was applied during the loading.

Table 5.1 *The applied loading regimes, the resulting strain and strain rate amplitudes in the peri-implant environment and the animal distribution.*

	loading regime		estimated strain and strain rate amplitude		group size (n)	
	frequency (Hz)	magnitude (N)	peak strain ($\mu\varepsilon$)	peak strain rate amplitude ($\mu\varepsilon\ s^{-1}$)	one week	four weeks
HF-LM	40	0.5	13	520	9	9
HF-HM	40	1	26	1040	8	8
LF-LM	2	10	260	520	9	9
LF-HM	2	20	520	1040	8	9

Specimen preparation and analysis

After sacrifice of the animals, the implants and their surrounding tissues were retrieved, processed into PMMA sections (refer to 2.2.1.2), stained (2.2.2.2) and analyzed (refer to 2.3.2)

5.3 Results

Animal and implant outcome

Implant surgery and *in vivo* mechanical loading were uneventful for both experimental periods. From a total of 138 implant samples, 5 samples were lost during histological processing (2 from the 1-week group and 3 from the 4-week group) and another 2 samples (from the 4-week group) were excluded due to peri-implant infection.

Quantification of peri-implant bone strains

Compressive loading of the rat limbs resulted in tensile strains on the medio-proximal surface of the tibiae. Over the range of load magnitudes applied, we found for each limb that the mean strains exhibited a linear relation to the applied loads both before and after implant insertion (R^2>0.99). Repeated measurements on each specimen showed high precision (intra-individual differences were as low to 6.45 % ± 2.27 % and 9.22 % ± 2.67 % for the intact and implanted tibiae, respectively). When compared to the measured strains in intact bone, the strains after implant placement were on average 35.3% lower.

As the experimental data were strongly affected by strain gauge placement, they could not be used directly for defining the desired strain rates. Instead they were used to validate established micro-finite element models, providing a three-dimensional quantification of the strain throughout the whole tibiae (Torcasio *et al*., 2011; Torcasio *et al*., 2012). We estimated maximum tensile strains at 25 % of the tibia length (hence corresponding to the strain gauge position and alignment) of ~260με for the implanted tibiae subjected to 10 N loading. These data were adopted to define the *in vivo* loading protocols by taking into account the linearity of the relationship applied loading - induced strain (1), a maximum loading force of 20 N (2) and assuming strain rate to be given by the product between strain magnitude and loading frequency (3); hence, we

estimated peak strains of 13, 26, 260 and 520 με to correspond to the HF-LM, HF-HM, LF-LM and LF-HM loading, respectively, and strain rates of 520 and 1040 με/s for the low-magnitude and high-magnitude loading regime, respectively (Table 5.1).

Histology

The histological images revealed bicortical bone apposition to the implant for both loaded and unloaded implants and for both healing periods (Figure 5.2). After 1 week, newly formed bone was observed along the implant surface in the medullar cavity, while active remodelling occurred at the cortex. After 4 weeks, the newly formed bone in the medulla was rearranged into denser and more homogeneous bone close to the implant surface. Furthermore, the healing of the peri-implant cortex was complete. No obvious differences between loaded and unloaded implants could be noticed on the histological sections.

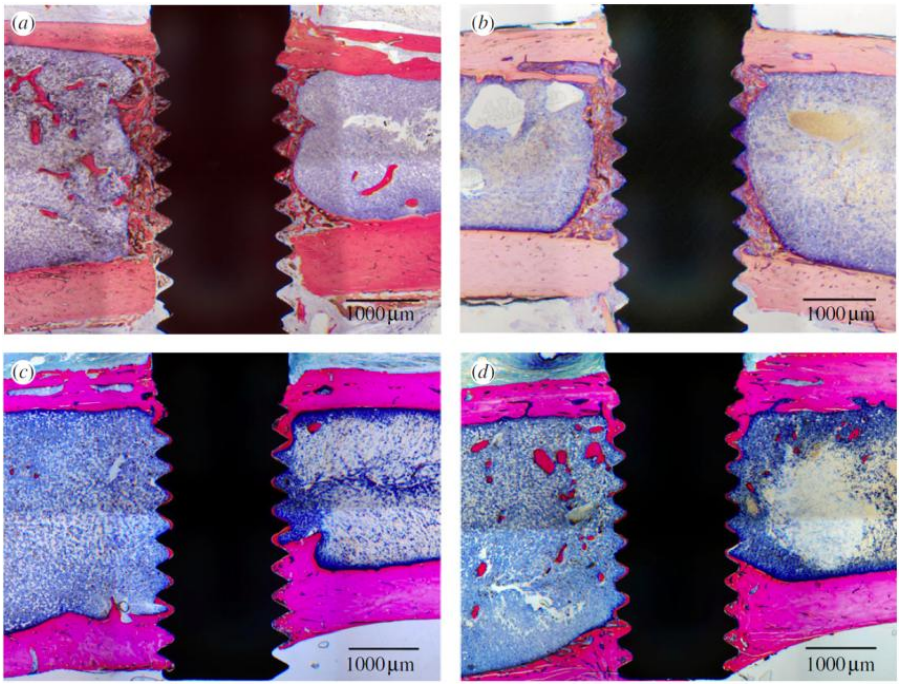

Figure 5.2 *Representative histological sections. Active osteogenesis was found adjacent to the implant in medulla after one week of healing for both (a) loaded and (b) unloaded implants. After four weeks of healing, remodelling of peri-implant bone led to denser medullar bone formation around both (c) loaded and (d) unloaded implants.*

Histomorphometry

BIC

In the peri-implant region of the cortex, 4 weeks of loading significantly increased BIC in case of HF-LM loading (40Hz-0.5N) and LF-HM loading (2Hz-20N) (79.8% ± 1.9% *vs*. 83.8% ± 1.3% and 78.6% ± 2.2% *vs*. 87.3% ± 1.1% respectively; unloaded *vs*. loaded; $p < 0.05$; two-way ANOVA followed by pairwise comparison) (Figure 5.3 a). In the medulla, a significant increase of BIC in response to loading was also found after 4 weeks of loading, but only in case of HF-LM loading (73.4% ± 4% *vs*. 79.1% ± 3.7%; unloaded *vs*. loaded; $p < 0.05$; two-way ANOVA followed by pairwise comparison) (Figure 5.3 b). No significant effect of the 4 loadings on BIC was found for the 1 week experiment.

Concerning BIC change over time, bone-implant contact at both cortex and medulla level significantly increased from 1 to 4 weeks for all loading regimes ($p < 0.01$; ANOVA).

BF

In the cortical peri-implant region, 1 week of loading significantly increased BF in ROI 1 in case of LF-HM (2Hz-20N) (36.2% ± 2.7% *vs*. 45.8% ± 3%; unloaded *vs*. loaded; $p < 0.05$; two-way ANOVA followed by pairwise comparison) (Figure 5.4). No effect of loading on BF, however, was identified either in the other ROIs or after 4 weeks of loading. In the medullar peri-implant region, no significantly different BF was detected between the unloaded and loaded implants of the 4 loading regimes.

In all assessed samples, peri-implant BF evolution over time (from 1 to 4 weeks of healing) was found to increase at the cortical level but to decrease at the medullar level ($p < 0.01$; ANOVA).

Similarly, with regard to BF relative to the distance to the implant surface, opposing results were found for the cortex and the medulla of all samples. At the cortex, the amount of bone was significantly lower in the region closest to the implant surface (ROI 1), compared to the other ROIs ($p < 0.01$; ANOVA followed by Tukey's HSD).

At the medulla, BF decreased with increasing distance from the implant surface (BF in ROI 1＞2＞3) (p＜0.01; ANOVA followed by Tukey's HSD).

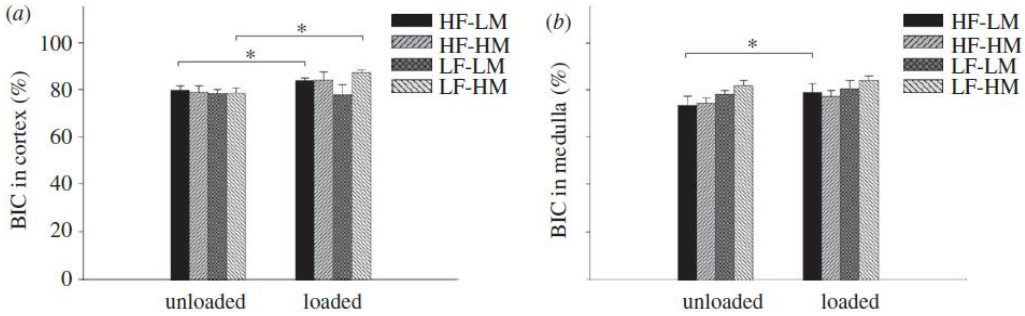

Figure 5.3 *Bone-to-implant contact (BIC) at (a) cortex and (b) medulla level for the four-week experiment. (Data from the one week experiment are not shown as no significant differences were observed; *: p<0.05; two-way ANOVA followed by pairwise comparison.)*

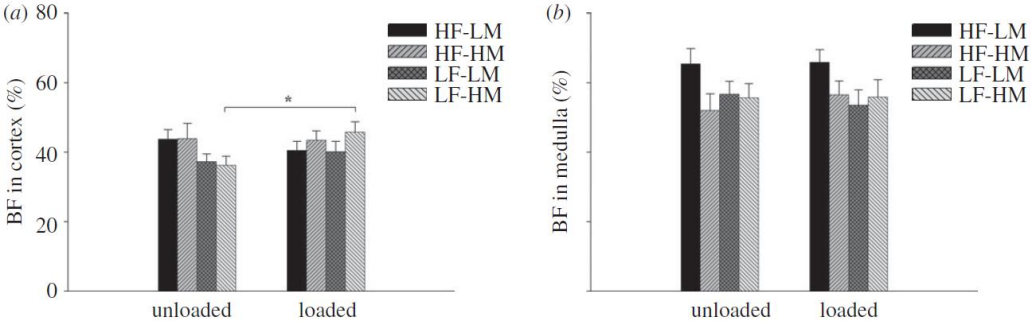

Figure 5.4 *Bone fraction (BF) for the region adjacent to the implant surface (ROI 1) at (a) cortical and (b) medullar level for the one-week experiment. (Data from the four-week experiment are not shown as no significant differences were observed; *: p<0.05; two-way ANOVA followed by pairwise comparison.)*

5.4 Discussion

In this study, different loading regimes were applied in order to evaluate the stimulatory effect of high- (*i.e.* 40 Hz) and low- (*i.e.* 2 Hz) frequency mechanical loading on implant osseointegration and peri-implant bone formation. In order to assess

additionally the influence of the loading magnitude, two loading forces varying by 2-fold within each frequency category were assigned.

According to Frost (Frost, 2004), loads on bones cause bone strains that generate signals detected by osteocytes and hence lead to cellular response and eventually to bone remodelling. The anabolic effect of loading on bone is evident when the bone strain induced by low-frequency loading goes beyond the 1000 με threshold (Frost, 2004). However, this does not apply to a high-frequency loading protocol, where low-magnitude events have been shown to be stimulatory to the bone (Ozcivici *et al*., 2010a). We intended to test whether the latter also applies to for peri-implant bone healing. With respect to the configuration limitations of the loading setup, 40 Hz and 2 Hz were selected as high- and low-frequency respectively. Specifically, the resonance of the loading system was observed during *ex vivo* tests when the loading frequency exceeded 50 Hz. To eliminate the systemic resonance which is harmful to the loading device and causes extra stimuli to the implant, the high-frequency regime was limited to 40 Hz. For both frequency categories, the magnitudes of loading were determined in such a way that identical strain rate amplitudes were obtained. In this way, the role of the strain rate amplitude – a determinant parameter of bone response to loading (LaMothe *et al*., 2005) – could be controlled. In a series of studies from our group (De Smet *et al*., 2006; De Smet *et al*., 2007; 2008), the amplitude of peri-implant strain favoring bone formation was found to be 250 to 1000 με at low-frequency (3 Hz) with strain rate amplitudes ranging from 267 to 1600με/s. In the present study, a strain of 260 and 520 με was induced when loading at low-frequency (2 Hz), resulting in strain rate amplitudes of 520 and 1040 με/s respectively. Accordingly, for the high-frequency loading (40 Hz), the estimated strain magnitudes of 13 and 26 με by loading would result in identical strain rate amplitudes. All loading categories could thus be considered lying within the range of positively influencing the peri-implant bone response.

Due to the advantages including the comparable bone remodelling rate to human (Baron *et al*., 1984), the accessibility for implant surgery and mechanical loading, the rat tibia was applied in the present research to study peri-implant bone healing.

Histological observations revealed a normal healing response after implantation, irrespective of the loading regime. These observations were corroborated by the histomorphometrical data: (1) Bone remodelling in the cortical peri-implant region led to an increased BIC and BF over time. Compared to the distant host bone, however, BF in the direct implant vicinity remained inferior, even after 4 weeks of healing. (2) In the peri-implant medullar area – an initial bone tissue-free region – massive woven bone was formed soon after implantation. The formed bone originated from the endosteum of the peri-implant cortex and grew along the implant surface. Subsequent remodelling of this newly formed bone led to less but denser bone, in close contact with the implant. With regard to the changes over time in this medullar region, implant osseointegration (as quantified by BIC) was found to increase from 1 to 4 weeks, whereas the bone volume in the vicinity of implant decreased for the same time period. This is in line with previous findings with the same animal model (Ogawa *et al*., 2011b).

The anabolic effects of high-frequency loading have been reported in several animal (Goodship *et al*., 2009; Hwang *et al*., 2009; Judex *et al*., 2007; Omar *et al*., 2008) and clinical trials (Gilsanz *et al*., 2006; Rittweger *et al*., 2010; Rubin *et al*., 2004). Hence it has been confirmed that bone can sense and respond to extremely small mechanical signals if they are applied at high-frequencies. Only a few studies investigated the effect of high-frequency loading on bone surrounding implants. Rubin & McLeod (Rubin and McLeod, 1994) investigated the effect of mechanical loading on bone growth into implants. Strains of 150 με were generated in the cortex immediately adjacent to the implant by means of host bone bending in the turkey ulna disuse model. The results showed that a 20-Hz loading regime induced the most favorable bone response, while the 1 Hz loading only prevented the bone resorption caused by disuse. Other studies on implants were performed using a rat tibia model in which high-frequency loading (12-100Hz, or 50Hz) was applied *via* whole body vibration. This loading was found to increase peri-implant bone formation in normal (Ogawa *et al*., 2011b) and in estrogen- deficient animals (Akca *et al*., 2007). In the current experimental setup, BIC, the criterion of osseointegration, was significantly increased in the peri-implant region in case of HF-LM loading (40Hz-0.5N). HF-HM loading (40Hz-1N), however, only showed a trend towards an increased BIC. These findings

agree with the notion that high-frequency mechanical loading can be osteogenic (Judex *et al*., 2007). However, this stimulatory effect may not require a high loading magnitude.

The effect of bio-physical stimulation at low-frequency loading (< 3Hz) on bone adaptation and regeneration has been well documented in rodent models using compressive loading (De Souza *et al*., 2005; Sugiyama *et al*., 2008; Tanaka *et al*., 2003; Warden and Turner, 2004), and implant healing set-ups (De Smet *et al*., 2006; De Smet *et al*., 2007; 2008; Leucht *et al*., 2007). Evidence is provided that, under low-frequency loading, bone is sensitive to the applied loading magnitude, with higher magnitude being more osteogenic (Cullen *et al*., 2001; Gross *et al*., 2002; Mosley *et al*., 1997). The findings of the low-frequency regimes applied in the current study demonstrated increased BIC and BF in the cortical bone solely when the load was applied at high magnitude (*i.e.* 20 N). Applying 10 N at 2 Hz did not influence the peri-implant healing response. Owing to the animal and technical restraints of the present study, the effect of higher loading forces (> 20 N) on the bone response could not be investigated. Despite these limitations, the findings suggest that the anabolic effect of low-frequency loading, which increases with increasing magnitude, also applies to peri-implant bone healing.

Although the osteogenic potential of high-frequency loading is evident, the peri-implant tissue response to the loading *via* different modes of application varies. Specifically, whole body vibration (WBV) seems to be superior to the localized loading. WBV has been found to extensively influence peri-implant bone remodelling and hence led to significant increases of BIC and BF (Akca *et al*., 2007; Ogawa *et al*., 2011a; Ogawa *et al*., 2011b). Compared to the control, more than 10% extra BIC was found in case of WBV after 4 weeks. This increase in BIC is almost 2-fold times the bone stimulating effect found with HF-LM loading. Moreover, the improved osseointegration by WBV can already be observed after 1 week of loading (Ogawa *et al*., 2011a). On the other hand, when the high-frequency loading was directly applied onto the implant, the loading failed to induce a pronounced peri-implant bone response (Zhang *et al*., 2012). The possible explanations for the superior stimulatory effect of

whole body vibration are (1) whole body vibration may lead to stochastic resonance of the applied vibrations, which could serve as an extra bone stimulus (Castillo *et al*., 2006; Tanaka *et al*., 2003); (2) the frequency span tested in whole body vibration is higher than the one used in the present study (up to 150 Hz *vs*. 40 Hz). As more efficient mechanotransduction goes along with increasing loading frequency (You *et al*., 2001), more osseous response could be associated with loading at higher frequency; (3) being no need of anesthesia during the application of whole body vibration, the side-effects and/or complications of daily usage of full anesthesia, which is performed on the animals in this compressive loading study, can be precluded; (4) the peri-implant strain distribution induced by different loading applications varies and inherently causes a different tissue response. However, measuring the exact strain the bone is exposed to *via* the whole body vibration set-up is difficult. Meanwhile, the strain measured in the present study corresponds to the bone surface level, thereby not exactly representing the strain at the bone-to-implant interface. Hence, for a better understanding of the biomechanical conditions with different experimental set-ups, further *in vitro* testing and numerical modelling is valuable.

In conclusion, mechanical loading at both high- and low- frequency can contribute to peri-implant bone healing. Higher loading magnitudes (and accompanying elevated tissue strains) are required under low-frequency loading to provoke a positive peri-implant bone response, compared to high-frequency loading. A sustained period of loading at high-frequency is needed to result in an overall enhanced osseointegration.

Acknowledgements: The authors declare no conflicts of interest. This study was supported by the Research Council of the KU Leuven (OT/07/059).

Chapter 6
Direct high-frequency stimulation of peri-implant rabbit bone: a pilot study.

This chapter is based on the publication "**Zhang X.**, Naert I., Van Schoonhoven D., Duyck J. Direct high-frequency stimulation of peri-implant rabbit bone: a pilot study. ***Clinical Implant Dentistry and Related Research*** 2012 August; 14(4):558-564."

Abstract

Objective: This study aimed to evaluate the effect of direct high-frequency mechanical stimulation on the peri-implant tissue healing.

Materials and methods: A total of 48 custom-made 2-mm diameter titanium implants were inserted in the tibial epiphyses of 12 rabbits. Half of the implants were stimulated by direct vibration (60±10 Hz) immediately after insertion for 1 and 4 weeks, respectively. The other half served as controls. The samples were collected after the animals were sacrificed and were histologically processed into paraffin sections and stained with haematoxylin and eosin. The bone fraction was measured in an area of 50 and 400 μm around the implant. To rate significant differences a one-way analysis of variance was used with a set at 5%.

Results: No significant difference in bone fraction was found between test and control groups. When the bone fractions of the 50 and 400 μm peri-implant regions were compared, a significantly larger bone fraction was found in the 50 μm peri-implant region for the 4-week stimulated group.

Conclusions: Histomorphometric analyses could not reveal a pronounced effect of direct immediate high-frequency implant loading.

Key words: high-frequency; implant; loading; rabbit.

6.1 Introduction

Bone is a metabolically active tissue capable of adapting its mass, shape, and structure to mechanical stimuli and repairing structural damage through the process of remodelling. The adaptation of bone in response to mechanical loading is considered to be a life-long process (Frost, 1992). It is clear that dynamic loading induces bone formation other than static loading (Hert *et al*., 1971; Robling *et al*., 2001b). Different *in vivo* studies support the notion that bone is sensitive to the applied strain rate (Judex and Zernicke, 2000; LaMothe *et al*., 2005; Mosley and Lanyon, 1998; Turner *et al*., 1995). Over the past decade, by use of different animal models, the high-frequency low-magnitude stimulation, also referred to as vibration, has been proven to actively stimulate osteogenesis and improve the skeleton quality (Torcasio *et al*., 2008). Most of the studies used an oscillating plate to induce whole body vibration as a stimulus.

For a long time it was assumed that mechanical loading during implant healing compromised peri-implant osteogenesis because of fibrous tissue formation, thereby impairing the osseointegration (Branemark *et al*., 1977; Branemark, 1983). Micromotion at the implant–bone interface in case of immediate implant loading can lead to inhibition of bone formation at the interface because it probably interferes with the development of adequate early scaffolding of the fibrin clot. This event might disrupt the reestablishment of a new vasculature to the healing tissue, which in turn interferes with the arrival of regenerative cells. Eventually, the healing process is rerouted into repair by collagenous scar tissue instead of bone regeneration (Brunski, 1999; Degidi and Piattelli, 2005). Ossification of regenerating tissue is only possible in case of a low hydrostatic strain environment and in the absence of shear strain (Carter *et al*., 1998). Whereas, high-peak strains impair bone mineral formation and osteogenic cell differentiation, physiologic bone loading (500-3,000 με) as such does not inhibit bone formation. Premature implant loading can promote early peri-implant osteogenesis in case of limited interfacial micromotion and an optimal biomechanical coupling between the implant and the surrounding tissues (Meyer *et al*., 2004; Piattelli *et al*., 1993; Romanos, 2004; Simmons *et al*., 1999; Simmons *et al*., 2001b). Such an optimal biomechanical coupling implies the transfer of compressive or tensile rather

than shear forces. Indeed, such loads on healing bone might even shorten the healing period (Vandamme *et al*., 2007c; Vandamme *et al*., 2008). As healing bone has lower mechanical properties compared with mature bone, equal loading will result in higher strains in immature bone. The load bearing capacity of healing bone is therefore less than mature mineralized bone. Both animal experiments (Duyck *et al*., 2005; Quinlan *et al*., 2005) and clinical studies (Attard and Zarb, 2005; Bischof *et al*., 2004; Degidi and Piattelli, 2005; Esposito *et al*., 2009a) have shown that immediately loaded oral implants acting as support for a prosthesis can osseointegrate provided that the forces and implant micro-motion are controlled (Buchter *et al*., 2005; Duyck *et al*., 2006; Vandamme *et al*., 2008).

Nowadays, there is a tendency to load implants immediately or soon after implantation. This limits the period of discomfort for the patients compared with the long healing times in the conventional loading protocol. As the treatment goes faster, it also offers psychosocial and economic benefits. The local mechanical loading situation is believed to be a strong determinant in the processes of tissue differentiation and bone formation/resorption around implants. Early/immediate loading might offer the potential to stimulate osteogenic effects during implant healing under specific conditions.

Considering the abundant evidence of the positive effect of high-frequency loading on both bone adaptation and regeneration in general (Judex *et al*., 2009), the idea of accelerating the osseointegration process and optimizing oral implant success through a therapeutically mechanical stimulation is tempting but not scientifically founded. This study therefore aims to evaluate the effect of high-frequency mechanical stimulation on the peri-implant tissue healing in the context of the optimization and acceleration of the osseointegration process.

6.2 Experimental design

Implants and Animals

Custom-made 2 mm diameter commercially pure titanium (grade 2, Goodfellow, Huntingdon, United Kingdom) implants were used (Figure 6.1). The screw design of the upper part allowed a solid connection with the vibration device (Figure 6.2).

Prior to surgery, the implants were cleaned ultrasonically, decontaminated by soaking in a 4% hydroxylfluoride (HF) buffered with a 20% HNO_3 solution for 30 seconds, and sterilized. By doing so, the implant surfaces were standardized into an average roughness (Sdr, %) of 1, which was determined by a scanning white-light interferometer (Wyko NT 3300; Veeco Metrology Inc., Tucson, AZ, USA). Twelve 6-month old female New Zealand white rabbits (body weight, 3.7 kg 1 0.5 kg) were selected for this experiment.

Surgery and Loading Protocol

Under general anesthesia (intravenous, Diprivan 1%, 0.4 ml/kg/h.; Astra Zeneca, Brussels, Belgium), a total of four implants were inserted in the two tibia epiphyses of each rabbit by two implant surgeries at 1 and 4 weeks before the sacrifice. During the first surgery, one implant was placed per leg. One of both implants received vibration stimulation; whereas, the other implant served as the unloaded control. After 3 weeks, a second implant was placed per leg. Again, one implant was loaded whereas the other one was not. After another week of healing, the animals were sacrificed with a 0.1 ml/kg intravenous injection of an embutramide, mebenzoniumiodide, and tetracaine hydrochloride solution (T61; Intervet, Mechelen, Belgium). By following this protocol, each rabbit contained a loaded and an unloaded implant that healed for 1 week and another loaded and unloaded implant that healed for 4 weeks.

A custom-made vibration device was used to apply the vibration (60 ±10 Hz). Immediately after the implantation, the implants of the test group received vibration for 10 min/day, 5 days/week. The control implants did not receive any vibration stimulation, but underwent the sham manipulations (mounting of the vibration device) (Figure 6.2).

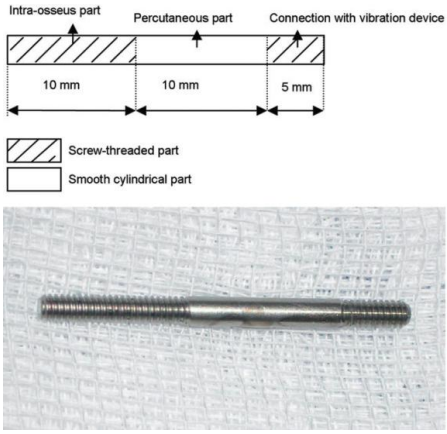

Figure 6.1 *Design of the implant.*

Figure 6.2 *The vibration device was mounted on the implant*

Figure 6.3 *Illustration of the 50- and 400-μm range of interest in which bone fraction measurements were performed. The white space in the center represents the cavity where the implant was removed*

Tissue Processing and Histomorphometry

Immediately after animal sacrifice, the samples were harvested. The tissues were fixed in 4% paraformaldehyde for 3 days. The samples were immersed in 0.5 M EDTA (pH 7.4) and formic acid (HCOOH, pH 3.7) at 4 ℃ until the decalcification was achieved. After demineralization, specimens were dehydrated through an ascending ethanol series prior to paraffin embedding. After paraffin embedding and freezing (-30 ℃), the

implants were gently removed, after which the samples were re-embedded. The most coronal part of the sample was cut into 5 µm thick sections (perpendicular to the implant axis) and stained with hematoxylin and eosin. The bone fraction in a region of interest (ROI) of 50 and 400 µm around the implant was evaluated by a semiautomatic system (Axiovision, Carl Zeiss Microimaging GmbH, Standort Göttingen, Germany) connected to a Zeiss light microscope (Figure 6.3). To eliminate the endochondral ossification which is mostly involved in long bone growth, the cartilage in the target region was excluded from the analysis (*i.e.* the mineral bone fraction = summation of all mineralized tissues in the ROI/(area of the ROI - area of cartilage in the ROI)).

6.3 Results

Means (SD) of the bone fraction in the 50 and 400 µm peri-implant areas are displayed in Figure 6.4. Neither in the 50 nor in the 400 µm peri-implant areas was a significant difference found between test and control groups. After a 4-week loading period, however, a significantly higher bone fraction was observed in the 50 µm compared with the 400 µm peri-implant region (Figure 6.4). This difference in bone fraction depending on the distance from the implant was not observed around the unloaded implants.

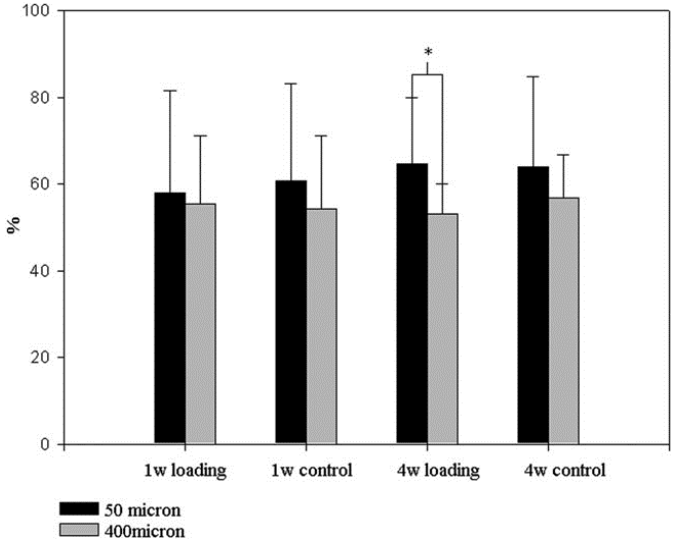

Figure 6.4 *Peri-implant bone fraction in the 50-µm and 400-µm peri-implant areas (*p < .05).*

6.4 Discussion

In this study, the changes of the bone fraction in the peri-implant area in response to high-frequency direct implant loading were investigated. No significant differences in bone fraction were found between the loaded and the control group.

For both loading conditions and both healing periods, there was a tendency for a higher bone fraction in the immediate vicinity of the implant (50 µm peri-implant region) compared with the broader (400 µm) peri-implant region. The fact that this tendency was seen around both unloaded as loaded implants, in combination with the fact that the loading conditions did not significantly affect the peri-implant bone fraction, suggests that the effect of implant installation on the bone in the immediate vicinity of the implants might have overruled a positive effect because of the mechanical stimulation. Only after 4 weeks of mechanical stimulation, a significantly higher bone fraction was found close to the implant compared with in a broader zone around the implant.

This bone densification near the implant was also described by Balatsouka *et al.* (Balatsouka *et al.*, 2005) who found a significant increase in bone density from 2 to 4 weeks. The bone density of newly formed mineralized bone in the bone bed sites without implants, however, did not demonstrate a difference over time.

In this study, the bone fraction – as a representation of the bone density – was measured as this is the parameter that is commonly used for the evaluation of the effect of bone stimuli. Also, the bone-to-implant contact is often used as a parameter to quantify the implant osseointegration. This could not be done in this study because the implants were removed from the bone samples. The choice for paraffin sectioning required this removal of the implants. Previously, the effect of such implant removal on the surrounding tissues was investigated by means of scanning electron microscopy (Slaets *et al.*, 2006). Implants removed only 1 to 3 days after insertion, showed scattered blood cells in a thin layer of (fibrin) matrix, which covered up to 30% of the implant surface. On implants removed after 1, 2, 4, or 6 weeks, some small sponge-like structures were rarely detected, which were devoid of cells. These structures were considered to be fibrous tissue or remnants of cells. The remaining surface of the

implants was comparable with the surface of a blank implant. This means that, despite the removal of an implant from 4 weeks healed bone, the peri-implant tissues can be considered as relatively intact.

Because of both internal mediators and external mechanical demands, the bone tissue dynamically responds to a number of metabolic, physical and endocrine stimuli, undergoing continual chemical exchange and structural remodelling. Recent research has suggested that bones display an extraordinary adaptive behavior toward high-frequency low-magnitude mechanical stimulation (Judex *et al*., 2009).

An early mechanical stimulation (implants healed for 1 week prior to stimulation) *via* indirect whole body vibration was applied on ovariectomized rats for 2 weeks at 50 Hz (Akca *et al*., 2007). The peri-implant bone response was quantified by micro-computed tomography and revealed an increased amount of relative bone volume in a 48 µm peri-implant area.

The current study, however, failed to demonstrate such an osteogenic effect of direct high-frequency loading. Besides, this effect might have been overruled by the healing response, another reason might be that because of the high-frequency loading directly applied onto the implant, a considerably interfacial micromotion between implant and the surrounding tissues might have been evoked. It has previously been shown and hence, this is generally accepted that large micromotions on the implant–bone interface lead to soft tissue encapsulation (fibroplasias) and therefore compromise osseointegration (Brunski, 1999; Degidi and Piattelli, 2005).

A third possible reason why the mechanical loading did not enhance bone formation might be an inefficient load transfer from the implant toward the surrounding tissues. It is known that peri-implant osteogenesis requires a limitation of the interfacial micromotion as well as an optimal force transfer (Vandamme *et al*., 2007c; Vandamme *et al*., 2008). The surface of the used implants (Sdr: 1%) might have been too smooth to establish an efficient biomechanical coupling during the initial healing period. Because of this lack of biomechanical coupling combined with the interfacial micromotion at the start of the mechanical stimulation, the mechanical stimulation failed to enhance bone formation (Wiskott and Belser, 1999).

In silico modelling might contribute to a better understanding of the biomechanical conditions of this experimental set-up. However, the roughness of the implants (Sdr: 1%) was purposely kept low so as to not interfere with the pure mechanical bone response, which was the aim of the study. As well established, surface roughening speeds up the healing process in the first weeks after implant installation compared with turned implants (Gahlert *et al*., 2007; Vandamme *et al*., 2008).

Further, to enhance osteogenesis around the implant, the strategy of biologic and/or geometric surface modification was explored in different animal studies. Coating with bioactive molecules on the implant surface (for instance, collagen and chondroitin sulphate, bone morphogenetic protein-2, calcium phosphate, bisphosphonate) might hold the potential to stimulate bone-to-implant contact (Stadlinger *et al*., 2009; Wikesjo *et al*., 2008) or does increase removal torque values (Ferguson *et al*., 2008). Nevertheless, in all the pervious mentioned studies, the relative peri-implant bone density was not found to be different, which is consistent with our results. It is likely, that in case of biologic and/or local mechanical stimulation, the osteogenic effect is more predominant in the vicinity of the bone–implant interface rather than at distance. This osteogenic effect is not necessarily translated into an increased peri-implant bone fraction, as explained above, but rather, in an increased bone-to-implant contact.

As mentioned previously, several oscillation studies (Judex *et al*., 2007; Rubin *et al*., 2001a; Rubin *et al*., 2001b; Sehmisch *et al*., 2009; Xie *et al*., 2008) indicated that very small load magnitudes (inducing 5 microstrains or less) may already have osteogenic potential when the stimulation is applied at high frequency (>30 Hz). Despite a similar loading regime used in this study, a convincing osteogenic effect could not be observed when the stimulation was directly evoked through an implant. A positive outcome might have been more likely though when the high-frequency loading was applied on the surrounding bone rather than directly onto the implant. This would avoid implant micro-motion, but could still stimulate the peri-implant tissues, which in turn might have a positive effect on peri-implant bone healing and eventually osseointegration. This is subject in ongoing investigation.

In conclusion, no pronounced effect of immediate high-frequency loading, which was applied at 60 ±10 Hz with the direct vibration setup in this study, could be observed on

the peri-implant bone response. The bone healing processes appeared to have a more important effect compared with the mechanical loading.

Acknowledgments: This study was supported by the Research Council of the KU Leuven (OT/07/059). The authors would like to thank Mrs. Lieve Ophalvens (Department of Pathology, UZ Leuven, Belgium) for her professional guidance on histology processing.

Chapter 7

Enhancement of implant osseointegration by direct high-frequency low-magnitude loading

This chapter is based on the publication "**Zhang X.**, Torcasio A., Vandamme K., Ogawa T., van Lenthe G.H., Naert I., Duyck J. Enhancement of implant osseointegration by high-frequency low-magnitude loading. ***PLoS ONE*** 2012;7(7): e40488."

Abstract

***Objective*:** Mechanical loading is known to play an important role in bone remodelling. This study aimed to evaluate the effect of high- and low-frequency axial loading, applied directly to the implant, on peri-implant bone healing and implant osseointegration.

***Materials and methods*:** Titanium implants were bilaterally installed in rat tibiae. For every animal, one implant was loaded (test) while the other one was not (control). The test implants were randomly divided into 8 groups according to 4 loading regimes and 2 experimental periods (1 and 4 weeks). The loaded implants were subject to an axial displacement. Within the high- (HF, 40 Hz) or low-frequency (LF, 8 Hz) loading category, the displacements varied 2-fold and were ranked as low- or high-magnitude (LM, HM), respectively. The strain rate amplitudes were kept constant between the two frequency groups. This resulted in the following 4 loading regimes: 1) HF-LM, 40 Hz-8 μm; 2) HF-HM, 40 Hz-16 μm; 3) LF-LM, 8 Hz-41 μm; 4) LF-HM, 8 Hz-82 μm. The tissue samples were processed for resin embedding and subjected to histological and histomorphometrical analyses. Data were analyzed statistically with the significance set at $p < 0.05$.

***Results*:** After loading for 4 weeks, HF-LM loading (40 Hz-8 μm) induced more bone-to-implant contact (BIC) at the level of the cortex compared to its unloaded control. No significant effect of the four loading regimes on the peri-implant bone fraction (BF) was found in the 2 experimental periods.

***Conclusions*:** The stimulatory effect of immediate implant loading on bone-to-implant contact was only observed in case of high-frequency (40 Hz) low-magnitude (8 μm) loading. The applied load regimes failed to influence the peri-implant bone mass.

Key words: implant; animal; osseointegration; loading frequency.

7.1 Introduction

Bone tissue is metabolically active in adapting its mass, shape and structure to mechanical stimuli through remodelling. Mechanical loading has been proven to direct the differentiation of mesenchymal stem cells towards the osteoblastic lineage and has therefore been introduced to facilitate fracture healing and to improve bone quality (Kelly and Jacobs, 2010; Ozcivici *et al*., 2010a; Ozcivici *et al*., 2010b; Schindeler *et al*., 2008). In animal studies, the anabolic effect of mechanical loading on bone tissue has been evidenced when applied at both high- and low-frequency (Judex *et al*., 2007; Ozcivici *et al*., 2010a).

The effect of mechanical loading on bone regeneration and adaptation also applies to bone around biomaterials, and more specifically around titanium implants (Duyck *et al*., 2006; Duyck *et al*., 2007; Isidor, 2006). Findings from *in vivo* studies have shown that force- (De Smet *et al*., 2005; De Smet *et al*., 2006; De Smet *et al*., 2008) or displacement- (Duyck *et al*., 2006; Duyck *et al*., 2007; Vandamme *et al*., 2007c; Vandamme *et al*., 2008) controlled mechanical loading at low-frequency ($<$10 Hz), when applied directly onto an implant, can improve bone formation in the peri-implant region and can therefore contribute to implant osseointegration. Recent research also revealed that high-frequency loading ($>$10 Hz), applied *via* whole body vibration, can lead to increased bone formation in the peri-implant surroundings and ultimately to an improved osseointegration (Akca *et al*., 2007; Ogawa *et al*., 2011a; Ogawa *et al*., 2011b).

Despite the above notions, further research on the peri-implant tissue response to mechanical loading at high- *versus* low-frequency is warranted due to the variety of animal models and of loading modes (*i.e.* the loading was directly or indirectly applied onto the implant) used in the aforementioned studies (De Smet *et al*., 2005; De Smet *et al*., 2006; De Smet *et al*., 2008; Duyck *et al*., 2006; Duyck *et al*., 2007; Isidor, 2006; Judex *et al*., 2007). Furthermore, the impact of the loading magnitude in high- *versus* low-frequency loading regimes is only partly unraveled. There is evidence that up to a

certain limit, the load-induced bone gain is determined by the loading magnitude in a low-frequency regime (Cullen *et al*., 2001; Gross *et al*., 2002; Mosley *et al*., 1997; Torrance *et al*., 1994). In case of high-frequency stimulation, however, the loading magnitude is reported to be less relevant (Garman *et al*., 2007b; Judex *et al*., 2007). To explore the therapeutic potential of high-frequency mechanical loading in titanium implant healing, it is valuable to fill this knowledge gap and hence to determine appropriate loading strategies.

By use of a rat tibia model and a displacement-controlled loading device, the present study aimed to investigate the influence of controlled mechanical loading, directly applied to the implant and immediately after implant installation, at high- *versus* low-frequency on peri-implant bone (re)modelling and implant osseointegration. It was hypothesized that (i) the peri-implant bone responds to high- and low-frequency loading; and that (ii) this bone response depends on the applied loading magnitude.

7.2 Experimental design

Animals and surgical procedure

Seventy-five male Wistar rats were used in the present study. Out of these, 8 rats were used for defining the desired strain magnitude induced by loading (*ex vivo* load calibration). The remaining 67 rats were used for *in vivo* loading. Custom-made cylindrical implants (⌀: 2 mm x L: 10 mm) were obtained from titanium rods (99.6% Ti, Goodfellow Cambridge Ltd., Huntingdon, England). The cylindrical endosseous part of the implant was screw-shaped; the percutaneous part was non-threaded hexagonal (Figure 7.1 A). The implants were cleaned in an ultrasonic bath with distilled water and etched with a solution of HF (4%) and HNO_3 (20%), resulting in a roughness value (Ra) of 0.45 µm. Implants were sterilized before surgery. The implants were inserted bi-laterally in the medio-proximal site of the tibia (refer to 2.1.1).

Ex vivo strain gauge measurement

Ex vivo strain gauge measurements were performed to correlate the loading magnitude (*i.e*. implant displacement) with the resulting peri-implant bone strain. For this purpose, 8 rat hind limbs were excised. After exposure of the medial surface of each tibia, an implant was inserted. The limb was placed on a rotating platform and fixated through clamping at the proximal (knee) and distal (ankle) joint. The position of the platform was determined in such a way that the implant and the loading pin were aligned (Figure 7.1 B). A single element strain gauge (type FLG-02-11, TML, Tokyo Sokki Kenkyujo Co., Ltd., Japan) was glued on the exposed bone surface of the tibia, 1 mm above the implant. The lead wires (type 3WP008, Feteris Components BV, UK) were connected at one end to the strain gauge through bondable terminals (TF-2SS, Feteris Components BV, UK) and at the other end to the acquisition system.

Loading was performed by using a custom-made displacement-controlled device (Duyck *et al*., 2004). This loading device consisted of a piezo translator (preloaded closed-loop LVPZT translator, P-841.60, ALT, Best, Netherland), which can induce a displacement of up to 120 µm, and a load cell (XFTC 100-M5M-1000N, FGP Sensors, Les Clayes Sous Bois Cedex, France) with a capacity of 1000 N in tension and 100 N in compression. Strain on the surface of peri-implant cortical bone was recorded during displacement of the implants over 30, 50, 70 and 90 µm at a frequency of 1 Hz. The strain reading system included the acquisition of the signal (SCXI 1314, NI, National Instruments, Austin, Texas, USA), amplification, conditioning (SCXI 1520, National Instruments) and transmission to the PC (SCXI 1600 DAQ module, National Instruments). Labview software (Labview 8.6, National Instruments) provided the necessary interface and read-out. The measurements were repeated 5 times with complete removal of the specimen from the device and repositioning. A linear regression analysis was performed to determine the relationship between the applied displacement (µm) and the resulting strain (µε).

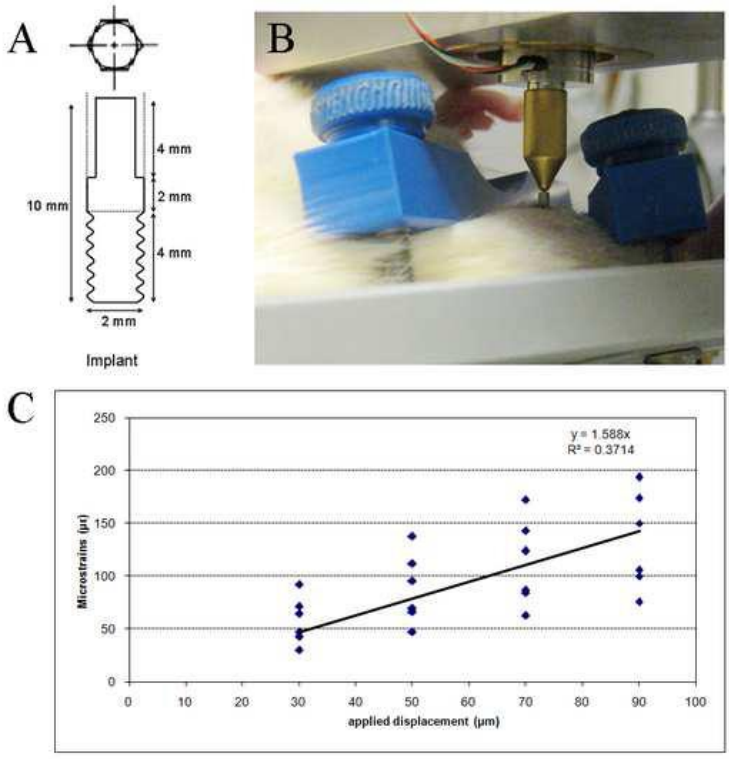

Figure 7.1 *(A) Commercially pure (c.p.) titanium custom-made screw-shaped implant (ISO M2 screw-thread protocol). (B) In vivo axial loading applied directly onto the implant. (C) Ex vivo strain gauge measurements data on the correlation between the loading magnitudes (i.e. implant displacement, μm) and the resulting peri-implant strain (με).*

In vivo mechanical loading

Rats were randomly allocated to 8 groups, corresponding to 4 loading regimes (Table 7.1) and 2 experimental periods (1 and 4 weeks). For each animal, one implant was loaded while the implant in the contralateral limb was unloaded. The loading regimes consisted of high- (40 Hz; HF) and low- (8 Hz; LF) frequency protocols. Within each frequency category, the loading magnitude was defined as such that the maximum induced strain in the high-magnitude loading regime was 2-fold the strain occurring in the low-magnitude protocols. The defined loading frequencies and magnitudes resulted in identical maximum strain rate amplitudes for HF-LM and LF-LM, and for HF-HM

and LF-HM. Loading was initiated one day post implant installation, and was applied axially (Figure 7.1 B). The load application took 10 minutes per session and was performed 5 times a week for 1 or 4 weeks, respectively. Anesthesia induced by isoflurane inhalation (Isoflurane USPR, Halocarbon, NJ, USA) was applied during the loading.

Specimen preparation and analysis

After sacrifice of the animals, the implants and their surrounding tissues were retrieved, processed into PMMA sections (refer to 2.2.1.2), stained (2.2.2.2) and analyzed (refer to 2.3.2)

7.3 Results

Animal and implant

Implant surgery and *in vivo* mechanical loading were performed uneventfully for all except 3 implants. A total of 131 samples we obtained, of which 5 were excluded because of peri-implant infection and 3 were lost during histological processing. The remaining 123 samples were successfully processed for histology and histomorphometry.

Ex vivo strain gauge measurement

The measurements on two limbs were not successful due to technical errors; these were not considered for analysis. For the measurements performed on the remaining 6 limbs, the regression between the applied loading displacement (μm) and the resulting strain (με) was determined (Figure 7.1 C). Based on the established correlation, strains of 13 με and 26 με for the HF-LM and HF-HM loading regimes, respectively, were estimated. For the LF-LM and LF-HM loading protocols, strains of 65 με and 130 με respectively were induced for the selected loading magnitudes (Table 7.1).

Table 7.1 *The applied loading regimes, the resulting mean strains and estimated strain rate amplitudes in the peri-implant environment, and the number of animals in each group.*

	Loading regime		Mean strain and estimated strain rate amplitude		Group size (n)	
	Frequency (Hz)	Magnitude (μm)	Strain (με)	Strain rate amplitude (με/s)	1-week	4-week
HF-LM	40	8	13	520	9	8
HF-HM	40	16	26	1040	8	8
LF-LM	8	41	65	520	9	9
LF-HM	8	82	130	1040	8	8

HF-LM: high-frequency low-magnitude; HF-HM: high-frequency high-magnitude; LF-LM: low-frequency low-magnitude; LF-HM: low-frequency high-magnitude.

Histology

The histological images revealed bicortical bone apposition to the implant for all the loaded and unloaded implants and for both healing periods (Figure 7.2). After 1 week, woven bone was formed along the implant surface in the medullar cavity, while remodelling occurred at the peri-implant cortex. After 4 weeks, the newly formed bone in the medulla was remodelled into lamellar bone close to the implant surface. Further, the healing of the peri-implant cortex was complete. No obvious differences between loaded and unloaded implant of the four loading regimes could be noticed on the histological sections.

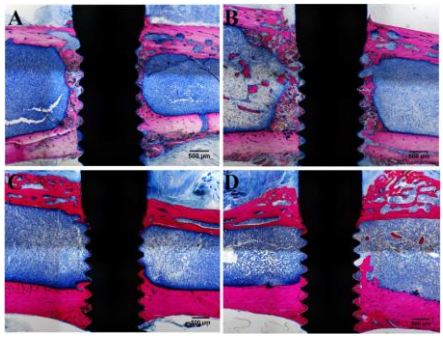

Figure 7.2 *Representative histological sections. Above: for the 1-week experiment, peri-implant bone formation was observed in the medulla around both unloaded (A) and loaded (B) implants. Below: for the 4-week experiment, bone remodelling resulted in a dense bone layer appositioned onto the implant surface in the medullar region for both unloaded (C) and loaded (D) implants.*

Histomorphometry

Bone-to-implant contact

Out of the 4 assessed loading regimes, only cortical BIC was significantly increased in case of HF-LM (40Hz-8μm) loading for 4 weeks, compared to the unloaded control (83.49 ±2.23% *vs.* 72.44 ±5.47%; loaded *vs.* unloaded; $p < 0.05$, ANOVA) (Figure 7.3 A). No further pronounced loading effect on BIC was detected in the medullar region for the 4 loading regimes (Figure 7.3 B).

Concerning the BIC changes over time, the BIC at the cortical level remained stable, whereas a significant increase from 1 to 4 weeks was observed at the medullar level ($p < 0.01$; ANOVA). This BIC change was observed in all 4 loading regimes.

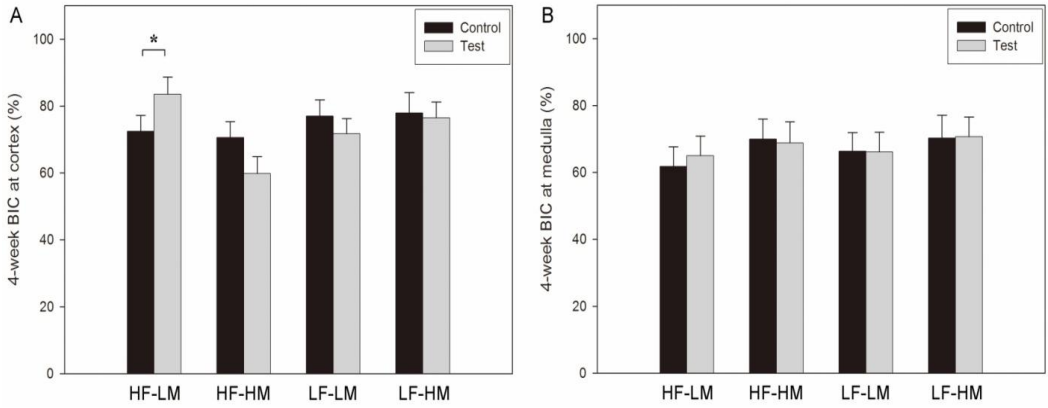

Figure 7.3 *Bone-to-implant contact (BIC) at the cortex (A) and the medulla (B) for the 4-week experiment. Data of the 1-week experiment are not shown as no significant differences were detected (*: $p < 0.05$; ANOVA).*

Bone fraction

The comparison between the unloaded and loaded implant revealed that the peri-implant BF of loaded implants did not significantly differ from the BF of the unloaded implants at both cortical and medullar level and for each loading regime.

As neither loading effect nor interactions between loading and time/ROI were detected for the 4 loading regimes, the BF data of the 4 loading regimes were pooled to assess the overall effect of time (*i.e*. the BF evolution over time) and ROI (*i.e*. the BF distribution in peri-implant region).

A significant increase of BF over time was observed at the cortical level ($p<0.01$; ANOVA). Inversely, a significant BF decrease from 1 to 4 weeks was detected at the medullar site ($p<0.01$; ANOVA) (Figure 7.4).

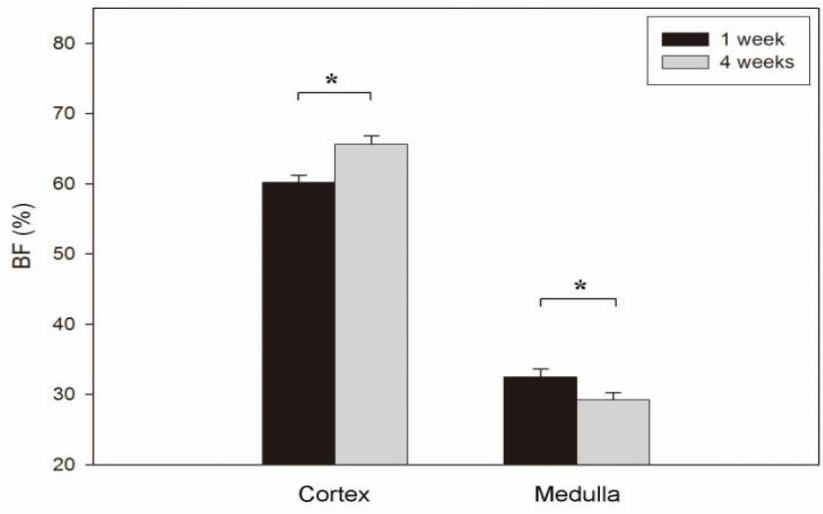

Figure 7.4 *Cortical and medullar bone fraction (BF) evolution from 1 to 4 weeks (*: p < 0.05; ANOVA).*

With regard to the BF distribution in the peri-implant region, again opposing results were found at cortex and medulla. At the cortex, BF significantly increased at further distance from the implant surface (BF in ROI 1<ROI 2<ROI 3, $p<0.01$; ANOVA followed by Tukey HSD). At the medulla, on the other hand, BF significantly decreased with increasing distance from the implant surface (BF in ROI 1 >ROI 2> ROI 3) ($p<0.01$; ANOVA followed by Tukey HSD) (Figure 7.5).

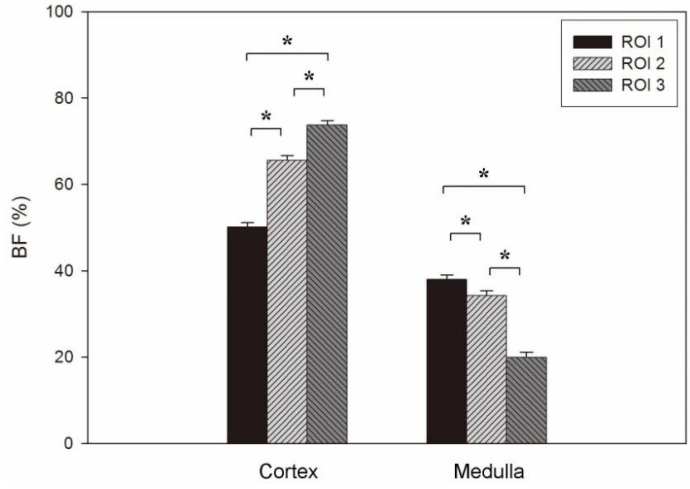

Figure 7.5 *Cortical and medullar bone fraction (BF) distribution in 3 regions of interest (ROI) (*: $p < 0.05$; ANOVA followed by Tukey HSD).*

7.4 Discussion

In the present study, implant osseointegration was assessed under immediate loading at either high- or low-frequency. It was hypothesized that (i) the peri-implant bone responds to high- and low-frequency loading; and that (ii) the response of the peri-implant bone depends on the applied loading magnitude. The main finding of the present study is that bone-to-implant contact is enhanced after 4 weeks of high-frequency low-magnitude loading. This effect, however, was not observed for the respective loading regime after 1 week of loading, or in case of high-frequency high-magnitude loading, or in case of low-frequency loading. Hence, the first study hypothesis is partly confirmed: a response of the peri-implant bone to direct immediate loading was only found in case of HF loading. At the same time, the suggested role of the loading magnitude (2^{nd} hypothesis) on the peri-implant bone response was confirmed.

According to Frost (Frost, 2004), bone (re)modelling is triggered when the tissue deformation (strain) induced by a low-frequency loading exceeds a certain threshold (*i.e.* 1000 με). On the other hand, when applied at high-frequency, bone can sense and respond to mechanical signals at low magnitudes (*i.e.* from 5 to 10 με) (Gilsanz *et al.*, 2006; Ozcivici *et al.*, 2010a). Besides the magnitude of the strain, the strain rate

amplitude (defined by both loading magnitude and frequency) is considered to be a determining factor for bone response to mechanical loading (Goodship *et al*., 1998; LaMothe *et al*., 2005). In order to define the role of the individual loading parameters (frequency, magnitude — corresponding to the displacement of the loading device, and strain rate amplitude) in immediate implant loading, 4 distinct but comparable loading regimes were defined in this study. The loading parameters were in part chosen based on reports of an anabolic effect of loading on bone (De Smet *et al*., 2005; De Smet *et al*., 2006; De Smet *et al*., 2007). The *ex vivo* calibration data provided information on which implant displacement was required to achieve a certain peri-implant bone strain. Considering the configuration of the loading device, 40 Hz and 8 Hz were selected as high- and low-frequency respectively. For both frequency categories, the loading magnitude was determined in such a way that identical strain rate amplitudes between the two frequency regimes were obtained. In studies from our group (De Smet *et al*., 2006; De Smet *et al*., 2007; 2008), the peri-implant strain rate amplitude favoring bone formation was found to be 267 με/s to 1600 με/s at low-frequency (3 Hz). In the present study, strain rate amplitudes of 520 με/s and 1040 με/s were achieved by loading magnitudes of 41 μm and 82 μm (leading to strains of 65 με and 130 με) for a low-frequency regime (8 Hz). Accordingly, for high-frequency loading (40 Hz), the estimated strains of 13 με and 26 με induced by loading magnitudes of 8 μm and 16 μm respectively resulted in identical strain rate amplitudes compared with the low-frequency regime. In this way, comparable strain rate amplitudes, anticipated to be anabolic to the peri-implant bone response, were achieved.

Histological observations revealed a normal healing response after implantation, irrespective of the loading regime. These observations were in line with the histomorphometrical data. At the cortex, bone remodelling led to a bone gain in the peri-implant cortex over time (BF increased from 1 to 4 weeks); while the remodelling did not necessarily influence the direct bone contact with the implant (BIC remained stable over time). Compared to the distant host bone, on the other hand, the bone fraction in the direct implant vicinity remained lower, even after 4 weeks of healing. Histologically, the more prominent presence of blood vessels, playing an active role in bone remodelling, in the implant's vicinity, may explain this lower peri-implant bone

fraction. In the peri-implant medullar area – an initially bone-free region – massive woven bone was formed soon after implantation. The formed bone originated from the endosteum of the peri-implant cortex and grew along the implant surface. Subsequent remodelling of this newly formed bone led to less but denser bone, in closer contact with the implant. With regard to the tissue evolution over time in this region, implant osseointegration (quantified as BIC) was found to increase from 1 to 4 weeks, whereas the bone mass (BF) around the implant decreased in the meantime. This is in line with previous findings with the same animal model (Ogawa *et al.*, 2011a; Ogawa *et al.*, 2011b).

The anabolic effects of high-frequency loading have been reported in a number of animal studies (Goodship *et al.*, 2009; Judex *et al.*, 2007; Omar *et al.*, 2008) and clinical trials (Gilsanz *et al.*, 2006; Rittweger *et al.*, 2010; Rubin *et al.*, 2004). Only few studies, however, investigated the effect of high-frequency loading on bone surrounding implants. De Smet *et al.* (De Smet *et al.*, 2007; De Smet *et al.*, 2011) applied the high-frequency (30 Hz) loading onto implants 7 days after implantation. They revealed a bone stimulating loading effect in the medullar region. However, no loading effect on implant osseointegration was found. The discrepancy from the findings of the present study (*i.e.* increased cortical osseointegration by HF-LM loading) may owe to the different time of loading. As De Smet *et al.* (De Smet *et al.*, 2007; De Smet *et al.*, 2011) adopted an implant-healing time of 7 days prior to the loading, the impact of loading on the differentiating cells and tissues in peri-implant region can be diminished, compared to the loading initiated one day after implantation.

In another study, applying a high-frequency loading of 40 Hz directly on the implant, failed to improve the osseointegration (Zhang *et al.*, 2012). In the mentioned study, however, a moment was applied instead of an axial force. Taking into account the detrimental effect of excessive micromotion and shear strains on osseointegration (Duyck *et al.*, 2006), it is logical that, in case of screw-shaped implants, load transfer from the implant to the surrounding tissues is more favorable in case of axial compared to rotational loading.

In the current experiment, HF-LM immediate loading was found to enhance bone-to-implant contact at the peri-implant cortex after loading for 4 weeks. Meanwhile, the high-magnitude loading at the same high-frequency failed to do so. In this respect, low-magnitude loading was better to promote cortical osseointegration. Furthermore, the gain in peri-implant cortical bone mass over time can be attributed to the inherent healing of the host tissue; neither low- nor high-magnitude loading was found to contribute significantly. Similar insignificant findings were observed in the peri-implant medulla. Potential loading effects are likely to be overruled by this active tissue repair and remodelling.

Similar to high-frequency loading, the effect of low-frequency loading on bone adaptation and regeneration has also been acknowledged (Judex *et al*., 2007; Ozcivici *et al*., 2010a). Well-controlled mechanical loading at low-frequency, when applied directly to the implant, either in an early or immediate loading protocol, can improve bone formation in the peri-implant region and implant osseointegration (De Smet *et al*., 2005; Duyck *et al*., 2006; Duyck *et al*., 2007; Vandamme *et al*., 2007c; Vandamme *et al*., 2008). Relatively small loading displacements were selected for the low-frequency loading regime in the current study. The resultant deformations by the loading were far below the (re)modelling threshold of 1000 με recommended by Frost (Frost, 2004). Although the applied strain rate amplitudes were identical to the ones in high-frequency loadings and considered osteogenic (De Smet *et al*., 2007; 2008), no significant effect of low-frequency loading on implant healing was found in the present experiment. The implication might be that (1) to induce a positive bone response to mechanical loading, at least one of the constituting elements of loading (*i.e*. magnitude or frequency) needs to go beyond a certain threshold; (2) after fulfillment of the above condition, the impact of loading element combination (*i.e*. strain rate amplitude) on bone response can be considered.

The exact mechanism of how mechanical loading affects bone is yet unclear. Compared to the high-frequency loading, the host tissue perceiving the low-frequency loading is more dependent on the loading magnitude. When keeping loading frequency and the number of loading events constant, variations in strain magnitude can explain

differences in the osteogenic response to the low-frequency loading. *I.e*. the larger the deformations generated in the bone, the greater the increases in bone mass (Cullen *et al*., 2001; Gross *et al*., 2002; Mosley *et al*., 1997; Torrance *et al*., 1994). This can be interpreted with relatively simple models such as the mechanostat (Frost, 2004) and the fluid flow theory (Klein-Nulend *et al*., 2005). According to the fluid flow theory, the load-induced fluid shear stress acts as the signal activating bone remodelling. The signal acts on osteocytes and cell processes in the lacunar-canalicular system. Therefore, the anabolic effect of low-frequency loading on bone is dependent on the loading magnitude which in turn affects the load-induced strain.

Under the high-frequency regime, the loading can also be sensed by the bone (Garman *et al*., 2007b; Judex and Rubin, 2010). Local strains on the tibia surface have been recorded to be less than 10με in case of whole body vibration (Judex *et al*., 2007; Xie *et al*., 2006). Apparently, the induced strain is extremely small, far less than the (re)modelling threshold of 1000 με for the low-frequency loading (Frost, 2004). Therefore, the notion has been called up that the anabolic response of the host tissue to the high-frequency loading was mainly dependent on the loading frequency, rather than the loading magnitude (Christiansen and Silva, 2006; Judex *et al*., 2007; Judex and Rubin, 2010). Explanations of this dependence were suggested by the theoretical models of You *et al*. (You *et al*., 2001) and Han *et al*. (Han *et al*., 2004). Their models were based on the facts that (1) osteocyte processes were attached along their length by tethering filaments, and (2) the actin filament bundle in dendritic processes led to a highly polarized cell whose processes were several hundred times stiffer than the osteocyte cell body (Han *et al*., 2004). Hence, the flow-induced drag on these filaments would produce a tension that could greatly amplify the very small whole tissue strains at the cellular level. By predicting the strain amplification ratio from the tissue to the cell level, they found that this amplification ratio not only increased with loading frequency, but also decreased with loading magnitude (You *et al*., 2001). Therefore, under high-frequency loading, low bone strains were amplified most, suggesting a more efficient mechanotransduction due to the cellular perception of the high-frequency signals. This “less is more” phenomenon is also supported by the findings of the high-frequency loadings in the present study.

In conclusion, the stimulatory effect of immediate implant loading on bone-to-implant contact was only observed in case of high-frequency (40 Hz) low-magnitude (8 μm) loading. The applied load regimes failed to influence the peri-implant bone mass.

Acknowledgements: Sincere gratitude was addressed to Mr. Michel De Cooman (Department of Electrical Engineering, ESAT, KU Leuven) for designing and constructing the loading device. This study was supported by the Research Council of KU Leuven (OT/07/059).

Chapter 8
General discussion and perspectives

The general objective of this thesis was to investigate the effect of high-frequency loading on osseointegration and bone remodelling of titanium implants.

Bone remodelling enables bone to renew and reshape itself in response to mechanical stimuli. Mechanical loading has been introduced to facilitate fracture healing of long bones and to improve bone quality owing to its potential to direct the differentiation of mesenchymal stem cells towards the osteoblastic lineage and to trigger bone remodelling (Ozcivici *et al*., 2010a; Ozcivici *et al*., 2010b). The impact of mechanical loading on bone regeneration and adaptation also applies around biomaterials, more specifically around titanium implants (Duyck *et al*., 2006; Duyck *et al*., 2007; Isidor, 2006).

In previous research, low-frequency loading protocols were often used to assess their anabolic effect and to identify ideal loading strategies (*e.g*. magnitude, duration, strain rate amplitude). Recently, *in vivo* studies indicated high-frequency loading as a potent osteogenic stimulus in case of osteoporotic bone (Garman *et al*., 2007a; Judex *et al*., 2007; Oxlund *et al*., 2003), fracture healing (Goodship *et al*., 2009; Leung *et al*., 2009), and bone defects (Leung *et al*., 2009; Omar *et al*., 2008; Wolf *et al*., 2001). Moreover, clinical trials have shown its potential to attenuate the bone loss due to bed-resting and to increase bone volume for low-BMD patients of both young females (Gilsanz *et al*., 2006) and postmenopausal senior women (Rubin *et al*., 2004; Verschueren *et al*., 2004). Therefore, the application of high-frequency loading was worth exploring in implant dentistry.

In this PhD project, the effect of mechanical loading on osseointegration and peri-implant remodelling was investigated to test the following hypotheses: (1) healing and healed peri-implant bone tissues respond differently to mechanical loading (*i.e*. immediate *versus* conventional loading), (2) high-frequency mechanical loading can stimulate osseointegration and peri-implant bone remodelling, (3), the effect of high-frequency loading on peri-implant bone depends on time-related parameters, (4) the effect of mechanical high-frequency loading on peri-implant bone depends on the applied loading parameters, in particular load magnitude and frequency, (5) the effect of high-frequency mechanical loading on peri-implant bone depends on the mode of

load application (whole body vibration *vs*. direct implant loading *vs*. indirect implant loading). .

Immediate versus conventional loading

To evaluate the peri-implant tissue response to immediate *versus* conventional implant loading, an established loading protocol (De Smet *et al*., 2005; De Smet *et al*., 2006; Slaets *et al*., 2009) was used **in Chapter 3**. This loading protocol adopted a physiological frequency (*i.e*. 3 Hz) to simulate the human mastication pace (Morimoto *et al*., 1984) and induced peri-implant bone strains of about 1000 με. The results of the study in Chapter 3 proved that the bone-to-implant contact was indeed increased in case of immediate compared to no loading after a 4-week healing period. The improvement of osseointegration by immediate loading is in line with previous findings (De Smet *et al*., 2005; Duyck *et al*., 2006; Duyck *et al*., 2007; Vandamme *et al*., 2007c; Vandamme *et al*., 2008). On the other hand, the conventional loading failed to influence the bone-to-implant contact. A report by Kim *et al*. (Kim *et al*., 2008), however, did indicate a higher degree of implant osseointegration in case of conventional loading compared to immediate loading. This increased bone-to-implant contact in case of conventional implant loading could be explained by the prolonged healing time (*i.e*. the extra load-free interval of 3 months for the conventional loading regime). In our study, the implants that were immediately loaded for 4 weeks obtained a similar degree of osseointegration (BIC: 77.67% ± 2.17%) to implants that received conventional loading for the same period (75.91% ± 6.71%) or that were left to heal for 8 weeks (76.1% ± 5.67%). These results suggested the potential of immediate loading to accelerate osseointegration.

In vitro and *in vivo* studies support the notion that the mechanical environment affects gene expression of the cells adjacent to implants (Kokkinos *et al*., 2009; Vandamme *et al*., 2011). Molecular analyses of our study revealed an increased osteoblastic gene expression (*i.e*. *Runx2*) in peri-implant tissue after loading for 7 days for both loading regimes. Moreover, conventional loading for 7 days induced a significant rise of anti-osteoclastic gene (*OPG*). Therefore, both loading regimes showed their influence favoring osteogenesis at the molecular scale. However, the peri-implant tissue in

response to the two loadings failed to present a pronounced difference from their unloaded controls.

Based on the above, the first hypothesis of this PhD thesis can be accepted. Healing and healed peri-implant tissues indeed respond differently to mechanical loading (*i.e.* immediate *versus* conventional loading).

Effect of high frequency loading

Being recognized as a potent signal for adaptive and reparative bone remodelling, mechanical loading at either low or high frequency can be a therapeutic reagent in favor of bone regeneration and adaptation in case of both normal and jeopardized bone conditions (*e.g.* osteoporosis) (Ozcivici *et al.*, 2010a). As increasing evidence indicates an anabolic effect of high-frequency loading *via* whole body vibration on bone regeneration and remodelling (Hwang *et al.*, 2009; Leung *et al.*, 2009; Omar *et al.*, 2008; Shi *et al.*, 2010), it leads to a tempting direction to explore the application of WBV in the implant dentistry (**Chapter 4**).

The stimulatory effect of high-frequency loading, *via* WBV, on peri-implant bone remodelling was confirmed in **Chapter 4 Study 4.1** using a step-wise frequency from 12 to 150 Hz. Compared to the unloaded control, the BIC increased up to 20% when loading for 25 days. A similar improvement of peri-implant bone and osseointegration was found when loading with less loading time, but with insertion of a load-free interval (**Chapter 4 Study 4.2**). When WBV was applied at high frequency with high acceleration (130-150 Hz at 0.3 g), significantly more bone-to-implant contact and peri-implant bone fraction was observed compared to the unloaded control and to the other loading modes with low/medium frequency (*i.e.* 12-30 Hz at 0.3g, 70-90 Hz at 0.075g) (**Chapter 4 Study 4.3**). **The second hypothesis, stating that high-frequency mechanical loading can stimulate osseointegration and peri-implant bone remodelling, is hereby confirmed.** To assess the influence of WBV duration on the peri-implant tissue response, four loading protocols, which varied in loading duration and rest time in-between loading sessions, were carried out in the second study of Chapter 4 (**Chapter 4 Study 4.2**). Extending loading duration alone did not significantly affect the positive effect of WBV. Inserting a load-free rest period in

between loading sessions, however, reinforced the positive effect of WBV. As reported before, the recovery of cell mechanosensitivity from its accommodation to the loading may be the explanation for the anabolic outcome of insertion of a rest period during loading (Robling *et al*., 2001a; Turner, 1999). **So, with the loading application *via* whole body vibration, the effect of high-frequency loading on peri-implant bone depends on time-related parameters. This can serve as an acceptance of the third hypothesis of this PhD thesis.**

The third study of Chapter 4 (**Chapter 4 Study 4.3**) was an attempt to further investigate the optimal combination of frequency and acceleration parameters of WBV. The loading frequency and acceleration was classified into three ranges (*i.e*. low, medium and high range) and was respectively applied with the combination of (1) low frequency with high acceleration, (2) medium frequency with medium acceleration, (3) medium frequency with high acceleration, (4) high frequency with low acceleration and (5) high frequency with high acceleration. It was observed that the loading mode of the high acceleration (0.3g) with high (130-150 Hz) frequency resulted in significantly more bone-to-implant contact and peri-implant bone fraction compared to the unloaded control, to the loading mode at low frequency (12-30 Hz at 0.3g) and to the medium frequency with medium acceleration (70-90 Hz at 0.075g) protocol. According to Judex *et al*. (Judex *et al*., 2007), the effect of high-frequency loading depends on the applied frequency rather than the loading magnitude. Our findings in Chapter 4 Study 4.3 were in line with this notion. When the loading magnitude was maintained, BIC was higher in case of high frequency loading (120-150Hz *vs*. 12-30 Hz) after 4 weeks.

Rubin & McLeod (Rubin and McLeod, 1994) investigated the effect of mechanical loading on peri-implant bone formation. Strains of 150 με were generated in the cortex of turkey ulnae immediately adjacent to the implant by means of bending of the ulnae. Their results showed that the 20-Hz loading regime induced the most favorable bone response, while the 1-Hz loading only prevented the bone disuse atrophy. In Chapter 5, a study in which a similar loading protocol was used, namely high-frequency (40 Hz) loading at a low strain magnitude (~13με). This indirect loading protocol improved the degree of implant osseointegration significantly at both the cortical and medullar

level after 4 weeks (**Chapter 5**). Meanwhile, the 40-Hz loading with increased strain magnitude (up to ~26με) failed to induce a significant peri-implant bone improvement, compared to the unloaded control.

The pilot study on direct implant loading (Chapter 6) did not reveal a significant effect of the loading on the peri-implant bone fraction. The possible reasons for the lack of loading effect on peri-implant bone are discussed in Chapter 6. There is still one point which is worth mentioning in the general discussion. The calibration of the peri-implant bone strain in response to the direct loading is crucial. The lack of the calibration made it difficult to interpret the experimental findings. In case of more controlled direct implant loading (Chapter 7), however, a stimulating effect of high-frequency (40 Hz) loading on bone-to-implant contact was found when the loading magnitude remained low (~13με). When the 40-Hz loading magnitude increased up to ~26 με, no difference of bone-to-implant contact can be found between the loading and the unloaded control.

Overall, the second and fourth hypothesis of this PhD thesis can be accepted. High-frequency mechanical loading can stimulate osseointegration and peri-implant bone remodelling with the application mode of WBV, indirect compression and direct implant loading. The effect of mechanical loading on peri-implant bone depends on the applied loading parameters, in particular load magnitude and frequency.

Direct loading versus indirect loading versus whole body vibration

In order to elaborate the effect of loading application mode (*i.e*. direct loading *vs*. indirect loading *vs*. whole body vibration), a horizontal comparison and evaluation from Chapter 4 to Chapter 7 was needed. Unfortunately, the main drawback which restrains us from making a systematic evaluation of the load application mode is the fact that the stress and strain at the bone implant interface as a result of the respective loading modes cannot be quantified and therefore compared. Although the improvement of peri-implant bone was found in the three modes of loading application, the whole body vibration seems to be a more practical way to apply high frequency

loading onto when compared to direct implant loading and indirect implant loading *via* compression. The reasons rely on the following concerns.

(1) Compared to the "constrained" direct and indirect implant loading, the "unconstrained" whole body vibration may in addition lead to muscle contraction and posture/stance adaptation in response to the loading. These were believed to result in an increased bone cell perception of the high-frequency loading signals (Gilsanz *et al*., 2006; Muir *et al*., 2011).

(2) Whole body vibration may lead to stochastic resonance of the applied vibrations, which could serve as an extra bone stimulus (Tanaka *et al*., 2003).

(3) Being no need of anesthesia during the application of whole body vibration, the side-effects and/or complications of daily usage of full anesthesia, which has to be performed on the animals in the direct and indirect (*via* compression) implant loading studies, could be precluded.

(4) The peri-implant strain distribution induced by different loading applications might vary and successively cause different tissue response. However, to measure the local strain on the bone accurately with the whole-body-vibration set-up is difficult. Even, the strain measured in the well-controlled loading studies (Chapter 5 and 7) is on the level of the bone surface, thus not representing the strain at the bone-to-implant interface. Hence, for a better understanding of the biomechanical conditions with different experimental set-ups, further *in vitro* testing and numerical modelling is required.

(5) From literature, the osteogenic effect of whole body vibration has also been intensively reported in the *in vivo* model of osteoporotic bone (Garman *et al*., 2007a; Judex *et al*., 2007; Oxlund *et al*., 2003), fracture healing (Goodship *et al*., 2009; Leung *et al*., 2009) and bony defect (Leung *et al*., 2009; Omar *et al*., 2008; Wolf *et al*., 2001).

In summary, the acceptance of the fifth hypothesis cannot be fully supported. Within the loading protocols and application modes tested in the thesis, we tend to believe that high frequency loading through WBV holds most potential.

Future perspectives

Based on the current literature, high-frequency loading can stimulate both normal and compromised bone. The findings of the present PhD research confirm this effect on peri-implant bone as well, as high-frequency loading contributes to peri-implant bone remodelling and favors osseointegration. Concerning the application strategy, it could be recommended to apply the high-frequency loading indirectly onto the implant *via* whole body vibration immediately after implantation. Moreover, an insertion of a load-free interval between loading sessions can reinforce the anabolic effect of the loading.

The main findings of this thesis are at the tissue level. Meanwhile, being short of the mechanical information at the bone-to-implant interface, it's difficult to explicitly resemble the relation between the peri-implant tissue response and the applied loading. Some interesting and valuable prospects for future researches are proposed:

- The investigation of the moleculars/signaling pathways responsible for the tissue response to high-frequency loading. In Chapter 3, an increased *Runx2* (the key transcript factor for osteoblast) was up-regulated by low frequency loading. It will be meaningful to study the osteoblast-related gene/protein expression in peri-implant tissues when the high-frequency loading was applied.
- The effect of high frequency loading on bone cell behavior and residing onto implant surface seems to be another interesting prospect of research. The *in vitro* osteocyte/osteoblast/MSCs culture with Ti disc is a widely-used model. With the high frequency loading applied into the culture system, the bone cell performance can be clearly observed and quantified in a well-controlled environment.
- If we consider the high frequency loading as a supplement tool for a better and faster peri-implant bone healing, it will be more valuable to assess the effect of high frequency loading in a more clinically challenging scenario, such as implantation in grafted bone.
- To have a precise mechanical feature at the bone-to-implant interface is an important challenge. The stiffness of the interface evolve over healing time and may be influenced by the additional loading The presence of implant can cause

severe metal artifacts, which jeopardized the quality of micro-CT images and may lead to a failed microCT based finite element model. How to resolve these problems may require creative experts and *in silico* modeling.

This PhD thesis may contribute to reveal the effect of high-frequency on peri-implant bone remodelling. With the findings reported in the thesis and the progresses gained in the prospective researches, we expect to improve the understanding on which genes/proteins in peri-implant tissues are responding to the high-frequency loading, how to (*i.e*. application mode) and what to (*i.e*. loading duration, frequency and magnitude) apply the high-frequency loading can achieved the optimal peri-implant bone healing, both for normal and compromised bone.

Summary

Oral implants are titanium screw-shaped devices that are inserted in jaw bone to support a dental prosthesis. Osseointegration is required for their clinical success and implies direct bone apposition onto the implant.

Despite high success rates of more than 90% after 15-years of follow-up, implants failures can occur in case of unfavorable conditions (*e.g*. compromised host bone, compromised blood circulation, low bone quantity, *etc*.).

Instead of delaying the loading, there is currently a trend to functionally load implants immediately or early after implantation in order to limit the period of discomfort for the patients. Those faster loading protocols also lead to satisfactory success rates, but cannot yet predictably be applied in all clinical situations (*e.g*. low primary implant stability, low bone quality, *etc*.).

Hence, it would be valuable to find a way to improve the reliability and speed, of implant osseointegration in order to optimize treatment outcomes also in compromised bone conditions. Mechanical loading is known to play a potent role in bone regeneration and adaptation. Recently, the interest in high-frequency mechanical loading, associated with low loading magnitude grows. Indeed, an increasing number of studies have shown their effect on enhancing bone formation in distraction osteogenesis and fracture healing of long bone. Clinical studies have shown an improvement of bone quality in both healthy and jeopardized conditions, such as in osteoporosis.

The overall objective of this PhD research was to investigate the effect of mechanical loading, in particular high-frequency loading, on peri-implant bone healing and remodelling. More specifically, the tissue response under different loading frequencies/magnitudes or loading modes has been assessed.

To investigate the response of healing *versus* healed peri-implant tissue to mechanical loading, the same loading was applied onto implants either immediately after implant insertion (immediate loading group) or after a healing time of 28 days (conventional loading group). Bone (re)modelling and vascularization in the peri-implant tissues were unaffected by both loading regimes. In the tissues of the implant's vicinity, however,

the observed gene expression changes were different in case of immediate *versus* conventional loading. Also an enhanced bone-to-implant contact was observed when loading was initiated immediately after implant insertion.

In the following experiments, the effect of different immediate loading regimes was evaluated. The tested loading regimes differed in loading magnitude, frequency, duration, and mode (whole body vibration, direct and indirect implant loading).

First, three consecutive experiments were performed to assess the effect of indirect high-frequency loading, *via* whole body vibration, on peri-implant bone remodelling. Both bone-to-implant contact and peri-implant bone density were significantly improved by the loading with a step-wise frequency band from 12 to 150 Hz at 0.3 g for around 10 min /day.

When the loading session was shortened to 1 min 15 sec, 2 min 30 sec, 5 min and twice 1 min 15 sec (with 4 h interval) respectively, the improvements of bone-to-implant contact and peri-implant bone density were still significant, compared to the unloaded controls. Among the tested loading sessions, the loading with a load-free interval presented the highest gain of peri-implant bone.

To investigate the optimized frequency and acceleration of whole body vibration, the vibration protocols of different combinations of loading frequency and acceleration were applied. For all combinations (*i.e*. 12-30 Hz at 0.3 g, 70-90 Hz at 0.3 g, 70-90 Hz at 0.075 g, 130-150 Hz at 0.3 g, and 130-150 Hz at 0.043 g), the loading combination with the highest frequency band and acceleration (*e.g*. 130-150 Hz at 0.3g) displayed the most favorable effect on BIC and BF, compared to the other test groups.

Second, besides whole body vibration, another indirect loading protocol was performed thereby compressing an implant-containing long bone through its axis. The controlled compression was applied at both high- and low-frequency. Higher loading magnitudes (and accompanying elevated tissue strains) were required under low-frequency loading to provoke a positive peri-implant bone response, compared to high-frequency loading. A sustained period of loading at high-frequency was needed to induce overall enhanced effect on the peri-implant bone.

After that, two studies were carried out to assess the effect of direct loading on peri-implant bone remodelling. In the first study, a small vibration motor was attached on the head of the implant to laterally stimulate the implant at 60±10 Hz. However, no pronounced bone response to the direct vibration was found. In the second study, a displacement-controlled loading was applied onto the implant through the implant axis. Four loading regimes were applied in this study: 1) HF-LM, 40 Hz-8 μm; 2) HF-HM, 40 Hz-16 μm; 3) LF-LM, 8 Hz-41 μm; 4) LF-HM, 8 Hz-82 μm. The stimulatory effect of immediate implant loading on bone-to-implant contact was only observed in case of high-frequency (40 Hz) low-magnitude (8 μm) loading. The applied load regimes failed to influence the peri-implant bone mass.

This series of studies confirmed the role of mechanical loading in peri-implant bone regeneration and remodelling. Although an influencing role was observed for all loading modes, we tend to believe that the high frequency loading through WBV holds most potential.

Samenvatting

Orale implantaten zijn titanium schroefvormige kunstwortels die in het kaaksbot geplaatst worden ter ondersteuning van een gebitsprothese. Om klinisch succes te waarborgen, is osseointegratie vereist, hetgeen directe botappositie tegen een functioneel belast implantaat impliceert.

Ondanks hoge succespercentages van meer dan 90% na 15 jaar follow-up, kunnen implantaten falen ten gevolge van ongunstige omstandigheden zoals gecompromit teerde botkwaliteit, botdoorbloeding e.d.

In plaats van osseointegratie af te wachten alvorens een implantaat functioneel te belasten, is er tegenwoordig ook een trend om implantaten vroeg of onmiddellijk na het plaatsen te belasten waardoor de periode van discomfort voor de patiënten beperkt wordt. Hoewel ook dit protocol het klinisch goed doet, is het minder voorspelbaar in diverse klinische situaties (vb. i.g.v. slechte botkwaliteit, beperkte primaire stabiliteit e.d.).

Om aan bovenstaande zaken te verhelpen, is het dus belangrijk om te zoeken naar manieren om de snelheid, voorspelbaarheid en kwaliteit van de implantaat osseointegratie te verbeteren om zo de prognose van implantaat therapie te verbeteren in het geval van gecompromitteerd bot of immediate belasting.

We weten dat mechanische belasting een belangrijke rol speelt in regeneratie en hermodelering van het bot. Meerdere studies geven aan dat hoog-frequente belasting (gecombineerd met een lage belastingsgrootte) een stimulerende rol kan spelen bij distractie osteogenese en fractuurheling. Ook klinische studies toonden een impact aan op de botkwaliteit in zowel gezonde als gecompromitteerde botcondities.

Het hoofddoel van deze thesis is het onderzoeken van het effect van mechanische belasting, in het bijzonder de hoog-frequente belasting, op de heling en hermodelering van het bot rond implantaten. Meer specifiek werd de weefselrespons rond implantaten nagegaan bij verschillende belastingsfrequentie en –grootte spectra en verschillende belastingsmodes.

In een eerste studie werd de peri-implantaat botrespons op belasting vergeleken tussen immediaat *versus* uitgesteld (28 d na implantatie) belaste implantaten. Hoewel zowel

de bothermodelering als de doorbloeding niet verschillenden tussen de immediaat en de uitgesteld belaste implantaten, waren er wel verschillen te zien in genexpressie. Ook werd een betere osseointegratie vastgesteld wanneer de belasting direct na implantatie werd aangebracht.

In de experimenten die daarop volgenden, werd de invloed van verschillende immediate belastingsprotocollen bestudeerd. Deze belastingsprotocollen varieerden in belastingsgrootte, -frequentie, -duur en –mode (whole body vibration, directe belasting, indirecte belasting).

Eerst werden 3 studies gedaan waarbij het effect van whole body vibration werd geëxploreerd. Hieruit bleek dat whole body vibration (12 tot 150 Hz, 0.3 g, ca. 10 min/dag) zorgt voor een significante toename in zowel bot-implantaat contact als peri-implantaat botdensiteit. Ook bij een verkorte belastingsduur (1 min.15 sec., 2 min.30 sec., 5 min., 2 x 1 min.15 sec. met een tijdsinterval tussen van 4 uur) was er nog steeds een significant stimulerend belastingseffect. Het belastingsprotocol waarbij de belasting kort (1 min. 15 sec.) in 2 sessies per dag, maar met een tijdsinterval van 4u werd aangbracht, had het grootste botstimulerende effect.

Om het effect van belastingsfrequentie en –acceleratie van de whole body vibration te evalueren werden opnieuw verschillende belastingsprotocollen uitgetest (12 to 30 Hz - 0.3 g, 70 to 90 Hz - 0.3 g, 70 to 90 Hz - 0.075 g, 130 to 150 Hz - 0.3 g, and 130 to 150 Hz - 0.043 g). Hierbij gaf het belastingsprotocol met de hoogste frequentie het beste resultaat.

Naast whole body vibration werd ook een andere manier van indirecte implantaatbelasting uitgetest, waarbij een lang been met daarin een implantaat, gecomprimeerd werd volgens zijn lengteas. Deze gecontroleerde belasting werd aangebracht aan zowel hoge als lage frequentie. Uit de resultaten van deze studie bleek dat grotere belastingsgroottes nodig waren om in geval van laag-frequente belasting een botstimulerend effect te bekomen en dit in tegenstelling tot de hoog-frequente belasting. De periode van belasting moest in geval van hoog-frequente belasting wel lang genoeg zijn om een algemene verbetering van de osseointegratie te bekomen. Hierna werden ook 2 studies uitgevoerd ter evaluatie van het effect van directe

belasting op het peri-implantaat bot. In de eerste studie werd een kleine vibratiemotor op het implantaat aangebracht waardoor deze laaste gestimuleerd werd aan 60 ± 10 Hz. Hierbij kon geen significant effect op het bot worden vastgesteld. In de tweede studie werd een toestel ontwikkeld waarbij de belasting nauwkeurig verplaatsingsgeco ntroleerd direct op het implantaat kon worden aangebracht. In deze studie werden 4 belastingsregimes (40 Hz-8 µm; 40 Hz-16 µm; 8 Hz-41 µm; 8 Hz-82 µm) geëvalueerd. Enkel in geval van hoog-frequente belasting (40 Hz) aan een lage belastingsgrootte (8 µm) werd een significant effect op het bot-implantaat contact vastgesteld. Er kon geen effect worden vastgesteld op de peri-implantaatbotdensiteit.

Deze reeks van studies bevestigden de rol van mechanische belasting op peri-implantaat bot regeneratie en remodeling. Hoewel een beïnvloedende effect werd waargenomen voor alle laden modi, hebben we de neiging om te geloven dat de hoge frequentie laden door middel van WBV heeft de meeste potentie.

References

Adell R, Lekholm U, Rockler B, Branemark PI (1981). A 15-year study of osseointegrated implants in the treatment of the edentulous jaw. *Int J Oral Surg* 10(6)*:*387-416.

Akagawa Y, Hashimoto M, Kondo N, Satomi K, Takata T, Tsuru H (1986). Initial bone-implant interfaces of submergible and supramergible endosseous single-crystal sapphire implants. *J Prosthet Dent* 55(1)*:*96-100.

Akca K, Sarac E, Baysal U, Fanuscu M, Chang TL, Cehreli M (2007). Micro-morphologic changes around biophysically-stimulated titanium implants in ovariectomized rats. *Head Face Med* 3(28.

Albrektsson T, Branemark PI, Hansson HA, Lindstrom J (1981). Osseointegrated titanium implants. Requirements for ensuring a long-lasting, direct bone-to-implant anchorage in man. *Acta Orthop Scand* 52(2)*:*155-170.

Arnsdorf EJ, Tummala P, Kwon RY, Jacobs CR (2009). Mechanically induced osteogenic differentiation--the role of RhoA, ROCKII and cytoskeletal dynamics. *J Cell Sci* 122(Pt 4)*:*546-553.

Attard NJ, Zarb GA (2005). Immediate and early implant loading protocols: a literature review of clinical studies. *J Prosthet Dent* 94(3)*:*242-258.

Avila G, Galindo P, Rios H, Wang HL (2007). Immediate implant loading: current status from available literature. *Implant Dent* 16(3)*:*235-245.

Balatsouka D, Gotfredsen K, Lindh CH, Berglundh T (2005). The impact of nicotine on bone healing and osseointegration. *Clin Oral Implants Res* 16(3)*:*268-276.

Baron R, Tross R, Vignery A (1984). Evidence of sequential remodeling in rat trabecular bone: morphology, dynamic histomorphometry, and changes during skeletal maturation. *Anat Rec* 208(1)*:*137-145.

Berglundh T, Abrahamsson I, Lang NP, Lindhe J (2003). De novo alveolar bone formation adjacent to endosseous implants. *Clin Oral Implants Res* 14(3)*:*251-262.

Bischof M, Nedir R, Szmukler-Moncler S, Bernard JP, Samson J (2004). Implant stability measurement of delayed and immediately loaded implants during healing. *Clin Oral Implants Res* 15(5)*:*529-539.

Bonewald LF, Johnson ML (2008). Osteocytes, mechanosensing and Wnt signaling. *Bone* 42(4)*:*606-615.

Botticelli D, Berglundh T, Buser D, Lindhe J (2003). Appositional bone formation in marginal defects at implants. *Clin Oral Implants Res* 14(1)*:*1-9.

Botticelli D, Berglundh T, Persson LG, Lindhe J (2005). Bone regeneration at implants with turned or rough surfaces in self-contained defects. An experimental study in the dog. *J Clin Periodontol* 32(5)*:*448-455.

Boyce BF, Xing L (2008). Functions of RANKL/RANK/OPG in bone modeling and remodeling. *Arch Biochem Biophys* 473(2)*:*139-146.

Branemark PI (1959). Vital microscopy of bone marrow in rabbit. *Scand J Clin Lab Invest* 11(Supp 38)*:*1-82.

Branemark PI, Hansson BO, Adell R, Breine U, Lindstrom J, Hallen O *et al.* (1977). Osseointegrated implants in the treatment of the edentulous jaw. Experience from a 10-year period. *Scand J Plast Reconstr Surg Suppl* 16(1-132.

Branemark PI (1983). Osseointegration and its experimental background. *J Prosthet Dent* 50(3)*:*399-410.

Branemark PI, Adell R, Albrektsson T, Lekholm U, Lundkvist S, Rockler B (1983). Osseointegrated titanium fixtures in the treatment of edentulousness. *Biomaterials* 4(1)*:*25-28.

Brunski JB, Moccia AF, Jr., Pollack SR, Korostoff E, Trachtenberg DI (1979). The influence of functional use of endosseous dental implants on the tissue-implant interface. I. Histological aspects. *J Dent Res* 58(10)*:*1953-1969.

Brunski JB (1999). In vivo bone response to biomechanical loading at the bone/dental-implant interface. *Adv Dent Res* 13(99-119.

Brunski JB, Puleo DA, Nanci A (2000). Biomaterials and biomechanics of oral and maxillofacial implants: current status and future developments. *Int J Oral Maxillofac Implants* 15(1)*:*15-46.

Buchter A, Wiechmann D, Koerdt S, Wiesmann HP, Piffko J, Meyer U (2005). Load-related implant reaction of mini-implants used for orthodontic anchorage. *Clin Oral Implants Res* 16(4)*:*473-479.

Burr DB, Robling AG, Turner CH (2002). Effects of biomechanical stress on bones in animals. *Bone* 30(5)*:*781-786.

Cameron HU, Pilliar RM, MacNab I (1973). The effect of movement on the bonding of porous metal to bone. *J Biomed Mater Res* 7(4)*:*301-311.

Carrillo Garcia C, Boronat Lopez A, Penarrocha Diago M (2008). Immediately restored dental implants for partial-arch applications. A literature update. *Med Oral Patol Oral Cir Bucal* 13(7)*:*E451-455.

Carter DR, Beaupre GS, Giori NJ, Helms JA (1998). Mechanobiology of skeletal regeneration. *Clin Orthop Relat Res* 355 Suppl)*:*S41-55.

Castillo AB, Alam I, Tanaka SM, Levenda J, Li J, Warden SJ *et al.* (2006). Low-amplitude, broad-frequency vibration effects on cortical bone formation in mice. *Bone* 39(5)*:*1087-1096.

Christiansen BA, Silva MJ (2006). The effect of varying magnitudes of whole-body vibration on several skeletal sites in mice. *Ann Biomed Eng* 34(7)*:*1149-1156.

Christiansen BA, Kotiya AA, Silva MJ (2009). Constrained tibial vibration does not produce an anabolic bone response in adult mice. *Bone* 45(4)*:*750-759.

Clark PA, Rodriguez A, Sumner DR, Hussain MA, Mao JJ (2005). Modulation of bone ingrowth of rabbit femur titanium implants by in vivo axial micromechanical loading. *J Appl Physiol* 98(5)*:*1922-1929.

Cornelini R, Artese L, Rubini C, Fioroni M, Ferrero G, Santinelli A *et al.* (2001). Vascular endothelial growth factor and microvessel density around healthy and failing dental implants. *Int J Oral Maxillofac Implants* 16(3)*:*389-393.

Cullen DM, Smith RT, Akhter MP (2000). Time course for bone formation with long-term external mechanical loading. *J Appl Physiol* 88(6)*:*1943-1948.

Cullen DM, Smith RT, Akhter MP (2001). Bone-loading response varies with strain magnitude and cycle number. *J Appl Physiol* 91(5)*:*1971-1976.

Datta HK, Ng WF, Walker JA, Tuck SP, Varanasi SS (2008). The cell biology of bone metabolism. *J Clin Pathol* 61(5)*:*577-587.

Davies JE (1998). Mechanisms of endosseous integration. *Int J Prosthodont* 11(5)*:*391-401.

Davies JE (2003). Understanding peri-implant endosseous healing. *J Dent Educ* 67(8)*:*932-949.

De Smet E, Jaecques S, Vandamme K, Vander Sloten J, Naert I (2005). Positive effect of early loading on implant stability in the bi-cortical guinea-pig model. *Clin Oral Implants Res* 16(4)*:*402-407.

De Smet E, Jaecques SV, Wevers M, Jansen JA, Jacobs R, Sloten JV *et al.* (2006). Effect of controlled early implant loading on bone healing and bone mass in guinea pigs, as assessed by micro-CT and histology. *Eur J Oral Sci* 114(3)*:*232-242.

De Smet E, Jaecques SV, Jansen JJ, Walboomers F, Vander Sloten J, Naert IE (2007). Effect of constant strain rate, composed of varying amplitude and frequency, of early loading on peri-implant bone (re)modelling. *J Clin Periodontol* 34(7)*:*618-624.

De Smet E, Jaecques SV, Jansen JJ, Walboomers F, Vander Sloten J, Naert IE (2008). Effect of strain at low-frequency loading on peri-implant bone (re)modelling: a guinea-pig experimental study. *Clin Oral Implants Res* 19(8)*:*733-739.

De Smet E, Jaecques SV, Wevers M, Sloten JV, Naert IE (2011). Constant Strain Rate and Peri-Implant Bone Modeling: An In Vivo Longitudinal Micro-CT Analysis. *Clin Implant Dent Relat Res.*

De Souza RL, Matsuura M, Eckstein F, Rawlinson SC, Lanyon LE, Pitsillides AA (2005). Non-invasive axial loading of mouse tibiae increases cortical bone formation and modifies trabecular organization: a new model to study cortical and cancellous compartments in a single loaded element. *Bone* 37(6)*:*810-818.

Degidi M, Piattelli A (2005). 7-year follow-up of 93 immediately loaded titanium dental implants. *J Oral Implantol* 31(1)*:*25-31.

Duyck J, Cooman MD, Puers R, Van Oosterwyck H, Sloten JV, Naert I (2004). A repeated sampling bone chamber methodology for the evaluation of tissue differentiation and bone adaptation around titanium implants under controlled mechanical conditions. *J Biomech* 37(12)*:*1819-1822.

Duyck J, Vrielinck L, Lambrichts I, Abe Y, Schepers S, Politis C *et al.* (2005). Biologic response of immediately versus delayed loaded implants supporting ill-fitting prostheses: an animal study. *Clin Implant Dent Relat Res* 7(3)*:*150-158.

Duyck J, Vandamme K, Geris L, Van Oosterwyck H, De Cooman M, Vandersloten J *et al.* (2006). The influence of micro-motion on the tissue differentiation around immediately loaded cylindrical turned titanium implants. *Arch Oral Biol* 51(1)*:*1-9.

Duyck J, Slaets E, Sasaguri K, Vandamme K, Naert I (2007). Effect of intermittent loading and surface roughness on peri-implant bone formation in a bone chamber model. *J Clin Periodontol* 34(11)*:*998-1006.

Ehrlich PJ, Lanyon LE (2002). Mechanical strain and bone cell function: a review. *Osteoporos Int* 13(9)*:*688-700.

Eriksson C, Ohlson K, Richter K, Billerdahl N, Johansson M, Nygren H (2007). Callus formation and remodeling at titanium implants. *J Biomed Mater Res A* 83(4)*:*1062-1069.

Esposito M, Hirsch JM, Lekholm U, Thomsen P (1998a). Biological factors contributing to failures of osseointegrated oral implants. (I). Success criteria and epidemiology. *Eur J Oral Sci* 106(1)*:*527-551.

Esposito M, Hirsch JM, Lekholm U, Thomsen P (1998b). Biological factors contributing to failures of osseointegrated oral implants. (II). Etiopathogenesis. *Eur J Oral Sci* 106(3)*:*721-764.

Esposito M, Grusovin MG, Achille H, Coulthard P, Worthington HV (2009a). Interventions for replacing missing teeth: different times for loading dental implants. *Cochrane Database Syst Rev* 1)*:*CD003878.

Esposito M, Grusovin MG, Chew YS, Coulthard P, Worthington HV (2009b). Interventions for replacing missing teeth: 1- versus 2-stage implant placement. *Cochrane Database Syst Rev* 3)*:*CD006698.

Ferguson SJ, Langhoff JD, Voelter K, von Rechenberg B, Scharnweber D, Bierbaum S *et al.* (2008). Biomechanical comparison of different surface modifications for dental implants. *Int J Oral Maxillofac Implants* 23(6)*:*1037-1046.

Fini M, Giavaresi G, Torricelli P, Borsari V, Giardino R, Nicolini A *et al.* (2004). Osteoporosis and biomaterial osteointegration. *Biomed Pharmacother* 58(9)*:*487-493.

Forwood MR, Bennett MB, Blowers AR, Nadorfi RL (1998). Modification of the in vivo four-point loading model for studying mechanically induced bone adaptation. *Bone* 23(3)*:*307-310.

Franchi M, Fini M, Martini D, Orsini E, Leonardi L, Ruggeri A *et al.* (2005). Biological fixation of endosseous implants. *Micron* 36(7-8)*:*665-671.

Fritton JC, Myers ER, Wright TM, van der Meulen MC (2005). Loading induces site-specific increases in mineral content assessed by microcomputed tomography of the mouse tibia. *Bone* 36(6)*:*1030-1038.

Frost HM (1992). Perspectives: bone's mechanical usage windows. *Bone Miner* 19(3)*:*257-271.

Frost HM (2004). A 2003 update of bone physiology and Wolff's Law for clinicians. *Angle Orthod* 74(1)*:*3-15.

Gahlert M, Gudehus T, Eichhorn S, Steinhauser E, Kniha H, Erhardt W (2007). Biomechanical and histomorphometric comparison between zirconia implants with varying surface textures and a titanium implant in the maxilla of miniature pigs. *Clin Oral Implants Res* 18(5)*:*662-668.

Gapski R, Wang HL, Mascarenhas P, Lang NP (2003). Critical review of immediate implant loading. *Clin Oral Implants Res* 14(5)*:*515-527.

Garman R, Gaudette G, Donahue LR, Rubin C, Judex S (2007a). Low-level accelerations applied in the absence of weight bearing can enhance trabecular bone formation. *J Orthop Res* 25(6)*:*732-740.

Garman R, Rubin C, Judex S (2007b). Small oscillatory accelerations, independent of matrix deformations, increase osteoblast activity and enhance bone morphology. *PLoS One* 2(7)*:*e653.

Geris L, Vandamme K, Naert I, Vander Sloten J, Van Oosterwyck H, Duyck J (2010). Mechanical loading affects angiogenesis and osteogenesis in an in vivo bone chamber: a modeling study. *Tissue Eng Part A* 16(11)*:*3353-3361.

Gilsanz V, Wren TA, Sanchez M, Dorey F, Judex S, Rubin C (2006). Low-level, high-frequency mechanical signals enhance musculoskeletal development of young women with low BMD. *J Bone Miner Res* 21(9)*:*1464-1474.

Goodship AE, Cunningham JL, Kenwright J (1998). Strain rate and timing of stimulation in mechanical modulation of fracture healing. *Clin Orthop Relat Res* 355 Suppl)*:*S105-115.

Goodship AE, Lawes TJ, Rubin CT (2009). Low-magnitude high-frequency mechanical signals accelerate and augment endochondral bone repair: preliminary evidence of efficacy. *J Orthop Res* 27(7)*:*922-930.

Gotfredsen K, Berglundh T, Lindhe J (2002). Bone reactions at implants subjected to experimental peri-implantitis and static load. A study in the dog. *J Clin Periodontol* 29(2)*:*144-151.

Gross TS, Srinivasan S, Liu CC, Clemens TL, Bain SD (2002). Noninvasive loading of the murine tibia: an in vivo model for the study of mechanotransduction. *J Bone Miner Res* 17(3)*:*493-501.

Han Y, Cowin SC, Schaffler MB, Weinbaum S (2004). Mechanotransduction and strain amplification in osteocyte cell processes. *Proc Natl Acad Sci U S A* 101(47)*:*16689-16694.

Hazenberg JG, Freeley M, Foran E, Lee TC, Taylor D (2006). Microdamage: a cell transducing mechanism based on ruptured osteocyte processes. *J Biomech* 39(11)*:*2096-2103.

Hert J, Liskova M, Landa J (1971). Reaction of bone to mechanical stimuli. 1. Continuous and intermittent loading of tibia in rabbit. *Folia Morphol (Praha)* 19(3)*:*290-300.

Hsieh YF, Turner CH (2001). Effects of loading frequency on mechanically induced bone formation. *J Bone Miner Res* 16(5)*:*918-924.

Huang H, Kamm RD, Lee RT (2004). Cell mechanics and mechanotransduction: pathways, probes, and physiology. *Am J Physiol Cell Physiol* 287(1)*:*C1-11.

Hwang SJ, Lublinsky S, Seo YK, Kim IS, Judex S (2009). Extremely small-magnitude accelerations enhance bone regeneration: a preliminary study. *Clin Orthop Relat Res* 467(4)*:*1083-1091.

Inman CL, Warren GL, Hogan HA, Bloomfield SA (1999). Mechanical loading attenuates bone loss due to immobilization and calcium deficiency. *J Appl Physiol* 87(1)*:*189-195.

Isidor F (1996). Loss of osseointegration caused by occlusal load of oral implants. A clinical and radiographic study in monkeys. *Clin Oral Implants Res* 7(2)*:*143-152.

Isidor F (1997). Histological evaluation of peri-implant bone at implants subjected to occlusal overload or plaque accumulation. *Clin Oral Implants Res* 8(1)*:*1-9.

Isidor F (2006). Influence of forces on peri-implant bone. *Clin Oral Implants Res* 17 Suppl 2(8-18.

Jemt T, Stenport V, Friberg B (2011). Implant treatment with fixed prostheses in the edentulous maxilla. Part 1: implants and biologic response in two patient cohorts restored between 1986 and 1987 and 15 years later. *Int J Prosthodont* 24(4)*:*345-355.

Judex S, Zernicke RF (2000). High-impact exercise and growing bone: relation between high strain rates and enhanced bone formation. *J Appl Physiol* 88(6)*:*2183-2191.

Judex S, Lei X, Han D, Rubin C (2007). Low-magnitude mechanical signals that stimulate bone formation in the ovariectomized rat are dependent on the applied frequency but not on the strain magnitude. *J Biomech* 40(6)*:*1333-1339.

Judex S, Gupta S, Rubin C (2009). Regulation of mechanical signals in bone. *Orthod Craniofac Res* 12(2)*:*94-104.

Judex S, Rubin CT (2010). Is bone formation induced by high-frequency mechanical signals modulated by muscle activity? *J Musculoskelet Neuronal Interact* 10(1)*:*3-11.

Katagiri T, Takahashi N (2002). Regulatory mechanisms of osteoblast and osteoclast differentiation. *Oral Dis* 8(3)*:*147-159.

Kawai Y, Taylor JA (2007). Effect of loading time on the success of complete mandibular titanium implant retained overdentures: a systematic review. *Clin Oral Implants Res* 18(4)*:*399-408.

Kelly DJ, Jacobs CR (2010). The role of mechanical signals in regulating chondrogenesis and osteogenesis of mesenchymal stem cells. *Birth Defects Res C Embryo Today* 90(1)*:*75-85.

Kim SH, Choi BH, Li J, Kim HS, Ko CY, Jeong SM *et al.* (2008). Peri-implant bone reactions at delayed and immediately loaded implants: an experimental study. *Oral Surg Oral Med Oral Pathol Oral Radiol Endod* 105(2)*:*144-148.

Kim Y, Oh TJ, Misch CE, Wang HL (2005). Occlusal considerations in implant therapy: clinical guidelines with biomechanical rationale. *Clin Oral Implants Res* 16(1)*:*26-35.

Klein-Nulend J, Bacabac RG, Mullender MG (2005). Mechanobiology of bone tissue. *Pathol Biol (Paris)* 53(10)*:*576-580.

Klinger A, Mijiritsky E, Kohavi D (2006). Biological and clinical rationale for early implant loading. *Compend Contin Educ Dent* 27(1)*:*29-34; quiz 35-26.

Kokkinos PA, Zarkadis IK, Kletsas D, Deligianni DD (2009). Effects of physiological mechanical strains on the release of growth factors and the expression of differentiation marker genes in human osteoblasts growing on Ti-6Al-4V. *J Biomed Mater Res A* 90(2)*:*387-395.

Kozlovsky A, Tal H, Laufer BZ, Leshem R, Rohrer MD, Weinreb M *et al.* (2007). Impact of implant overloading on the peri-implant bone in inflamed and non-inflamed peri-implant mucosa. *Clin Oral Implants Res* 18(5)*:*601-610.

Kuruvilla SJ, Fox SD, Cullen DM, Akhter MP (2008). Site specific bone adaptation response to mechanical loading. *J Musculoskelet Neuronal Interact* 8(1)*:*71-78.

LaMothe JM, Hamilton NH, Zernicke RF (2005). Strain rate influences periosteal adaptation in mature bone. *Med Eng Phys* 27(4)*:*277-284.

Lee JY, Kim SG, Moon SY, Lim SC, Ong JL, Lee KM (2009). A short-term study on immediate functional loading and immediate nonfunctional loading implant in dogs: histomorphometric evaluation of bone reaction. *Oral Surg Oral Med Oral Pathol Oral Radiol Endod* 107(4)*:*519-524.

Lee KC, Maxwell A, Lanyon LE (2002). Validation of a technique for studying functional adaptation of the mouse ulna in response to mechanical loading. *Bone* 31(3)*:*407-412.

Leonard G, Coelho P, Polyzois I, Stassen L, Claffey N (2009). A study of the bone healing kinetics of plateau versus screw root design titanium dental implants. *Clin Oral Implants Res* 20(3)*:*232-239.

Leucht P, Kim JB, Wazen R, Currey JA, Nanci A, Brunski JB *et al.* (2007). Effect of mechanical stimuli on skeletal regeneration around implants. *Bone* 40(4)*:*919-930.

Leung KS, Shi HF, Cheung WH, Qin L, Ng WK, Tam KF *et al.* (2009). Low-magnitude high-frequency vibration accelerates callus formation, mineralization, and fracture healing in rats. *J Orthop Res* 27(4)*:*458-465.

Li YJ, Batra NN, You L, Meier SC, Coe IA, Yellowley CE *et al.* (2004). Oscillatory fluid flow affects human marrow stromal cell proliferation and differentiation. *J Orthop Res* 22(6)*:*1283-1289.

Liddelow G, Klineberg I (2011). Patient-related risk factors for implant therapy. A critique of pertinent literature. *Aust Dent J* 56(4)*:*417-426; quiz 441.

Linder L, Albrektsson T, Branemark PI, Hansson HA, Ivarsson B, Jonsson U *et al.* (1983). Electron microscopic analysis of the bone-titanium interface. *Acta Orthop Scand* 54(1)*:*45-52.

Livak KJ, Schmittgen TD (2001). Analysis of relative gene expression data using real-time quantitative PCR and the 2(-Delta Delta C(T)) Method. *Methods* 25(4)*:*402-408.

Loening AM, Gambhir SS (2003). AMIDE: a free software tool for multimodality medical image analysis. *Mol Imaging* 2(3)*:*131-137.

Marco F, Milena F, Gianluca G, Vittoria O (2005). Peri-implant osteogenesis in health and osteoporosis. *Micron* 36(7-8)*:*630-644.

Matsuo M, Nakamura T, Kishi Y, Takahashi K (1999). Microvascular changes after placement of titanium implants: scanning electron microscopy observations of machined and titanium plasma-sprayed implants in dogs. *J Periodontol* 70(11)*:*1330-1338.

McCracken M, Zinn K, Lemons JE, Thompson JA, Feldman D (2001). Radioimaging of implants in rats using Tc-99m-MDP. *Clin Oral Implants Res* 12(4)*:*372-378.

Mellal A, Wiskott HW, Botsis J, Scherrer SS, Belser UC (2004). Stimulating effect of implant loading on surrounding bone. Comparison of three numerical models and validation by in vivo data. *Clin Oral Implants Res* 15(2)*:*239-248.

Mertens C, Steveling HG (2011). Early and immediate loading of titanium implants with fluoride-modified surfaces: results of 5-year prospective study. *Clin Oral Implants Res*.

Meyer U, Joos U, Mythili J, Stamm T, Hohoff A, Fillies T *et al.* (2004). Ultrastructural characterization of the implant/bone interface of immediately loaded dental implants. *Biomaterials* 25(10)*:*1959-1967.

Miyata T, Kobayashi Y, Araki H, Ohto T, Shin K (2000). The influence of controlled occlusal overload on peri-implant tissue. Part 3: A histologic study in monkeys. *Int J Oral Maxillofac Implants* 15(3)*:*425-431.

Monjo M, Lamolle SF, Lyngstadaas SP, Ronold HJ, Ellingsen JE (2008). In vivo expression of osteogenic markers and bone mineral density at the surface of fluoride-modified titanium implants. *Biomaterials* 29(28)*:*3771-3780.

Morimoto T, Inoue T, Nakamura T, Kawamura Y (1984). Frequency-dependent modulation of rhythmic human jaw movements. *J Dent Res* 63(11)*:*1310-1314.

Mosley JR, March BM, Lynch J, Lanyon LE (1997). Strain magnitude related changes in whole bone architecture in growing rats. *Bone* 20(3)*:*191-198.

Mosley JR, Lanyon LE (1998). Strain rate as a controlling influence on adaptive modeling in response to dynamic loading of the ulna in growing male rats. *Bone* 23(4)*:*313-318.

Muir J, Judex S, Qin YX, Rubin C (2011). Postural instability caused by extended bed rest is alleviated by brief daily exposure to low magnitude mechanical signals. *Gait Posture* 33(3)*:*429-435.

Murai K, Takeshita F, Ayukawa Y, Kiyoshima T, Suetsugu T, Tanaka T (1996). Light and electron microscopic studies of bone-titanium interface in the tibiae of young and mature rats. *J Biomed Mater Res* 30(4)*:*523-533.

Naert I, Duyck J, Vandamme K (2012). Occlusal overload and bone/implant loss. *Clin Oral Implants Res* 23 Suppl 6(95-107.

Novaes AB, Jr., de Souza SL, de Barros RR, Pereira KK, Iezzi G, Piattelli A (2010). Influence of implant surfaces on osseointegration. *Braz Dent J* 21(6)*:*471-481.

Ogawa T, Possemiers T, Zhang X, Naert I, Chaudhari A, Sasaki K *et al.* (2011a). Influence of whole-body vibration time on peri-implant bone healing: a histomorphometrical animal study. *J Clin Periodontol* 38(2)*:*180-185.

Ogawa T, Zhang X, Naert I, Vermaelen P, Deroose CM, Sasaki K *et al.* (2011b). The effect of whole-body vibration on peri-implant bone healing in rats. *Clin Oral Implants Res* 22(3)*:*302-307.

Omar H, Shen G, Jones AS, Zoellner H, Petocz P, Darendeliler MA (2008). Effect of low magnitude and high frequency mechanical stimuli on defects healing in cranial bones. *J Oral Maxillofac Surg* 66(6)*:*1104-1111.

Omar O, Svensson S, Zoric N, Lenneras M, Suska F, Wigren S *et al.* (2010). In vivo gene expression in response to anodically oxidized versus machined titanium implants. *J Biomed Mater Res A* 92(4)*:*1552-1566.

Omar OM, Lenneras ME, Suska F, Emanuelsson L, Hall JM, Palmquist A *et al.* (2011). The correlation between gene expression of proinflammatory markers and bone formation during osseointegration with titanium implants. *Biomaterials* 32(2)*:*374-386.

Oxlund BS, Ortoft G, Andreassen TT, Oxlund H (2003). Low-intensity, high-frequency vibration appears to prevent the decrease in strength of the femur and tibia associated with ovariectomy of adult rats. *Bone* 32(1)*:*69-77.

Ozcivici E, Luu YK, Adler B, Qin YX, Rubin J, Judex S *et al.* (2010a). Mechanical signals as anabolic agents in bone. *Nat Rev Rheumatol* 6(1)*:*50-59.

Ozcivici E, Luu YK, Rubin CT, Judex S (2010b). Low-level vibrations retain bone marrow's osteogenic potential and augment recovery of trabecular bone during reambulation. *PLoS One* 5(6)*:*e11178.

Parfitt AM (2001). The bone remodeling compartment: a circulatory function for bone lining cells. *J Bone Miner Res* 16(9)*:*1583-1585.

Pearce AI, Richards RG, Milz S, Schneider E, Pearce SG (2007). Animal models for implant biomaterial research in bone: a review. *Eur Cell Mater* 13(1-10.

Piattelli A, Ruggeri A, Franchi M, Romasco N, Trisi P (1993). An histologic and histomorphometric study of bone reactions to unloaded and loaded non-submerged single implants in monkeys: a pilot study. *J Oral Implantol* 19(4)*:*314-320.

Pilliar RM, Lee JM, Maniatopoulos C (1986). Observations on the effect of movement on bone ingrowth into porous-surfaced implants. *Clin Orthop Relat Res* 208)*:*108-113.

Probst A, Spiegel HU (1997). Cellular mechanisms of bone repair. *J Invest Surg* 10(3)*:*77-86.

Quinlan P, Nummikoski P, Schenk R, Cagna D, Mellonig J, Higginbottom F *et al.* (2005). Immediate and early loading of SLA ITI single-tooth implants: an in vivo study. *Int J Oral Maxillofac Implants* 20(3)*:*360-370.

Quirynen M, Naert I, van Steenberghe D (1992). Fixture design and overload influence marginal bone loss and fixture success in the Branemark system. *Clin Oral Implants Res* 3(3)*:*104-111.

Rangert B, Jemt T, Jorneus L (1989). Forces and moments on Branemark implants. *Int J Oral Maxillofac Implants* 4(3)*:*241-247.

Rittweger J, Beller G, Armbrecht G, Mulder E, Buehring B, Gast U *et al.* (2010). Prevention of bone loss during 56 days of strict bed rest by side-alternating resistive vibration exercise. *Bone* 46(1)*:*137-147.

Robling AG, Burr DB, Turner CH (2000). Partitioning a daily mechanical stimulus into discrete loading bouts improves the osteogenic response to loading. *J Bone Miner Res* 15(8)*:*1596-1602.

Robling AG, Burr DB, Turner CH (2001a). Recovery periods restore mechanosensitivity to dynamically loaded bone. *J Exp Biol* 204(Pt 19)*:*3389-3399.

Robling AG, Duijvelaar KM, Geevers JV, Ohashi N, Turner CH (2001b). Modulation of appositional and longitudinal bone growth in the rat ulna by applied static and dynamic force. *Bone* 29(2)*:*105-113.

Robling AG, Hinant FM, Burr DB, Turner CH (2002). Improved bone structure and strength after long-term mechanical loading is greatest if loading is separated into short bouts. *J Bone Miner Res* 17(8)*:*1545-1554.

Robling AG, Turner CH (2009). Mechanical signaling for bone modeling and remodeling. *Crit Rev Eukaryot Gene Expr* 19(4)*:*319-338.

Romanos G, Froum S, Hery C, Cho SC, Tarnow D (2010). Survival rate of immediately vs delayed loaded implants: analysis of the current literature. *J Oral Implantol* 36(4)*:*315-324.

Romanos GE, Toh CG, Siar CH, Wicht H, Yacoob H, Nentwig GH (2003). Bone-implant interface around titanium implants under different loading conditions: a histomorphometrical analysis in the Macaca fascicularis monkey. *J Periodontol* 74(10)*:*1483-1490.

Romanos GE (2004). Present status of immediate loading of oral implants. *J Oral Implantol* 30(3)*:*189-197.

Rosenberg ES, Torosian JP, Slots J (1991). Microbial differences in 2 clinically distinct types of failures of osseointegrated implants. *Clin Oral Implants Res* 2(3)*:*135-144.

Rubin C, Turner AS, Bain S, Mallinckrodt C, McLeod K (2001a). Anabolism. Low mechanical signals strengthen long bones. *Nature* 412(6847)*:*603-604.

Rubin C, Xu G, Judex S (2001b). The anabolic activity of bone tissue, suppressed by disuse, is normalized by brief exposure to extremely low-magnitude mechanical stimuli. *FASEB J* 15(12)*:*2225-2229.

Rubin C, Turner AS, Mallinckrodt C, Jerome C, McLeod K, Bain S (2002). Mechanical strain, induced noninvasively in the high-frequency domain, is anabolic to cancellous bone, but not cortical bone. *Bone* 30(3)*:*445-452.

Rubin C, Recker R, Cullen D, Ryaby J, McCabe J, McLeod K (2004). Prevention of postmenopausal bone loss by a low-magnitude, high-frequency mechanical stimuli: a clinical trial assessing compliance, efficacy, and safety. *J Bone Miner Res* 19(3)*:*343-351.

Rubin CT, Lanyon LE (1984). Regulation of bone formation by applied dynamic loads. *J Bone Joint Surg Am* 66(3)*:*397-402.

Rubin CT, McLeod KJ (1994). Promotion of bony ingrowth by frequency-specific, low-amplitude mechanical strain. *Clin Orthop Relat Res* 298)*:*165-174.

Sasaki H, Koyama S, Yokoyama M, Yamaguchi K, Itoh M, Sasaki K (2008). Bone metabolic activity around dental implants under loading observed using bone scintigraphy. *Int J Oral Maxillofac Implants* 23(5)*:*827-834.

Schindeler A, McDonald MM, Bokko P, Little DG (2008). Bone remodeling during fracture repair: The cellular picture. *Semin Cell Dev Biol* 19(5)*:*459-466.

Seeman E (2006). Osteocytes--martyrs for integrity of bone strength. *Osteoporos Int* 17(10)*:*1443-1448.

Sehmisch S, Galal R, Kolios L, Tezval M, Dullin C, Zimmer S *et al.* (2009). Effects of low-magnitude, high-frequency mechanical stimulation in the rat osteopenia model. *Osteoporos Int* 20(12)*:*1999-2008.

Shi HF, Cheung WH, Qin L, Leung AH, Leung KS (2010). Low-magnitude high-frequency vibration treatment augments fracture healing in ovariectomy-induced osteoporotic bone. *Bone* 46(5)*:*1299-1305.

Silva MJ, Brodt MD (2008). Mechanical stimulation of bone formation is normal in the SAMP6 mouse. *Calcif Tissue Int* 82(6)*:*489-497.

Simmons CA, Valiquette N, Pilliar RM (1999). Osseointegration of sintered porous-surfaced and plasma spray-coated implants: An animal model study of early postimplantation healing response and mechanical stability. *J Biomed Mater Res* 47(2)*:*127-138.

Simmons CA, Meguid SA, Pilliar RM (2001a). Differences in osseointegration rate due to implant surface geometry can be explained by local tissue strains. *J Orthop Res* 19(2)*:*187-194.

Simmons CA, Meguid SA, Pilliar RM (2001b). Mechanical regulation of localized and appositional bone formation around bone-interfacing implants. *J Biomed Mater Res* 55(1)*:*63-71.

Slaets E, Carmeliet G, Naert I, Duyck J (2006). Early cellular responses in cortical bone healing around unloaded titanium implants: an animal study. *J Periodontol* 77(6)*:*1015-1024.

Slaets E, Carmeliet G, Naert I, Duyck J (2007). Early trabecular bone healing around titanium implants: a histologic study in rabbits. *J Periodontol* 78(3)*:*510-517.

Slaets E, Naert I, Carmeliet G, Duyck J (2009). Early cortical bone healing around loaded titanium implants: a histological study in the rabbit. *Clin Oral Implants Res* 20(2)*:*126-134.

Soballe K, Hansen ES, H BR, Jorgensen PH, Bunger C (1992). Tissue ingrowth into titanium and hydroxyapatite-coated implants during stable and unstable mechanical conditions. *J Orthop Res* 10(2)*:*285-299.

Srinivasan S, Agans SC, King KA, Moy NY, Poliachik SL, Gross TS (2003). Enabling bone formation in the aged skeleton via rest-inserted mechanical loading. *Bone* 33(6)*:*946-955.

Srinivasan S, Ausk BJ, Poliachik SL, Warner SE, Richardson TS, Gross TS (2007). Rest-inserted loading rapidly amplifies the response of bone to small increases in strain and load cycles. *J Appl Physiol* 102(5)*:*1945-1952.

Stadelmann VA, Terrier A, Pioletti DP (2008). Microstimulation at the bone-implant interface upregulates osteoclast activation pathways. *Bone* 42(2)*:*358-364.

Stadlinger B, Bierbaum S, Grimmer S, Schulz MC, Kuhlisch E, Scharnweber D *et al.* (2009). Increased bone formation around coated implants. *J Clin Periodontol* 36(8)*:*698-704.

Sugiyama T, Saxon LK, Zaman G, Moustafa A, Sunters A, Price JS *et al.* (2008). Mechanical loading enhances the anabolic effects of intermittent parathyroid hormone (1-34) on trabecular and cortical bone in mice. *Bone* 43(2)*:*238-248.

Szmukler-Moncler S, Salama H, Reingewirtz Y, Dubruille JH (1998). Timing of loading and effect of micromotion on bone-dental implant interface: review of experimental literature. *J Biomed Mater Res* 43(2)*:*192-203.

Takeda T, Narita T, Ito H (2004). Experimental study on the effect of mechanical stimulation on the early stage of fracture healing. *J Nihon Med Sch* 71(4)*:*252-262.

Tanaka SM, Alam IM, Turner CH (2003). Stochastic resonance in osteogenic response to mechanical loading. *FASEB J* 17(2)*:*313-314.

Torcasio A, van Lenthe GH, Van Oosterwyck H (2008). The importance of loading frequency, rate and vibration for enhancing bone adaptation and implant osseointegration. *Eur Cell Mater* 16(56-68.

Torcasio A, Zhang X, Van Oosterwyck H, Duyck J, van Lenthe GH (2011). Use of micro-CT-based finite element analysis to accurately quantify peri-implant bone strains: a validation in rat tibiae. *Biomech Model Mechanobiol*.

Torcasio A, Zhang X, Duyck J, van Lenthe GH (2012). 3D characterization of bone strains in the rat tibia loading model. *Biomech Model Mechanobiol* 11(3-4)*:*403-410.

Torrance AG, Mosley JR, Suswillo RF, Lanyon LE (1994). Noninvasive loading of the rat ulna in vivo induces a strain-related modeling response uncomplicated by trauma or periostal pressure. *Calcif Tissue Int* 54(3)*:*241-247.

Traini T, Assenza B, San Roman F, Thams U, Caputi S, Piattelli A (2006). Bone microvascular pattern around loaded dental implants in a canine model. *Clin Oral Investig* 10(2)*:*151-156.

Turner CH, Forwood MR, Otter MW (1994). Mechanotransduction in bone: do bone cells act as sensors of fluid flow? *FASEB J* 8(11)*:*875-878.

Turner CH, Owan I, Takano Y (1995). Mechanotransduction in bone: role of strain rate. *Am J Physiol* 269(3 Pt 1)*:*E438-442.

Turner CH (1999). Toward a mathematical description of bone biology: the principle of cellular accommodation. *Calcif Tissue Int* 65(6)*:*466-471.

Turner CH (2006). Bone strength: current concepts. *Ann N Y Acad Sci* 1068(429-446.

Turner CH, Warden SJ, Bellido T, Plotkin LI, Kumar N, Jasiuk I *et al.* (2009). Mechanobiology of the skeleton. *Sci Signal* 2(68)*:*pt3.

Umemura Y, Ishiko T, Yamauchi T, Kurono M, Mashiko S (1997). Five jumps per day increase bone mass and breaking force in rats. *J Bone Miner Res* 12(9)*:*1480-1485.

Umemura Y, Sogo N, Honda A (2002). Effects of intervals between jumps or bouts on osteogenic response to loading. *J Appl Physiol* 93(4)*:*1345-1348.

Vandamme K, Naert I, Geris L, Sloten JV, Puers R, Duyck J (2007a). Histodynamics of bone tissue formation around immediately loaded cylindrical implants in the rabbit. *Clin Oral Implants Res* 18(4)*:*471-480.

Vandamme K, Naert I, Geris L, Vander Sloten J, Puers R, Duyck J (2007b). Influence of controlled immediate loading and implant design on peri-implant bone formation. *J Clin Periodontol* 34(2)*:*172-181.

Vandamme K, Naert I, Geris L, Vander Sloten J, Puers R, Duyck J (2007c). The effect of micro-motion on the tissue response around immediately loaded roughened titanium implants in the rabbit. *Eur J Oral Sci* 115(1)*:*21-29.

Vandamme K, Naert I, Vander Sloten J, Puers R, Duyck J (2008). Effect of implant surface roughness and loading on peri-implant bone formation. *J Periodontol* 79(1)*:*150-157.

Vandamme K, Holy X, Bensidhoum M, Logeart-Avramoglou D, Naert IE, Duyck JA *et al.* (2011). In vivo molecular evidence of delayed titanium implant osseointegration in compromised bone. *Biomaterials* 32(14)*:*3547-3554.

Verborgt O, Gibson GJ, Schaffler MB (2000). Loss of osteocyte integrity in association with microdamage and bone remodeling after fatigue in vivo. *J Bone Miner Res* 15(1)*:*60-67.

Verschueren SM, Roelants M, Delecluse C, Swinnen S, Vanderschueren D, Boonen S (2004). Effect of 6-month whole body vibration training on hip density, muscle strength, and postural control in postmenopausal women: a randomized controlled pilot study. *J Bone Miner Res* 19(3)*:*352-359.

Vignoletti F, Johansson C, Albrektsson T, De Sanctis M, San Roman F, Sanz M (2009). Early healing of implants placed into fresh extraction sockets: an experimental study in the beagle dog. De novo bone formation. *J Clin Periodontol* 36(3)*:*265-277.

Warden SJ, Turner CH (2004). Mechanotransduction in the cortical bone is most efficient at loading frequencies of 5-10 Hz. *Bone* 34(2)*:*261-270.

Weber HP, Morton D, Gallucci GO, Roccuzzo M, Cordaro L, Grutter L (2009). Consensus statements and recommended clinical procedures regarding loading protocols. *Int J Oral Maxillofac Implants* 24 Suppl(180-183.

Wikesjo UM, Huang YH, Xiropaidis AV, Sorensen RG, Rohrer MD, Prasad HS *et al.* (2008). Bone formation at recombinant human bone morphogenetic protein-2-coated titanium implants in the posterior maxilla (Type IV bone) in non-human primates. *J Clin Periodontol* 35(11)*:*992-1000.

Wiskott HW, Belser UC (1999). Lack of integration of smooth titanium surfaces: a working hypothesis based on strains generated in the surrounding bone. *Clin Oral Implants Res* 10(6)*:*429-444.

Wiskott HW, Cugnoni J, Scherrer SS, Ammann P, Botsis J, Belser UC (2008). Bone reactions to controlled loading of endosseous implants: a pilot study. *Clin Oral Implants Res* 19(11)*:*1093-1102.

Wolf S, Augat P, Eckert-Hubner K, Laule A, Krischak GD, Claes LE (2001). Effects of high-frequency, low-magnitude mechanical stimulus on bone healing. *Clin Orthop Relat Res* 385)*:*192-198.

Xie L, Jacobson JM, Choi ES, Busa B, Donahue LR, Miller LM *et al.* (2006). Low-level mechanical vibrations can influence bone resorption and bone formation in the growing skeleton. *Bone* 39(5)*:*1059-1066.

Xie L, Rubin C, Judex S (2008). Enhancement of the adolescent murine musculoskeletal system using low-level mechanical vibrations. *J Appl Physiol* 104(4)*:*1056-1062.

You L, Cowin SC, Schaffler MB, Weinbaum S (2001). A model for strain amplification in the actin cytoskeleton of osteocytes due to fluid drag on pericellular matrix. *J Biomech* 34(11)*:*1375-1386.

Zarb GA, Schmitt A (1990). The longitudinal clinical effectiveness of osseointegrated dental implants: the Toronto study. Part III: Problems and complications encountered. *J Prosthet Dent* 64(2)*:*185-194.

Zhang X, Naert I, Van Schoonhoven D, Duyck J (2012). Direct High-Frequency Stimulation of Peri-Implant Rabbit Bone: A Pilot Study. *Clin Implant Dent Relat Res* 14(4):558-564.

Curriculum vitae

Name	Xiaolei Zhang
Date of birth	26th Dec.1977
Place of birth	Wuhan, China
Street address	Kapucijnenvoer 7 blok a - box 7001, 3000 Leuven, Belgium
Email	xiaolei.zhang@med.kuleuven maxzhang09@hotmail.com

Academic and professional curriculum

1996.9-2001.7	**School of Stomatology, Wuhan University** *Bachelor of Stomatology*
2001.9-2006.7	**School of Stomatology, Wuhan University** *PhD* (under supervision of Prof. Bin Peng)
2006.8-2008.8	**School and Hospital of Stomatology, Tongji University** *Dental practitioner and lecturer*
2008.9-2015.11	**Dental School, KU Leuven** *PhD* (under supervision of Prof. Joke Duyck, Prof. Ignace Naert and Prof. van Lenthe)
2012.3-present	**School and Hospital of Stomatology, Sun Yat-sen University** *Endodontist and associate professor*

Publications in peer reviewed journals

Zhang X., Duyck, J., Vandamme, K., Naert, I., Carmeliet, G. Ultrastructural characterization of the implant interface response to loading. ***Journal of Dental Research*** 2014 Mar;93(3):313-8.

Ogawa T. †, Vandamme K. †, **Zhang X.**, Naert I., Possemiers T., Chaudhari A., Sasaki K., Duyck J*. Stimulation of titanium implant osseointegration through high frequency

vibration loading is enhanced when applied at high acceleration. ***Calcified Tissue International*** 2014 Nov;95(5):467-75. (†: co-first author; *: corresponding author)

Zhang W.[†], **Zhang X.**[†], Junqi Ling[*], Wei Liu, Xinchun Zhang, Jinglei Ma and Jianmao Zheng. Proliferation and odontogenic differentiation of BMP2 gene transfected stem cells from human tooth apical papilla: An *in vitro* study. ***International Journal of Molecular Medicine*** 2014 Oct;34(4):1004-12. (†: co-first author; *: corresponding author)

Tian Y., **Zhang X.**, Zhang K., Song Z., Wang R., Huang S., Lin Z. Effect of Enterococcus faecalis lipoteichoic acid on apoptosis in human osteoblast-like cells. ***Journal of Endodontics*** 2013 May;39(5):632-7.

Zhang X., Torcasio A., Vandamme K., Ogawa T., van Lenthe G.H., Naert I., Duyck J. Enhancement of implant osseointegration by high-frequency low-magnitude loading. ***PLoS ONE*** 2012;7(7)e40488.

Zhang X., Vandamme K., Torcasio A., Ogawa T., van Lenthe G.H., Naert I., Duyck J. *In vivo* assessment of the effect of controlled high- and low-frequency mechanical loading on peri-implant bone healing. ***Journal of the Royal Society Interface*** 2012 Jul 7;9(72):1697-704.

Zhang X., Naert I., Van Schoonhoven D., Duyck J. Direct high-frequency stimulation of peri-implant rabbit bone: a pilot study. ***Clinical Implant Dentistry and Related Research*** 2012 August; 14(4):558-564.

Torcasio A., **Zhang X.**, Duyck J., van Lenthe G.H. 3D characterization of bone strains in the rat tibia loading model. ***Biomechanics and Modeling in Mechanobiology*** 2012 Feb; 11(3):403-10.

Torcasio A., **Zhang X.**, Van Oosterwyck H., Duyck J., van Lenthe G.H. Use of micro-CT-based finite element analysis to accurately quantify peri-implant bone strains: a validation in rat tibiae. ***Biomechanics and Modeling in Mechaniobiology*** 2012 May;11(5):743-50.

Ogawa T., Possemiers T., **Zhang X.**, Naert I., Chaudhari A., Sasaki K., Duyck J. Influence of loading time on the impact of whole body vibration on peri-implant bone healing: a histomorphometrical study on rat. ***Journal of Clinical Periodontology*** 2011 Feb;38(2):180-5.

Ogawa T., **Zhang X.**, Naert I., Vermaelen P., Deroose C.M., Sasaki K., Duyck J. The effect of whole body vibration on peri-implant bone healing in rats. ***Clinical Oral Implants Research*** 2011 Mar;22(3):302-7.

Ogawa T., Suzuki T., Oishi N., **Zhang X.**, Naert I., Sasaki K. Relationship between tactile sensation and occlusal loading condition of mandibular premolars and molars. ***Odontology*** 2011 Jul;99(2):193-6.

Zhang X., Peng B., Fan M., Bian Z., Chen Z. Effect of estrogen-deficiency on RANKL and OPG synthesis in periapical lesions induced in rats. ***Journal of Endodontics*** 2007 Sept; 33(9): 1053-6.

Xiong H., Peng B., Wei L., **Zhang X.**, Wang L. Effect of an Estrogen-deficient State and Alendronate Therapy on Bone Loss Resulting from Experimental Periapical Lesions in Rats. ***Journal of Endodontics*** 2007 Nov;33(11):1304-8.

Zhang X., Peng B. Immunolocalization of receptor activator of NF kappa B ligand in rat periapical lesions. ***Journal of Endodontics*** 2005 Aug; 31(8):574-7.

Publications at international conferences and symposia

Ogawa T., Possemiers T., **Zhang X.**, Naert I., Chaudhari A., Sasaki K., Duyck J. (2011). Time effect of whole body vibration on peri-implant bone healing. IADR/AADR General Session. San Diego, Abstract No. 143479. 16-19 March 2011.

Zhang X., Duyck, J., Naert, I., Carmeliet, G. (2010). Effect of immediate and delayed loading on peri-implant bone healing. IADR General Session. Barcelona, Abstract No. 131659.14-17 July 2010.

Ogawa T., **Zhang X.**, Naert I., Vermaelen P., Deroose CM., Sasaki K., Duyck J. (2010) Effect of whole body vibration loading on peri-implant bone healing. IADR General Session. Barcelona, Abstract No. 3771. 14-17 July 2010.

Torcasio A., **Zhang X**., Duyck J., van Lenthe G. (2010). "Quantification of the peri-implant bone strains in the rat tibia compression model". ESB2010- The European Society of Biomechanics. Edinburgh, UK. Abstract No. CD-ROM 279. 5-8 July.